

PB 262 823

DOT HS-802 108

ELECTROMAGNETIC INTERFERENCE EFFECTS ON MOTOR VEHICLE ELECTRONIC CONTROL AND SAFETY DEVICES

Volume II-Measurements, Analysis and Testing

Contract No. DOT-HS-5-01097

November 1976

Final Report

PREPARED FOR:

U.S. DEPARTMENT OF TRANSPORTATION

National Highway Traffic Safety Administration

Washington, D.C. 20590

**REPRODUCED BY
NATIONAL TECHNICAL
INFORMATION SERVICE
U. S. DEPARTMENT OF COMMERCE
SPRINGFIELD, VA. 22161**

Document is available to the public through
the National Technical Information Service,
Springfield, Virginia 22161

This document is disseminated under the sponsorship of the Department of Transportation in the interest of information exchange. The United States Government assumes no liability for its contents or use thereof.

1. Report No. DOT HS 802 108		2. Government Accession No.		3. Recipient's Catalog No.	
4. Title and Subtitle Electromagnetic Interference Effects on Motor Vehicle Electronic Control and Safety Devices Volume 2 - Measurements, Analysis and Testing				5. Report Date November 1976	
				6. Performing Organization Code	
7. Author(s) R.H. Espeland, D.H. Layton, B.D. Warner & L.R. Teters				8. Performing Organization Report No.	
9. Performing Organization Name and Address U.S. Department of Commerce Office of Telecommunications Institute for Telecommunication Sciences Boulder, Colorado 80302				10. Work Unit No. (TRAIS)	
				11. Contract or Grant No. DoT-HS-5-01097	
12. Sponsoring Agency Name and Address U.S. Department of Transportation National Highway Traffic Safety Administration 400 Seventh St, SW Washington, DC 20590				13. Type of Report and Period Covered Final Report of Period March 1, 1975 July 1, 1976	
				14. Sponsoring Agency Code	
15. Supplementary Notes					
16. Abstract This report contains the results of a test series to evaluate the electrical environment of a motor vehicle during normal operating conditions and a summary of power supply variations and electrical signal transient characteristics. Both source and coupled signals were measured. A computerized coupling analysis program was used to determine the effects of body shielding, aperture size, and cable lengths on signal coupling in the 100 to 200 MHz band between a simulated mobile radio emission and a modeled air-cushion restraint system cable as it might be used in a motor vehicle. A series of susceptibility tests were performed on an electronic speed control system and an antiskid control module to determine functional upset levels of injected signals at critical circuit ports on these devices. The upset criteria were based on performance departures from normal, resulting from the injection of interfering signals. The injected signals were designed to represent levels and durations characteristic of those generated within the vehicle or coupled from external sources.					
17. Key Words Electrical signals, automotive, interference, coupled signals, measurements, transients, power supply variations, aperture size, shielding, susceptibility testing.			18. Distribution Statement Document is available to the public through the National Technical Information Service, Springfield, Virginia 22161		
19. Security Classif. (of this report) UNCLASSIFIED		20. Security Classif. (of this page) UNCLASSIFIED		21. No. of Pages	22. Price

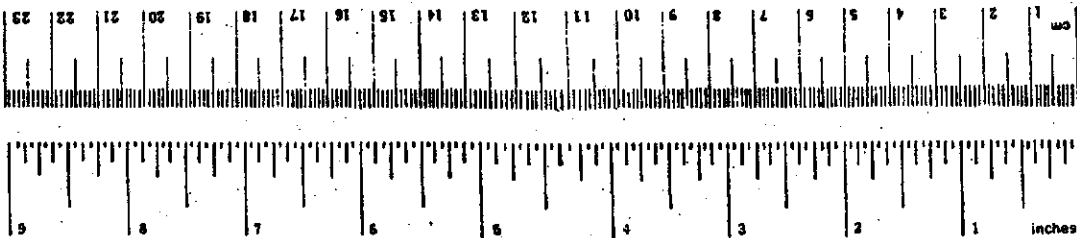
METRIC CONVERSION FACTORS

Approximate Conversions to Metric Measures

Symbol	When You Know	Multiply by	To Find	Symbol
LENGTH				
in	inches	2.5	centimeters	cm
ft	feet	30	centimeters	cm
yd	yards	0.9	meters	m
mi	miles	1.6	kilometers	km
AREA				
in ²	square inches	6.5	square centimeters	cm ²
ft ²	square feet	0.09	square meters	m ²
yd ²	square yards	0.8	square meters	m ²
mi ²	square miles	2.6	square kilometers	km ²
	acres	0.4	hectares	ha
MASS (weight)				
oz	ounces	28	grams	g
lb	pounds	0.45	kilograms	kg
	short tons (2000 lb)	0.9	metric tons	t
VOLUME				
tsp	teaspoons	5	milliliters	ml
Tbsp	tablespoons	15	milliliters	ml
fl oz	fluid ounces	30	milliliters	ml
c	cups	0.24	liters	l
pt	pints	0.47	liters	l
qt	quarts	0.96	liters	l
gal	gallons	3.8	liters	l
ft ³	cubic feet	0.03	cubic meters	m ³
yd ³	cubic yards	0.76	cubic meters	m ³
TEMPERATURE (exact)				
°F	Fahrenheit temperature	5/9 (after subtracting 32)	Celsius temperature	°C

Approximate Conversions from Metric Measures

Symbol	When You Know	Multiply by	To Find	Symbol
LENGTH				
mm	millimeters	0.04	inches	in
cm	centimeters	0.4	inches	in
m	meters	3.3	feet	ft
km	kilometers	0.6	miles	mi
AREA				
cm ²	square centimeters	0.16	square inches	in ²
m ²	square meters	1.2	square yards	yd ²
km ²	square kilometers	0.4	square miles	mi ²
ha	hectares (10,000 m ²)	2.5	acres	
MASS (weight)				
g	grams	0.035	ounces	oz
kg	kilograms	2.2	pounds	lb
t	metric tons (1000 kg)	1.1	short tons	
VOLUME				
ml	milliliters	0.03	fluid ounces	fl oz
l	liters	2.1	pints	pt
l	liters	1.06	quarts	qt
l	liters	0.26	gallons	gal
m ³	cubic meters	35	cubic feet	ft ³
m ³	cubic meters	1.3	cubic yards	yd ³
TEMPERATURE (exact)				
°C	Celsius temperature	9/5 (then add 32)	Fahrenheit temperature	°F



*1 in = 2.54 cm exactly. Conversion factors are approximate and rounded. See NBS Special Publication 280, Units of Measure, for details. P. 4-2.25, 4-2.26, 4-2.27, 4-2.28, 4-2.29, 4-2.30, 4-2.31, 4-2.32, 4-2.33, 4-2.34, 4-2.35, 4-2.36, 4-2.37, 4-2.38, 4-2.39, 4-2.40, 4-2.41, 4-2.42, 4-2.43, 4-2.44, 4-2.45, 4-2.46, 4-2.47, 4-2.48, 4-2.49, 4-2.50, 4-2.51, 4-2.52, 4-2.53, 4-2.54, 4-2.55, 4-2.56, 4-2.57, 4-2.58, 4-2.59, 4-2.60, 4-2.61, 4-2.62, 4-2.63, 4-2.64, 4-2.65, 4-2.66, 4-2.67, 4-2.68, 4-2.69, 4-2.70, 4-2.71, 4-2.72, 4-2.73, 4-2.74, 4-2.75, 4-2.76, 4-2.77, 4-2.78, 4-2.79, 4-2.80, 4-2.81, 4-2.82, 4-2.83, 4-2.84, 4-2.85, 4-2.86, 4-2.87, 4-2.88, 4-2.89, 4-2.90, 4-2.91, 4-2.92, 4-2.93, 4-2.94, 4-2.95, 4-2.96, 4-2.97, 4-2.98, 4-2.99, 4-3.00.

TABLE OF CONTENTS

	<u>Page</u>
LIST OF ILLUSTRATIONS	v
LIST OF TABLES	viii
ABSTRACT	1
1. INTRODUCTION	2
2. INTERNALLY GENERATED MOTOR VEHICLE ELECTRICAL SIGNALS	4
2.1 Measurement Plans and Methodology	4
2.2 Internal Electrical Sources	7
2.2.1 Light Switch	7
2.2.2 Air Conditioner Clutch	13
2.2.3 Starter Solenoid and Starter	16
2.2.4 Ignition System	16
2.2.5 Turn Signal and Emergency Flashers	21
2.2.6 Transient Simulator	24
2.2.7 Fan Motor	25
2.2.8 Alternator	29
2.2.9 Windshield Wiper Motor	31
2.2.10 Horn	31
2.2.11 General Vehicle Noise (Broadband Noise)	34
2.3 Power Supply Variations and Severe Transient Characteristics	34
2.3.1 Voltage Regulation	36
2.3.2 Transients	37
2.3.3 Electrical and Accessory Noise	38
2.4 Chassis DC Resistance Measurements	38
3. FIELD-TO-WIRE COUPLING ANALYSIS	42
3.1 The FTWCAP Model	42
3.2 Program Adaptation	44
3.3 Coupling Analysis	46
4. SUBSYSTEM SUSCEPTIBILITY TESTING	61
4.1 Testing Preparation and Procedures	61
4.1.1 Procurement of Equipment & Descriptive Documentation	62
4.1.2 Preparation of Subsystems for Interface and Operational Synthesis	62
4.1.3 Test Series	63

	<u>Page</u>
4.2 Test Activities (Speed Control System)	63
4.2.1 Speed Control System	63
4.2.2 Speed Control System Test Plan	64
4.3 Speed Control Test Results	69
4.3.1 Circuit Impedances	71
4.3.2 RF Pulse Testing	71
4.3.3 DC Pulse Testing	82
4.4 Test Activities (AntiSkid Brake System)	89
4.4.1 Antiskid Braking System	89
4.4.2 Antiskid Braking System Test Plan	91
4.5 Antiskid Brake System Results	105
4.5.1 Circuit Impedance	106
4.5.2 RF Pulse Testing	106
4.5.3 CW Testing	118
4.5.4 DC Pulse Testing	118
5. SUMMARY AND CONCLUSIONS	126
6. ACKNOWLEDGEMENTS	130
7. REFERENCES	130

LIST OF ILLUSTRATIONS

		<u>Page</u>
Figure 2.1	Measurements Techniques	8
Figure 2.2	Light Switch Signals	14
Figure 2.3	Air-Conditioner Clutch Waveforms	15
Figure 2.4	Starter Solenoid and Starter Waveforms	17
Figure 2.5	Ignition System Waveforms	19
Figure 2.6	Turn Signal and Emergency Flasher Waveforms	22
Figure 2.7	Transient Simulator Waveforms	26
Figure 2.8	Fan Motor Waveforms	27
Figure 2.9	Alternator Waveforms	30
Figure 2.10	Windshield Wiper Motor Waveforms	32
Figure 2.11	Horn Waveforms	33
Figure 2.12	General Vehicle Noise (Broadband)	35
Figure 2.13	Test Equipment	40
Figure 3.1	Air Cushion Restraint System	45
Figure 3.2	Cable Bundle Diagram	47
Figure 3.3	Vehicle Model Reference Grid	48
Figure 3.4	Power Density and Shielding Attenuation vs. Frequency	52
Figure 3.5	Wire Shielding Attenuation vs. Frequency	53
Figure 3.6	Amplitude of Received Signal vs. Frequency (wire ends A_1 , B_1 , and A_2)	54
Figure 3.7	Amplitude of Received Signal vs. Frequency (wire end A_1)	55
Figure 3.8	Amplitude of Received Signal vs. Frequency (wire end A_2)	56
Figure 3.9	Amplitude of Received Signal vs. Frequency (wire end B_1)	57
Figure 3.10	Amplitude of Received Signal vs. Frequency (132 in. and 110 in.)	60

LIST OF ILLUSTRATIONS (cont.)

	<u>Page</u>	
Figure 4.1	Speed Control System	65
Figure 4.2	Speed Control Electronics	65
Figure 4.3	Speed Control Sensor Input Impedance	72
Figure 4.4	Speed Control Power Line Input Impedance	73
Figure 4.5	Speed Control Line Input Impedance	74
Figure 4.6	Test Configuration	75
Figure 4.7	Interference Pulses (RF)	77
Figure 4.8	Sensor Line Test Results (Speed Control System)	80
Figure 4.9	Control Line Test Results (Speed Control System)	81
Figure 4.10	Power Line Test Results (Speed Control System)	83
Figure 4.11	Interference Pulses (DC)	87
Figure 4.12	Interference Pulses (Exponential Shaping)	90
Figure 4.13	Generalized Block Diagram of an Antiskid Brake Controller	92
Figure 4.14	Wheel and Vehicle Velocity Interrelationship	93
Figure 4.15	Antiskid Module Test Diagram	98
Figure 4.16	Waveforms Representing the Acceleration-Deceleration Cycle of an Antiskid Control Module	100
Figure 4.17	Wheel-Sensor Type Signals Showing the Effect of Brake Modulation	102
Figure 4.18	Skid Control System	103
Figure 4.19	Wheel and Axle Control Schematics	104
Figure 4.20	Antiskid Sensor Input Impedance	107
Figure 4.21	Antiskid Power Line Input Impedance	108
Figure 4.22	Antiskid Sensor Line Test Results (Single point - RF Pulses)	109
Figure 4.23	Antiskid Sensor Line Test Results (Dual Input - RF Pulse)	110
Figure 4.24	Antiskid Accelerate-Decelerate Cycles with Brake Modulation	113

LIST OF ILLUSTRATIONS (cont.)

	<u>Page</u>
Figure 4.25 Antiskid Accelerate-Decelerate Cycles Showing System Upset Conditions	114
Figure 4.26 Antiskid Accelerate-Decelerate Cycles with System Upset Conditions	115
Figure 4.27 An Antiskid Sensor Signal with RF Pulse Signals Superimposed	117
Figure 4.28 Antiskid Power Line Test Results	119
Figure 4.29 Antiskid Sensor Line Test Results (Dual Input - CW)	120
Figure 4.30 Antiskid Sensor Line Test Results (Single Point - CW)	121
Figure 4.31 Antiskid Accelerate-Decelerate Cycles with System Upset Conditions	124
Figure 4.32 Antiskid Sensor Signal with DC Pulses Superimposed.	125

LIST OF TABLES

		<u>Page</u>
Table 2.1	Proposed Tests for Signal Sources and Distribution	5
Table 2.2	Source Waveform Summary	9
Table 2.3	Coupled Waveform Summary	11
Table 2.4	Automotive Voltage Regulation Characteristics	36
Table 2.5	Automotive Transient Voltage Characteristics	37
Table 2.6	Summary of Automotive Electrical Continuous Noise Characteristics	39
Table 2.7	Chassis DC Resistance Measurements	41
Table 3.1	Power Density, Fuselage Shielding and Cable Shielding	50
Table 3.2	Amplitude of Received Signals at Designated Load Points (dB)	51
Table 4.1	RF Pulse Tests (Speed Control Unit)	67
Table 4.2	Mobile Radio Frequencies	68
Table 4.3	DC Pulse Tests (Speed Control Unit)	70
Table 4.4	Upset Test Data (RF Pulses) Sensor Line	79
Table 4.5	Upset Test Data (DC Pulses) Sensor Line	84
Table 4.6	DC Pulse Tests (Sensor Line - Speed Control System)	85
Table 4.7	DC Pulse Tests (Control Line - Speed Control System)	88
Table 4.8	RF Pulse Tests (Anti-skid Module)	95
Table 4.9	CW Tests (Antiskid Module)	96
Table 4.10	DC Pulse Tests (Antiskid Module)	97
Table 4.11	Control Board Pin Connections	105
Table 4.12	Antiskid Module Test Record	112
Table 4.13	DC Pulse Tests (Sensor Line)	123

ELECTROMAGNETIC INTERFERENCE EFFECTS
ON MOTOR VEHICLE ELECTRONIC CONTROL AND SAFETY DEVICES

VOLUME 2 - MEASUREMENTS, ANALYSIS, AND TESTING

R.H. Espeland, D.H. Layton, B.D. Warner, and L.R. Teters*

ABSTRACT

This report contains the results of a test series to evaluate the electrical environment of a motor vehicle during normal operating conditions and a summary of power supply variations and electrical signal transient characteristics. Both source and coupled signals were measured.

A computerized coupling analysis program was used to determine the effects of body shielding, aperture size, and cable lengths on signal coupling in the 100 to 200 MHz band between a simulated mobile radio emission and a modeled air-cushion restraint system cable as it might be used in a motor vehicle.

A series of susceptibility tests were performed on an electronic speed control system and an antiskid control module to determine functional upset levels of injected signals at critical circuit ports on these devices. The upset criteria were based on performance departures from normal, resulting from the injection of interfering signals. The injected signals were designed to represent levels and durations characteristic of those generated within the vehicle or coupled from external sources.

Key Words: Electrical signals, automotive, interference, coupled signals, measurements, transients, power supply variations, aperture size, shielding, susceptibility testing.

* The authors are with the Institute for Telecommunication Sciences, Office of Telecommunications, U.S. Department of Commerce, Boulder, Colorado 80302.

1. INTRODUCTION

In recognition of the potential EMC/EMI problems associated with the introduction of electronic systems for control and safety of motor vehicles, the National Highway Traffic Safety Administration (NHTSA) of the U.S. Department of Transportation initiated an investigation to determine the range of possible problems and to develop preliminary design guidelines to assist equipment and system designers in circuit and configuration selection and control.

An earlier study (Espeland, et al., 1975) produced documents and models regarding the following areas of research:

- 1) computer analysis models to determine sensitivities of electronic circuits and subsystems,
- 2) a file of potential interference sources internal to the vehicle,
- 3) a file of potential interference sources external to the vehicle,
- 4) computer analysis models to determine the conducted and coupled transfer of signals in the cabling and wiring circuits of the vehicle, and
- 5) a guide of validation tests and preliminary guidelines.

This present study specifies a research effort to expand the general guidelines for packaging and installation of electronic safety and control devices on motor vehicles so as to affect electromagnetic compatibility among the devices and the electromagnetic and electrical environment of the vehicle. These guidelines are based on the results of tests and measurements conducted to evaluate the electrical environment of motor vehicles, on conductive and radiative susceptibility tests of selected electronic subsystems, and on current research and studies conducted by the automotive and electronics industries. The results of this program are reported in two volumes. The results obtained from the measurements (electrical environment), the analysis of coupled signals, and the subsystem susceptibility testing are contained in Volume 2. The extension and clarification of the work on automotive EMC guidelines is

reported in Volume 3 under the same title.

Section 2 of this report deals mainly with a measurement program to study the characteristics of signals generated by the normal operation of the electrical and electromechanical devices of the motor vehicle. Data were recorded at the source and at remote points within the primary power and control system to determine the amplitude, duration, and frequency responses of these generated signals. Typical control actions for which signals are generated are the activation or deactivation of the light switch and flashers, solenoids, and motors. The alternator, ignition system, and vibrators (horn and buzzer) are also sources. A review of power supply variations and severe transient characteristics resulting from the previous study were included to complete this section.

A field-to-wire coupling analysis of the effects of body shielding, aperture sizes (such as windows, door seams, grills, etc.), and cable lengths and terminating impedances on coupled signals from external fields is reported in Section 3, using an air-cushion restraint system cable and simulated mobile radio emission as the study example. The program used in this analysis is related to the wire-to-wire coupling analysis program reported in the earlier study (Espeland et al., 1975).

Section 4 reports on the methodology and results of injected signal susceptibility testing using an electronic speed control subsystem and an antiskid control module. A direct drive test facility operated by the Air Force Weapons Laboratory (AFWL) at Kirtland AFB, NM was used for these tests. The interference test signals were selected to be similar to those types observed in the source measurements work (Section 2). Various system upset conditions were observed and reported.

The results and conclusions obtained from these tasks are used in part as a basis for the automotive EMC guidelines report in Volume 3.

2. INTERNALLY GENERATED MOTOR VEHICLE ELECTRICAL SIGNALS

2.1 Measurement Plans and Methodology

This section gives the results of the tests conducted to evaluate the internal electrical environment of a motor vehicle. The objective of these measurements was to collect information on source signals and their distribution to aid in establishing guidelines to achieve electromagnetic compatibility between vehicle electronic circuits.

The general measurements philosophy followed in the performance of this task was to record first the signal characteristics at the source (varying operating conditions to determine the potential range of characteristics) and then to observe the degree of coupling of these signals to points of interest throughout the vehicle. The combined source and distribution data comprise an information set for any particular source.

A proposed test plan (Espeland et al., 1975) was used as a reference document in conducting these source evaluation tests. This plan (Table 2.1) details the types and locations of measurements to be made, emphasizing the source characteristics as well as possible signal distribution.

The electrical and electromechanical devices on which measurements were made are as follows:

- 1) the light switch,
- 2) the air conditioner clutch,
- 3) the starter and starter solenoid,
- 4) the ignition system,
- 5) the turn signal and emergency flashers,
- 6) the field dump transient simulator,
- 7) the fan motor,
- 8) the alternator,
- 9) the windshield wiper motor,

Reproduced from
best available copy.



Table 2.1 Proposed Test for Source Signals and Distribution

TEST POINTS	OPERATING CONDITIONS	ENGINE RUNNING		DIRECTIONAL SIGNALS		EMERGENCY FLASHER		WINDSHIELD WIPER (ELECTRIC)		WARNING BUZZER		HEATER & AIR COND		FAN		AIR COND CLUTCH		STARTER CRANKING		ALTERNATOR		HEADLAMP SWITCHING		MAXIMUM LAMP LOAD		
		SOLE / 2000 / 3000	DISTRIBUTOR	D-FLASHER	LEFT	RIGHT	EMERG. WIPER SWITCH	INT	INT	INT	INT	INT	INT	INT	INT	INT	INT	INT	INT	INT	INT	INT	INT	INT	INT	INT
SCOPE SYNC																										
MAIN BUS		1, 3	1, 3	1, 3	1, 3	1, 3	1, 3	1, 3	1, 3	1, 3	1, 3	1, 3	1, 3	1, 3	1, 3	1, 3	1, 3	1, 3	1, 3	1, 3	1, 3	1, 3	1, 3	1, 3	1, 3	1, 3
IGNITION SWITCH		1, 3	1, 3	1, 3	1, 3	1, 3	1, 3	1, 3	1, 3	1, 3	1, 3	1, 3	1, 3	1, 3	1, 3	1, 3	1, 3	1, 3	1, 3	1, 3	1, 3	1, 3	1, 3	1, 3	1, 3	1, 3
TERMINALS COIL		1, 3, 6	1, 3, 6	1, 3, 6	1, 3, 6	1, 3, 6	1, 3, 6	1, 3, 6	1, 3, 6	1, 3, 6	1, 3, 6	1, 3, 6	1, 3, 6	1, 3, 6	1, 3, 6	1, 3, 6	1, 3, 6	1, 3, 6	1, 3, 6	1, 3, 6	1, 3, 6	1, 3, 6	1, 3, 6	1, 3, 6	1, 3, 6	1, 3, 6
FRONT DIRECTION SIGNAL		1, 2, 3	1, 2, 3	1, 2, 3	1, 2, 3	1, 2, 3	1, 2, 3	1, 2, 3	1, 2, 3	1, 2, 3	1, 2, 3	1, 2, 3	1, 2, 3	1, 2, 3	1, 2, 3	1, 2, 3	1, 2, 3	1, 2, 3	1, 2, 3	1, 2, 3	1, 2, 3	1, 2, 3	1, 2, 3	1, 2, 3	1, 2, 3	1, 2, 3
REAR DIRECTION SIGNAL		1, 2, 3	1, 2, 3	1, 2, 3	1, 2, 3	1, 2, 3	1, 2, 3	1, 2, 3	1, 2, 3	1, 2, 3	1, 2, 3	1, 2, 3	1, 2, 3	1, 2, 3	1, 2, 3	1, 2, 3	1, 2, 3	1, 2, 3	1, 2, 3	1, 2, 3	1, 2, 3	1, 2, 3	1, 2, 3	1, 2, 3	1, 2, 3	1, 2, 3
REAR PARKING LAMP		1, 2, 3	1, 2, 3	1, 2, 3	1, 2, 3	1, 2, 3	1, 2, 3	1, 2, 3	1, 2, 3	1, 2, 3	1, 2, 3	1, 2, 3	1, 2, 3	1, 2, 3	1, 2, 3	1, 2, 3	1, 2, 3	1, 2, 3	1, 2, 3	1, 2, 3	1, 2, 3	1, 2, 3	1, 2, 3	1, 2, 3	1, 2, 3	1, 2, 3
WINDSHIELD WIPER MOTOR		1, 2, 3	1, 2, 3	1, 2, 3	1, 2, 3	1, 2, 3	1, 2, 3	1, 2, 3	1, 2, 3	1, 2, 3	1, 2, 3	1, 2, 3	1, 2, 3	1, 2, 3	1, 2, 3	1, 2, 3	1, 2, 3	1, 2, 3	1, 2, 3	1, 2, 3	1, 2, 3	1, 2, 3	1, 2, 3	1, 2, 3	1, 2, 3	1, 2, 3
AIR CONDITIONER CLUTCH		1, 2, 3	1, 2, 3	1, 2, 3	1, 2, 3	1, 2, 3	1, 2, 3	1, 2, 3	1, 2, 3	1, 2, 3	1, 2, 3	1, 2, 3	1, 2, 3	1, 2, 3	1, 2, 3	1, 2, 3	1, 2, 3	1, 2, 3	1, 2, 3	1, 2, 3	1, 2, 3	1, 2, 3	1, 2, 3	1, 2, 3	1, 2, 3	1, 2, 3
O/S FLASHER OUTPUT		1, 2, 3	1, 2, 3	1, 2, 3	1, 2, 3	1, 2, 3	1, 2, 3	1, 2, 3	1, 2, 3	1, 2, 3	1, 2, 3	1, 2, 3	1, 2, 3	1, 2, 3	1, 2, 3	1, 2, 3	1, 2, 3	1, 2, 3	1, 2, 3	1, 2, 3	1, 2, 3	1, 2, 3	1, 2, 3	1, 2, 3	1, 2, 3	1, 2, 3
EMERGENCY FLASHER OUTPUT		1, 2, 3	1, 2, 3	1, 2, 3	1, 2, 3	1, 2, 3	1, 2, 3	1, 2, 3	1, 2, 3	1, 2, 3	1, 2, 3	1, 2, 3	1, 2, 3	1, 2, 3	1, 2, 3	1, 2, 3	1, 2, 3	1, 2, 3	1, 2, 3	1, 2, 3	1, 2, 3	1, 2, 3	1, 2, 3	1, 2, 3	1, 2, 3	1, 2, 3
IGNITION COIL POSITIVE TERMINAL		1, 3, 6	1, 3, 6	1, 3, 6	1, 3, 6	1, 3, 6	1, 3, 6	1, 3, 6	1, 3, 6	1, 3, 6	1, 3, 6	1, 3, 6	1, 3, 6	1, 3, 6	1, 3, 6	1, 3, 6	1, 3, 6	1, 3, 6	1, 3, 6	1, 3, 6	1, 3, 6	1, 3, 6	1, 3, 6	1, 3, 6	1, 3, 6	1, 3, 6
WARNING BUZZER		1, 3	1, 3	1, 3	1, 3	1, 3	1, 3	1, 3	1, 3	1, 3	1, 3	1, 3	1, 3	1, 3	1, 3	1, 3	1, 3	1, 3	1, 3	1, 3	1, 3	1, 3	1, 3	1, 3	1, 3	1, 3
HEADLAMP HIGH		1, 3	1, 3	1, 3	1, 3	1, 3	1, 3	1, 3	1, 3	1, 3	1, 3	1, 3	1, 3	1, 3	1, 3	1, 3	1, 3	1, 3	1, 3	1, 3	1, 3	1, 3	1, 3	1, 3	1, 3	1, 3
TERMINALS LOW		1, 3	1, 3	1, 3	1, 3	1, 3	1, 3	1, 3	1, 3	1, 3	1, 3	1, 3	1, 3	1, 3	1, 3	1, 3	1, 3	1, 3	1, 3	1, 3	1, 3	1, 3	1, 3	1, 3	1, 3	1, 3
BATTERY		1, 3	1, 3	1, 3	1, 3	1, 3	1, 3	1, 3	1, 3	1, 3	1, 3	1, 3	1, 3	1, 3	1, 3	1, 3	1, 3	1, 3	1, 3	1, 3	1, 3	1, 3	1, 3	1, 3	1, 3	1, 3
ALTERNATOR		1, 3	1, 3	1, 3	1, 3	1, 3	1, 3	1, 3	1, 3	1, 3	1, 3	1, 3	1, 3	1, 3	1, 3	1, 3	1, 3	1, 3	1, 3	1, 3	1, 3	1, 3	1, 3	1, 3	1, 3	1, 3

Table 2.1 (Continued) Proposed Test for Source Signals and Distribution

Tests:

1. Voltage waveform reference to device ground to show voltage transients under as many operating conditions as possible.
2. Voltage waveform from battery ground to device ground to detect ground differential voltages in a possible ground loop condition.
3. Spectrum measurement of voltage waveform to determine the frequency/power content of the device load.
4. Current probe measurement of device current.
5. Battery and terminal to device and lead to examine effects of line drop.
6. Power spectrum of device current.
(This test would be expected to be the same as the voltage spectrum. It may prove effective in isolating device analysis from outside interference.)

Equipment:

H. P. 1207 B Scope

H. P. 1207 B Scope

UA - 6A Spectrum Analyzer
(Federal Scientific)

H. P. 1207 B Scope

H. P. 456 A Current Probe

H. P. 1207 B Scope

UA - 6A Spectrum Analyzer
H. P. 456 A Current Probe with
Adaptor

- 10) the horn, and
- 11) the general vehicle noise (broadband noise).

The results and data from these tests are presented in the next section.

The signals recorded are generally of four forms: 1) direct current voltage level changes caused by switching equipment on or off the primary power source, 2) transients or decaying sinusoidal waveforms that are generated during the switching actions, 3) periodic waveforms generated by vibrating systems or rotating machinery, and 4) high frequency pulses or bursts associated with rf transmitting equipment or with (intentional or unintentional) resonance in electronic circuits. Two methods of data recording and analysis were used in these tests. They are shown in Figure 2.1, and represent recording in the time domain and in the frequency domain. Most of the data was taken in real-time using an oscilloscope display recorded photographically.

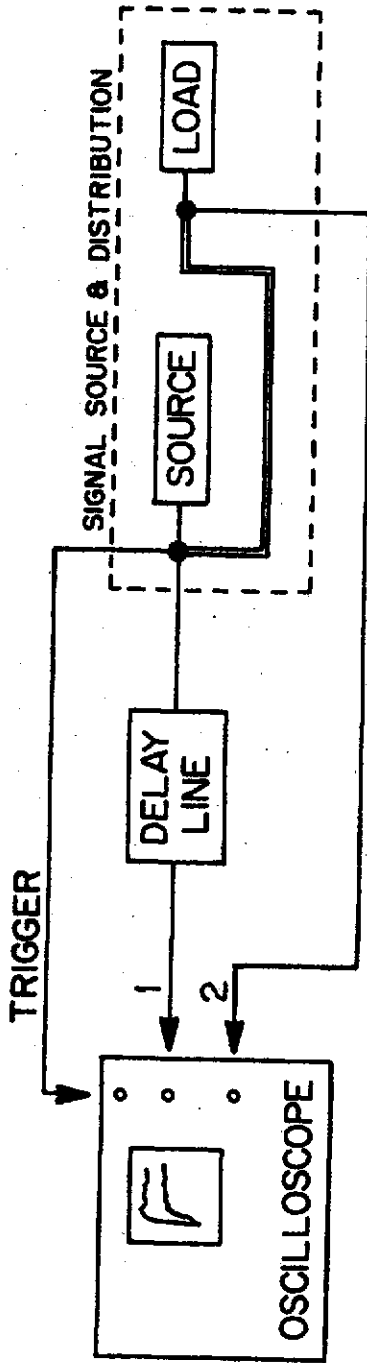
2.2 Internal Electrical Sources

The objective in compiling the data for this section was to present, in the most useful manner, all of the available data on electrical sources within a motor vehicle. Although the bulk of the material presented in this section resulted from the tests described above, certain useful data from other references (Espeland, et al., 1975) is included where appropriate.

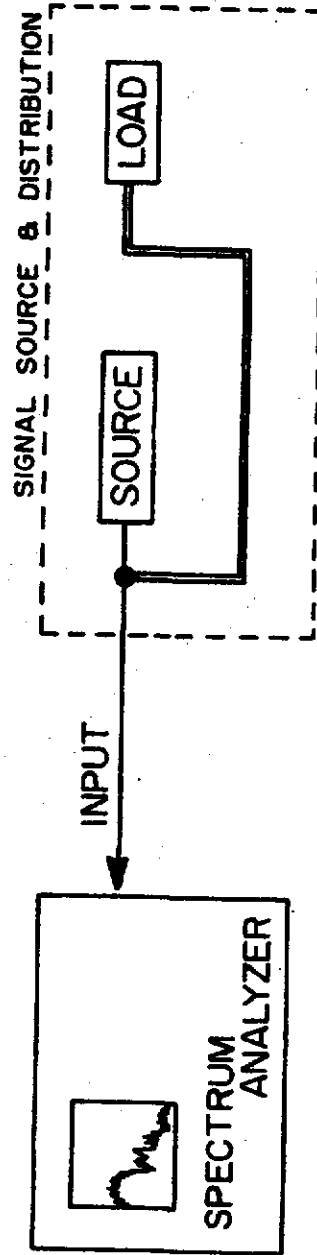
Summary Tables (2.2) and (2.3) describe the signal studies. The pertinent information in the tables define the signal (type, amplitude, and duration) and the source and event that caused it. The format used to present the data from the individual sources includes a circuit diagram, a description of the sources and their functions, tracings of the signals and waveforms recorded, and observations of the signal characteristics. These data are in Figures 2.2 through 2.12. In the circuit diagram at the top of each figure, an arrow is used to indicate the location at which the signals are generated.

2.2.1 Light Switch

The main light switch controls the park and tail lights and head



a.) Time-domain Records



b.) Frequency-domain Records

Figure 2.1 Measurement Techniques

Table 2.2 Source Waveform Summary

EQUIPMENT (SOURCE)	WAVEFORM	DURATION (FREQUENCY)	AMPLITUDE	FIGURE NO.
Light Switch	1.) Switching Transient (Low Beam)	.2 s	≈1.0 V	2.2 (a)
	2.) Switching Transient (High Beam)	.2 s	≈1.0 V	2.2 (b)
	3.) Switching Transient (High Beam)	.2 s	≈1.0 V	2.2 (c)
	4.) Switching Transient (High Beam)	.2 s	≈1.0 V	2.2 (d)
Air Conditioner Clutch	1.) Switching Transient (On-Off)	60 ms	70 V	2.3 (c)
Starter Solenoid and Starter	1.) Starter Solenoid (Switching Pulse)	(On-Off)	12 V	2.4 (a)
	2.) Main Bus (Disabled)	(On-Off)	12 V	2.4 (a)
Ignition System	1.) Ignition Spark	(RPM Dependent)	9 V	2.5 (a)
	2.) Breaker Points	(RPM Dependent)	700 V	2.5 (a), (b)
	3.) Distributor Output	(RPM Dependent)	≈15 KV	2.5 (d), (e)
	4.) Spark Plug	(RPM Dependent)	≈12 KV	2.5 (f), (g)
Turn Signal and Emergency Flashers	1.) T.S. Flasher Output (On-Off)	.25 s	≈12 V	2.6 (b), (c)
	2.) Emergency Flasher		≈12 V	2.6 (d)

Table 2.2 (cont.) Source Waveform Summary

EQUIPMENT (SOURCE)	WAVEFORM	DURATION (FREQUENCY)	AMPLITUDE	FIGURE NO.
Transient Simulator	Simulated Transient	250 ms	≈ 50 V	2.7 (a), (b)
Fan Motor	1.) Fan Motor 2.) Switching Transient and Decaying Sinewave	≈ 555 Hz .4 ms (Variable)	≈ 100 mV ≈ 7 V ≈ 2.5 V	2.8 (a) 2.8 (d), (e) (f), (g), (h)
Alternator	Alternator Output	(RPM Dependent ≈ 900 Hz)	60 mV	2.9 (a)
Windshield Wiper	1.) Motor 2.) Switching Waveform	(RPM Dependent ≈ 500 Hz) .1 s	≈ .3 V 12 V	2.10 (b) 2.10 (a)
Horn	Horn	(≈ 350 Hz)	≈ 3 V	2.11 (a)
Broadband Noise	1.) Ignition Key Buzzer 2.) Horn 3.) Engine Idling			2.12 (b) 2.12 (c) 2.12 (d)

Table 2.3 Coupled Waveforms Summary

EQUIPMENT (SOURCE)	LOCATION	WAVEFORM	DURATION (FREQUENCY)	AMPLITUDE	FIGURE NO.
Light Switch	1.) Turn Signal Lamp	Spike	100 ms	150 mV	2.2 (a)
	2.) Turn Signal Lamp	Spike	100 ms	300 mV	2.2 (b)
	3.) Low Beam Lamp	Spike	100 ms	200 mV	2.2 (c)
	4.) Low Beam Lamp (Bulb Removed)	Spike	5 ms	+700 mV -1.2 V	2.2 (d)
Air Conditioner Clutch	Main Bus	Spike (Noise)	250 ms	300 mV	2.3 (b)
Starter Solenoid and Starter	Battery	Spike and Cogging	(While Cranking)	7 V 1 V	2.4 (b), (c) and (d)
Ignition System	1.) Battery Plus Terminal	Pulse	(RPM Dependent)	50 mV	2.5 (c)
	2.) Main Bus	Pulse	(RPM Dependent)	1 V	2.5 (c)
	3.) Spark Plus Wire (NO Arc Across Plug)	Damped Sinewave	(RPM Dependent)	≈ 35 KV	2.5 (h)
Turn Signal and Emergency Flashers	1.) Lamp Ground Wire	Spike	40 us	≈ 100 mV	2.6 (e)
	2.) Parking Lamp Wire	Spike	20 us	≈ 600 mV	2.6 (f)
	3.) Back-Up Lamp Wire	Spike	20 us	≈ 300 mV	2.6 (g)
	4.) Back-Up Lamp Wire (Lamp Removed)	Spike	10 us	≈ 750 mV	2.6 (h)

Table 2.3 (cont) Coupled Waveforms Summary

EQUIPMENT (SOURCE)	LOCATION	WAVEFORM	DURATION (FREQUENCY)	AMPLITUDE	FIGURE NO.
Transient Simulator	Windshield Wiper	Spike	200 ms	150 mV	2.7 (d)
Fan Motor	Main Bus Right Front Parking Lamp	Sinewave	(555 Hz)	50 mV	2.8 (c)
Alternator	1.) Main Bus	Ripple	(=900 Hz)	20 mV	2.9 (c)
	2.) Main Bus (Abnormal)	Ripple	(=900 Hz)	=6 V	2.9 (d)
Windshield wiper	1.) Main Bus	Ripple	(=500 Hz)	.2 V	2.10 (d)
	2.) Battery Terminal	Ripple	(=500 Hz)	=30 mV	2.10 (c)
Horn	Main Bus	Periodic (Noisy)	(=350 Hz)	60 mV	2.11 (c), (d)
Broadband Noise	1.) Main Bus	(Broadband Noise)	0-100 MHz		2.12 (b)
	2.) Main Bus	(Broadband Noise)	0-100 MHz		2.12 (c)
	3.) Main Bus	(Broadband Noise)	0-100 MHz		2.12 (d)

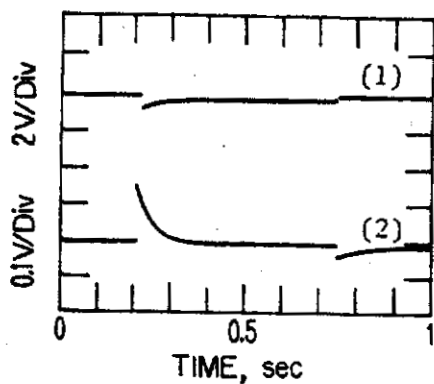
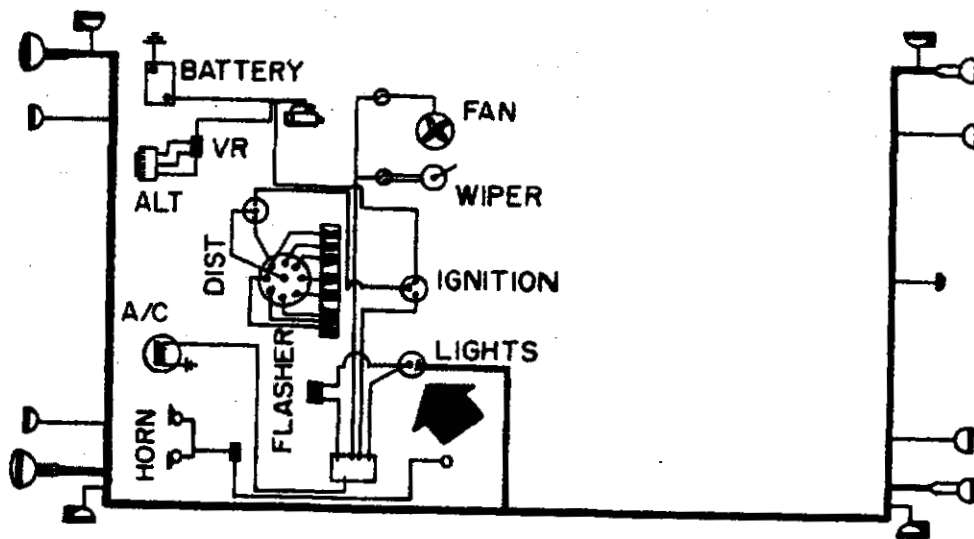
lights. Additional light switches include the stop light switch, the back-up light switch, the high-low beam switch and accessory lamp switches and controls. As these switches are activated, a load is placed on the primary power bus (battery) and energy is coupled to adjacent wires, which often produces transients. The data presented in Figure 2.2 shows the main bus load and selected transients.

Figure 2.2 (a) shows a 200 mV line drop when the low beams are turned "on." A transient of 150 mV occurs at the right front turn signal lamp when the low beam is switched on, and a transient with peak amplitude of -40 mV occurs at the same point when the low beam is switched "off." Figure 2.2 (b) shows that a positive transient of 400 mV occurs at the turn signal lamp when the high beam is turned "on."

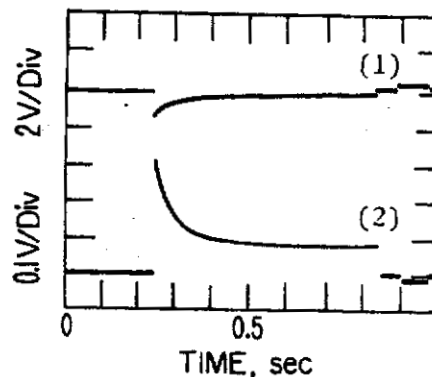
Further documentation of transients associated with the activation of light switches is shown in Figure 2.2 (c) and 2.2 (d). Figure 2.2 (c) shows the waveforms at the low beam lamp when the high beam is switched "on" and "off." An amplitude of 240 mV is reached at the "on" time. In Figure 2.2 (d) the low beam lamps were removed, thus the wires are open circuits. Larger and sharper transients occur, reaching amplitudes of +0.75 V and -1.2 V. This test simulates a condition of burned out lamps.

2.2.2 Air-Conditioner Clutch

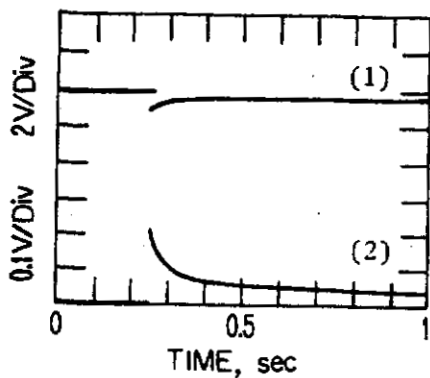
The air-conditioner compressor is driven from a pulley coupled by belt to the crank-shaft drive pulley. When the air-conditioner switch is activated, the compressor is coupled to the pulley by means of an electromagnetic clutch. The clutch imposes a 3.75 A load on the power supply. Transients occur when the air-conditioner switch is turned "on" and "off." The data in Figure 2.3 (a) show the switching "on" and "off" of the air-conditioner compressor. A large transient (80 V) is generated when the compressor clutch is released. Some coupling of this signal to the main bus is evident in the lower trace of Figure 2.3 (b). This high-frequency noise recorded has an amplitude of 0.4 V (p-p). The waveforms in Figure 2.3 (c) and 2.3 (d) show greater detail of the



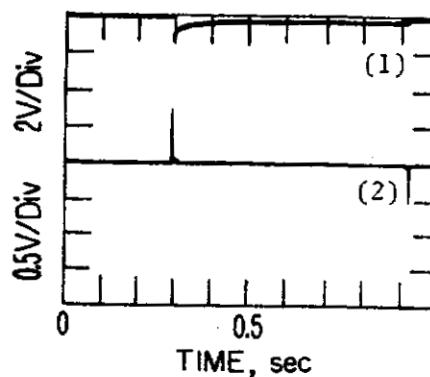
(a) 1 Main bus (low beam on-off)
2 Right front turn-signal lamp



(b) 1 Main bus (high beam on-off)
2 Right front turn-signal lamp

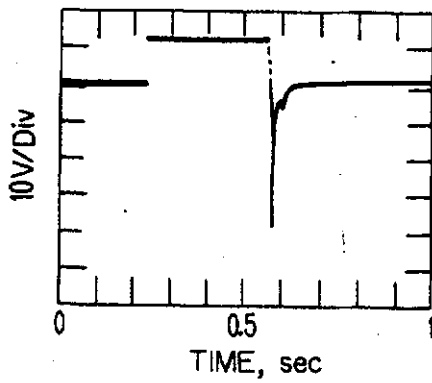
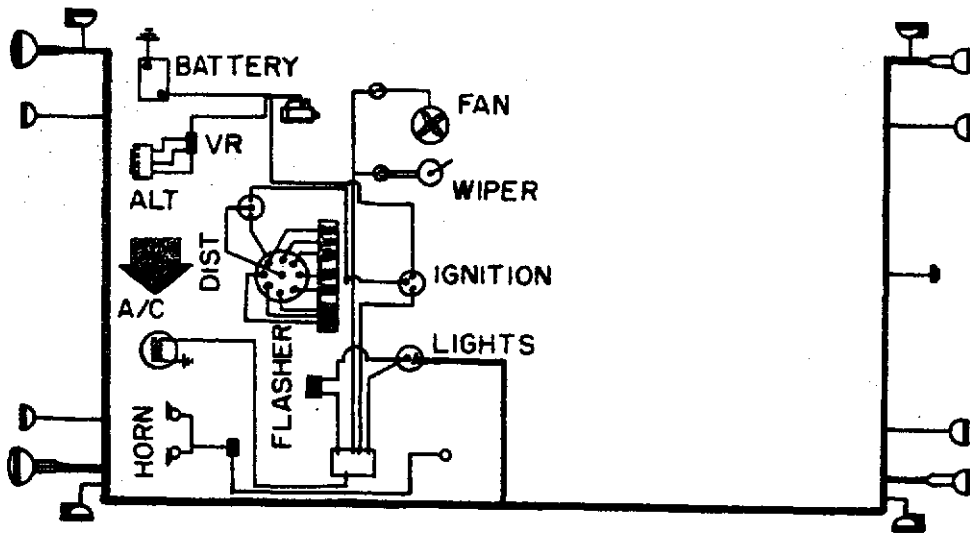


(c) 1 Main bus (high beam on-off)
2 Right front low beam lamp

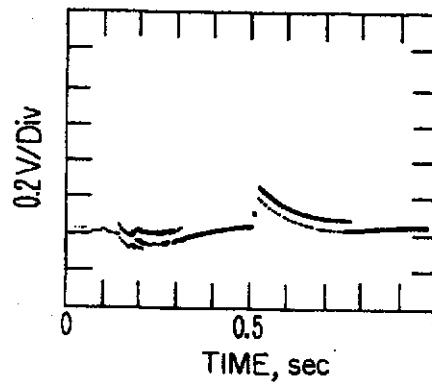


(d) 1 Main bus (high beam on-off)
2 Right front low beam lamp (lamp removed)

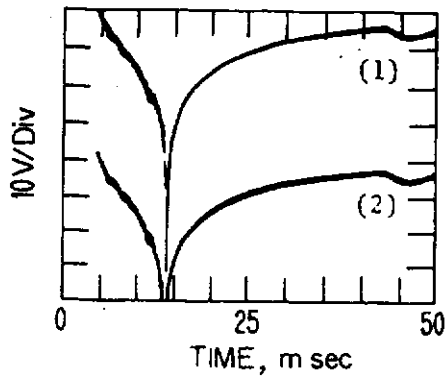
Figure 2.2 Light Switch Signals



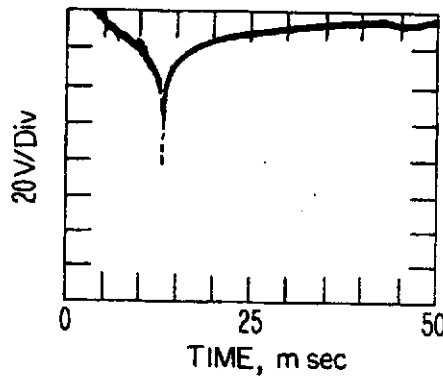
(a) Air-conditioner clutch (on-off)



(b) Main bus (clutch on-off)



(c) 1 Air-conditioner clutch (off)
2 Air-conditioner switch (off)



(d) Air-conditioner clutch (off)

Figure 2.3 Air-conditioner Clutch Waveforms

transient occurring as the clutch is shut off.

2.2.3 Start Solenoid and Starter

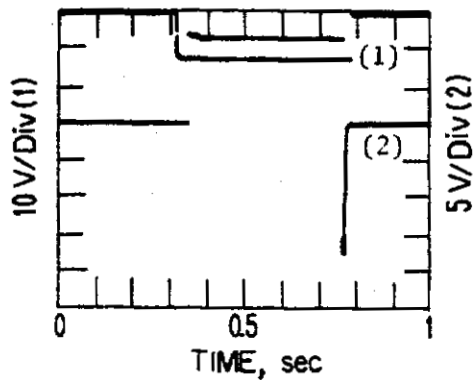
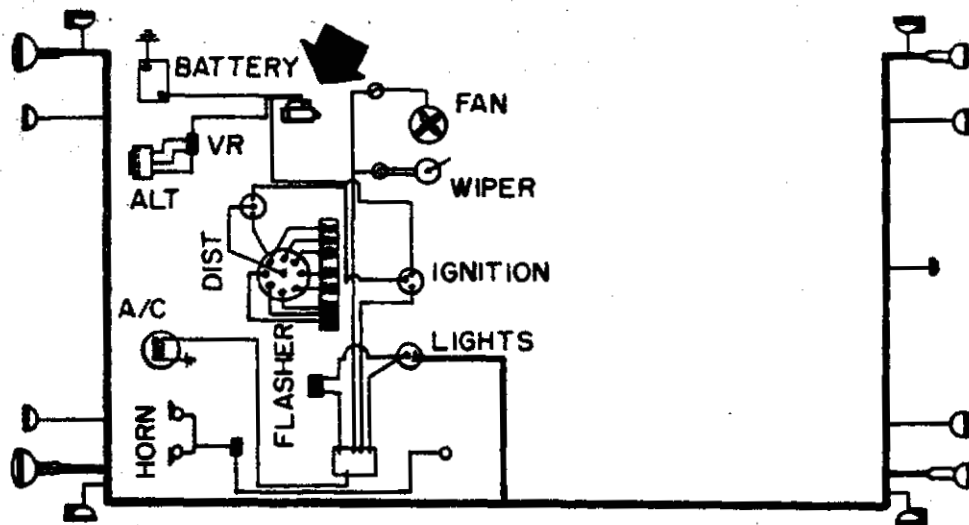
The starter solenoid is activated in the start position of the ignition switch. The solenoid closes a switch which connects the starter directly to the battery. When the ignition switch is turned to the "start" position, the power (12 V) is removed from the main power bus. This is evident from the top trace of Figure 2.4 (a). The voltage on the main bus drops 12 V to ground and 25 ms later the solenoid circuit is energized, as evidenced by the 12 V increase on the lower trace. When the ignition switch is released from "start" and returns to "run," this condition is reversed. Also, an 18 V transient is generated at the solenoid circuit.

The data in Figure 2.4 (b) shows the dc coupled waveform measured at the battery (plus) terminal at the initiation of the "start" or cranking action. The initial 7.5 V drop is caused by the engagement of the starter drive gear onto the flywheel. This is a solenoid action also. The .5 V sinusoidal waveform that follows is known as "cogging" caused by the variation in cranking load as the gas in each cylinder is compressed and then the pressure released.

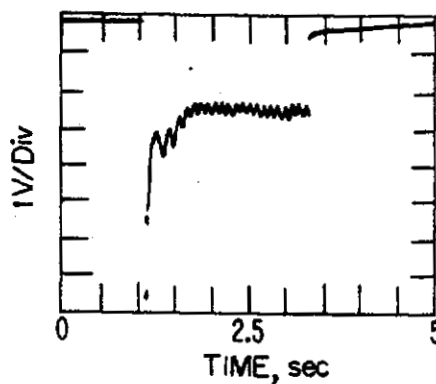
The data in Figure 2.4 (c) and 2.4 (d) show the effect of the plug misfiring during crank and run. In Figure 2.4 (c), the waveform shows the starter engagement and initial cogging. After 1 s, the engine starts and the battery voltage returns to the 12 V level. Some alternator noise (ripple) is evident, and it has a marked periodicity, because only the right-bank cylinders were firing. (The wires of the left bank were removed from the plugs.) In Figure 2.4 (d), only the front right plug wire remained attached to the plug, with all the others removed. The engine did not start, but the firing of the single cylinder is apparent in the waveform.

2.2.4 Ignition System

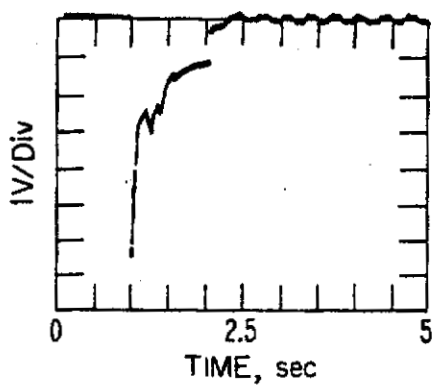
The ignition system, which is powered from the 12 V battery through the ignition switch, consists of a primary circuit and a secondary



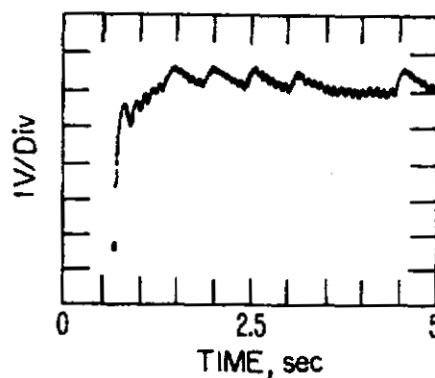
(a) 1 Main bus (starter on-off)
2 Starter solenoid



(b) Battery (engine cranking - did not start)



(c) Battery (engine started - left bank misfiring)



(d) Battery (engine cranking - right front plug only - firing)

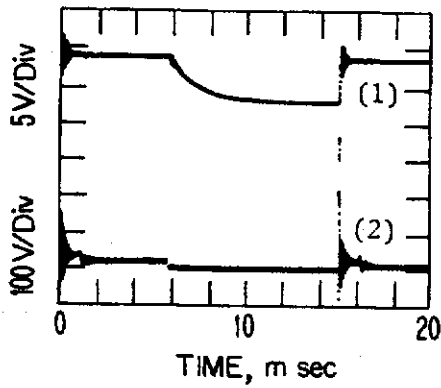
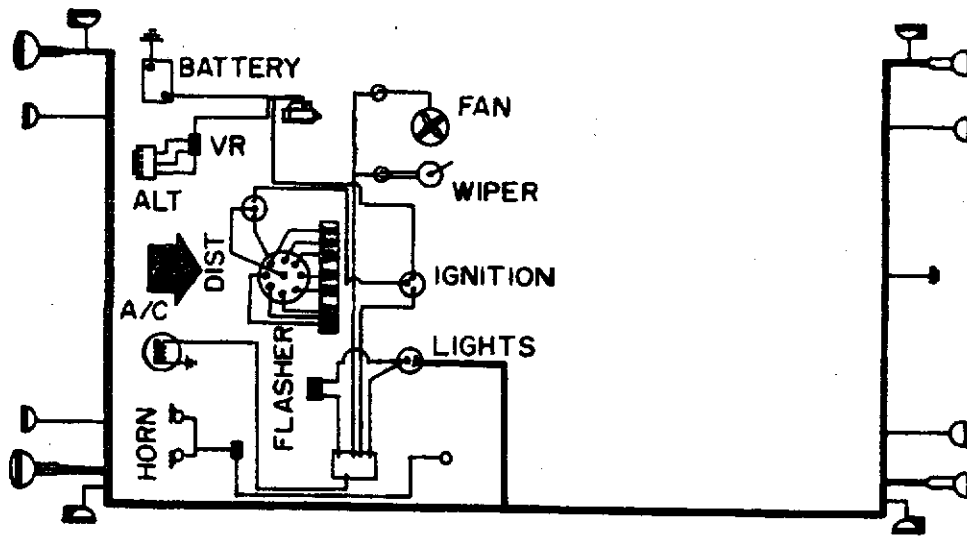
Figure 2.4 Starter Solenoid and Starter Waveforms

circuit. The primary ignition circuit includes the primary winding of the coil, a condenser, and breaker points operated from a cam. In solid-state ignition systems, electronic switches may supplement the breaker points or an armature and pick-up coil may replace the breaker points. The secondary windings of the coil, the distributor, and the spark plugs make up the secondary circuit. The function of the ignition system is to provide a high-voltage spark in the cylinder head near the peak of the compression stroke. This fires the gas mixture, and the expansion of the burning gas powers the engine.

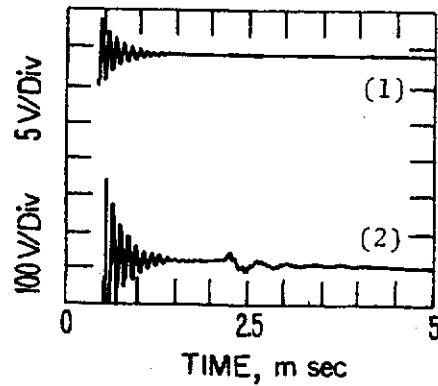
The data shown in Figures 2.5 (a), (b), and (c) are waveforms measured in the primary circuit, and those waveforms measured in Figures 2.5 (d), (e), (f), (g), and (h) are measured in the secondary circuit.

The upper trace in Figure 2.5 (a) shows the dc waveform at the battery side of the ignition coil. This point is common to both windings of the coil. As the breaker points open, the test-point voltage is raised to the battery voltage (13 V) and remains at that voltage until the points close (at about 6 ms). Then the voltage drops to a steady-state 6 V (4 ms) and holds until the breaker points open again. The primary side of the coil and the ignition wire to the ignition switch are a voltage dividing network between the battery and ground. At the time of the breaker opening and the corresponding firing of the spark plug, a damped sinusoidal waveform occurs. Peak amplitudes are 6 V at the battery wire and 360 V at the breaker points. The period of the damped sine wave is measured at about 10 kHz in Figure 2.5(b). The sinusoidal waveform measured on the main fuse of the primary power circuit reaches a peak of 1 V. At the battery terminal, the waveform is less than 0.1 V. These data are recorded in Figure 2.5 (c).

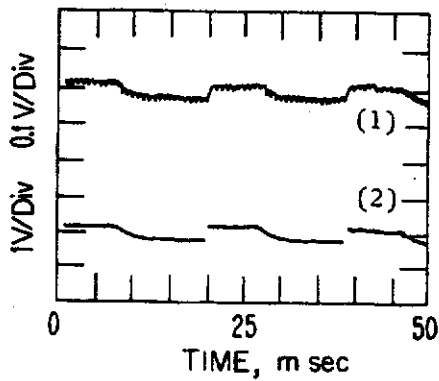
The waveform in Figure 2.5 (d) was recorded at the distributor output. The waveform repeats at approximately 3 ms (this is subject to engine speed variation) with two principal spikes in each set. The first spike occurs with the breaking of the points. A short duration waveform as large as 15,000 V in some cases occurs at that time. It is followed by an offset and a ringing (sinusoidal) waveform as shown in



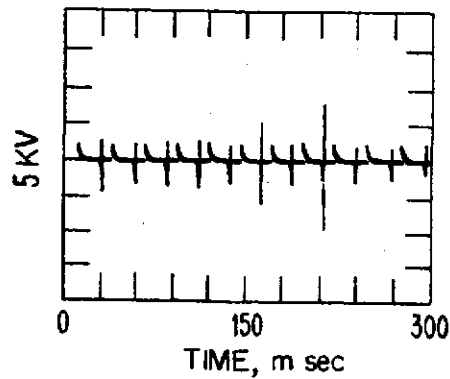
(a) 1 Ignition coil (battery)
2 Breaker points



(b) 1 Ignition coil (battery)
2 Breaker points

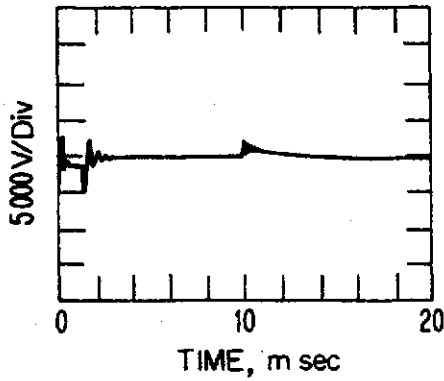
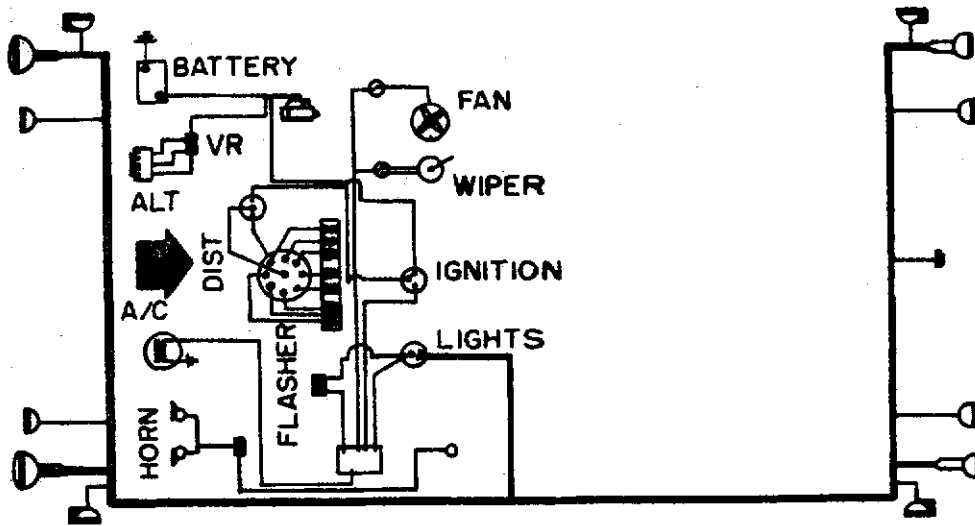


(c) 1 Battery terminal (plus)
2 Main bus

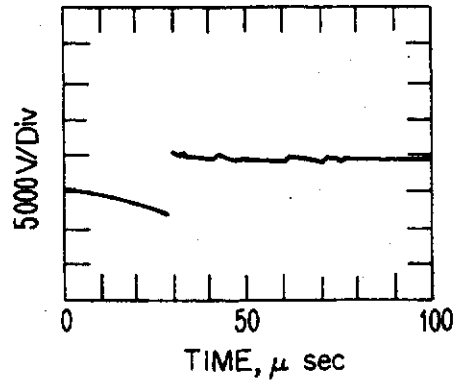


(d) Distributor output
(to spark plugs)

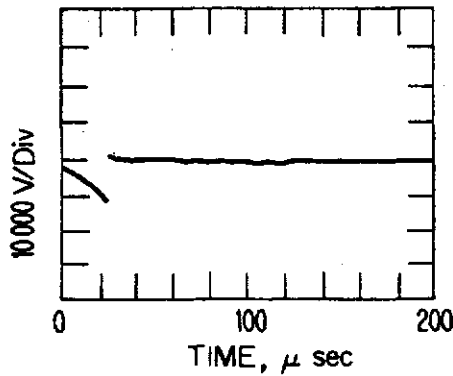
Figure 2.5 Ignition System Waveforms



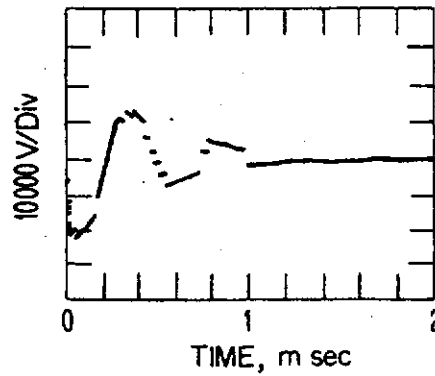
(e) Distributor output
(to spark plugs)



(f) Spark plug
(normal spark)



(g) Spark plug
(normal spark)



(h) Spark plug (no arc
across the plug)

Figure 2.5 (cont) Ignition System Waveforms

Figure 2.5 (e). A ringing occurs at about 10 ms with the closing of the breaker points. These waveforms are evident in both Figures 2.5 (d) and 2.5 (e). The remaining figures show data recorded at the spark plugs. Figures 2.5 (f) and 2.5 (g) show the first few milliseconds of the spark waveform. Peak negative values of about 10,000 V are observed. These waveforms occur with normal spark. The amplitudes and duration will vary with time, with spark plug, and with engine speed and load. However, they are typical waveforms.

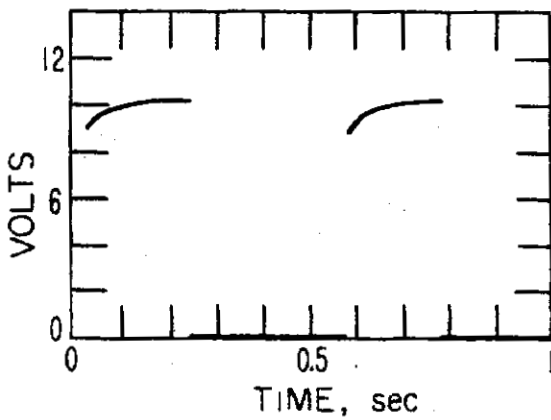
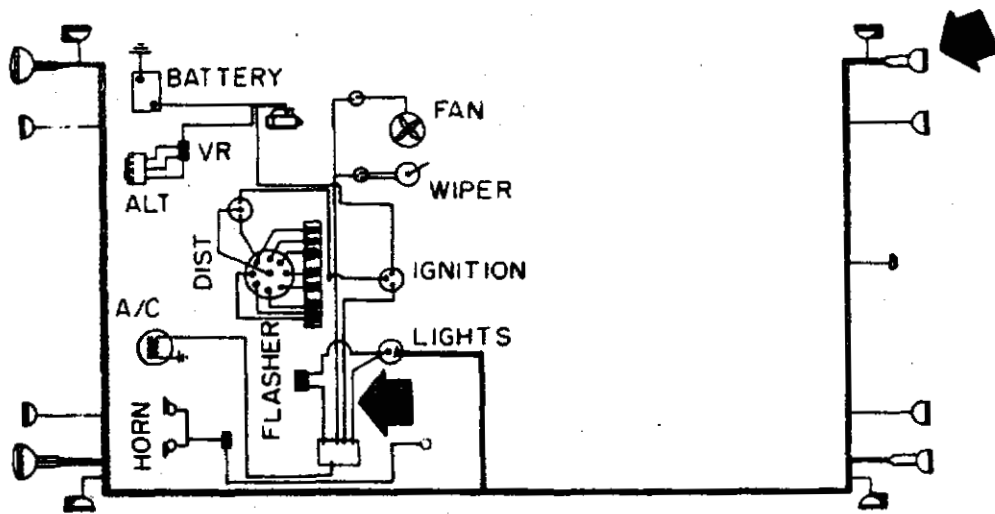
Figure 2.5 (h) represents an abnormal spark condition. The spark plug wire has been removed from the spark plug at a distance prohibiting a spark to the plug or to a ground point. A pronounced ringing of 1 ms duration occurs with peak negative/positive excursions of $-24000/+14000$ V.

2.2.5 Turn Signal and Emergency Flashers

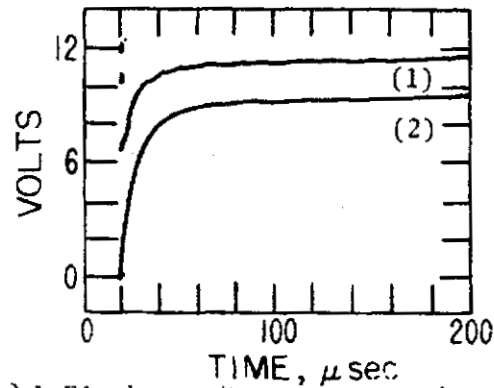
The turn-signal flasher is a device used to cause all required signal lamps to flash when the turn signal flasher switch is activated. The flash rate is between 60 and 120 flashes per minute, and the current "on" between 30% and 75% of the time. Variations within these limits are determined by the type of device, lamp load, and normal production tolerances. The flasher switch connects and disconnects appropriate lamps to the power bus. This produces a rectangular pulse that varies between ground and the power supply voltage. This voltage level change occurs at the flasher unit and at the several lamps that are driven. The emergency flasher serves a similar function to a different set of lights.

Turn-signal and emergency flasher waveforms presented in Figures 2.6 (a), (b), (c), and (d) show the characteristics of the pulse that is generated by the flasher. The data in Figures 2.6 (e), (f), (g), and (h) show the characteristics of coupled or induced waveform resulting from these pulses.

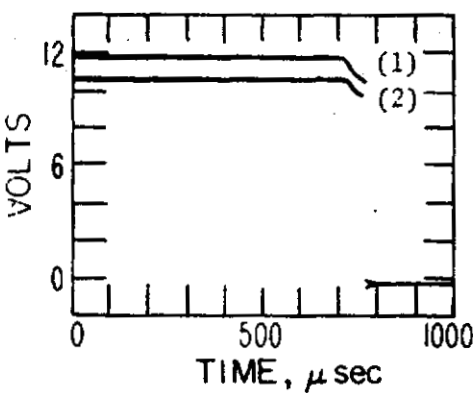
Figure 2.6 (a) describes the switching pulse produced by the turn-signal flasher at the right rear turn-signal lamp. This shows a flash rate of approximately 107 flashes per minute with an "on" time of about



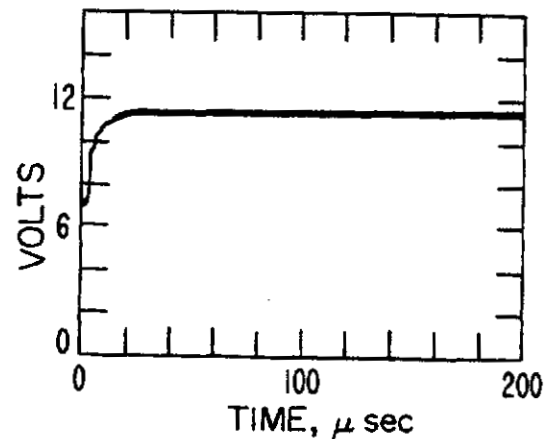
(a) Right rear lamp (turn signal waveform)



(b) 1 Flasher output turn signal
2 Right rear lamp "on"

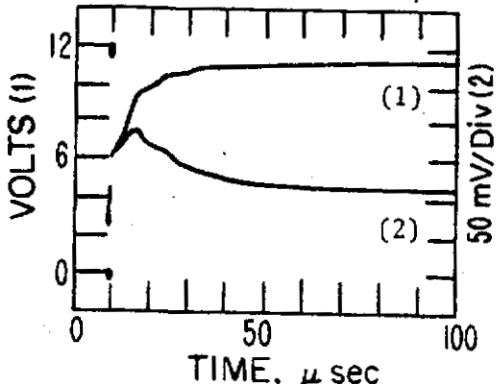
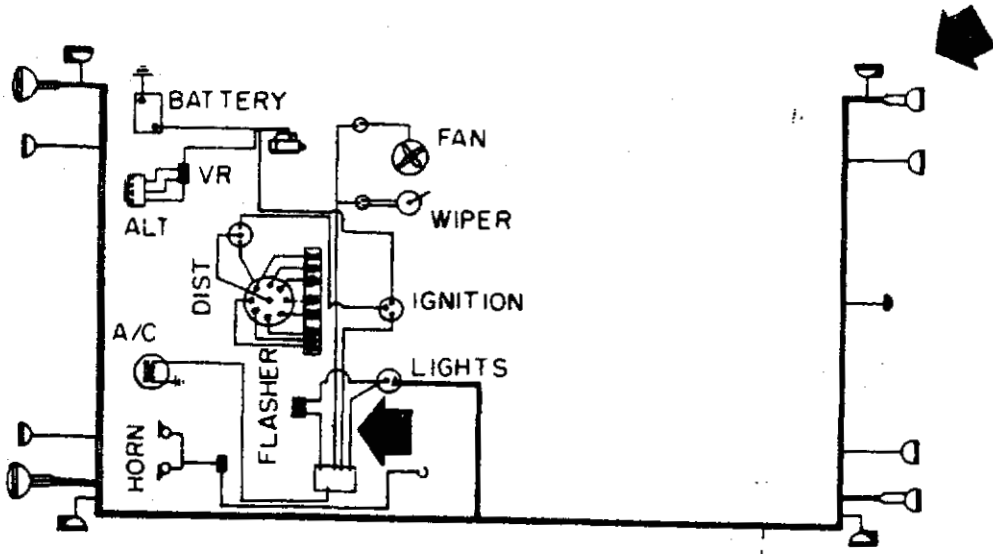


(c) 1 Flasher output {turn signal}
2 Right rear lamp { "off" }

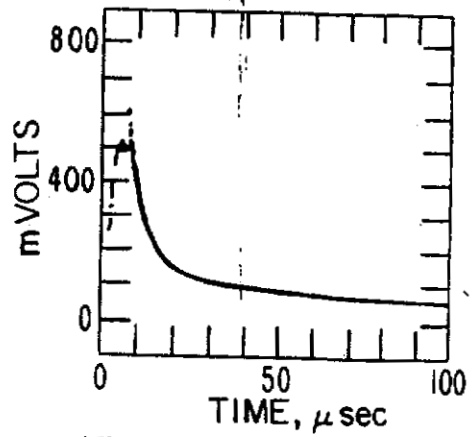


(d) Emergency flasher waveform ("on")

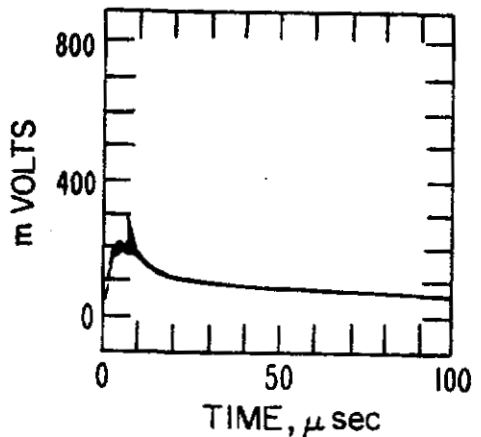
Figure 2.6 Turn Signal and Emergency Flasher Waveforms



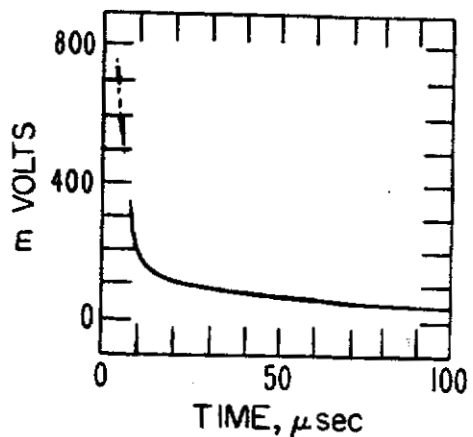
(e) 1 Turn-signal "on"
2 Lamp ground wire .



(f) Parking lamp wire (T.S., "off")



(g) Back-up lamp wire
(T.S., "off")



(h) Back-up lamp wire
(T.S., "off" - lamp removed)

Figure 2.6 (cont) Turn Signal and Emergency Flasher Waveforms

40%. Maximum amplitude reaches 10.2 V. Detailed information of the leading edge of the turn signal pulse is shown in Figure 2.6 (b) as measured at the flasher output and at the right rear lamp. The pulse has a rise time of about 20 μ s. A similar display of the trailing edge is shown in Figure 2.6 (c). Observe that the sweep time is 100 μ s/div in Figure 2.6 (c) compared to 20 μ s/div in Figure 2.6 (b). The data in Figure 2.6 (d) is a record of the emergency flasher output and shows a very similar "on" waveform as shown in Figure 2.6 (b) for the turn-signal. The data in Figure 2.6 (e) compares the pulse at origin (turn-signal output) to the signal developed across the ground wire at the rear lamp. The peak amplitude reached is about 190 mV.

The data in Figures 2.6 (f) thru 2.6 (h) show induced or coupled waveforms. The signal source is the trailing edge of the turn signal pulse (Figure 2.6 (c)). The induced signals are recorded from parking lamp and back-up lamp wires. Recorded amplitudes are as follows: 1) parking lamp, 600 mV; 2) back-up lamp (normal), 250 mV; and 3) back-up lamp (bulb removed), 700 mV. Removing the bulb simulates an abnormal condition that could occur with a broken wire or burned out bulb.

2.2.6 Transient Simulator

Several types of automotive power bus transients can develop from normal and abnormal functions in the automobile. These are described in Section 2.3. The abnormal transients and their effects are difficult to measure because of variations in voltage and characteristics.

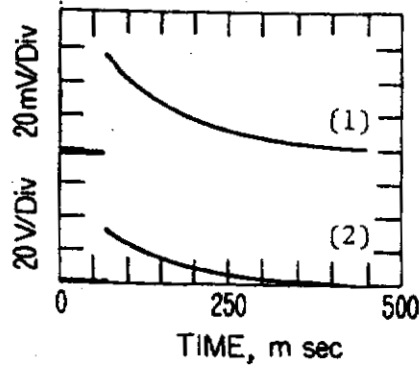
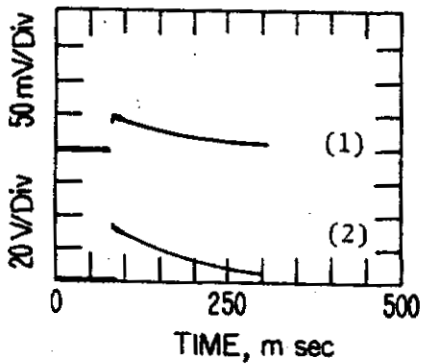
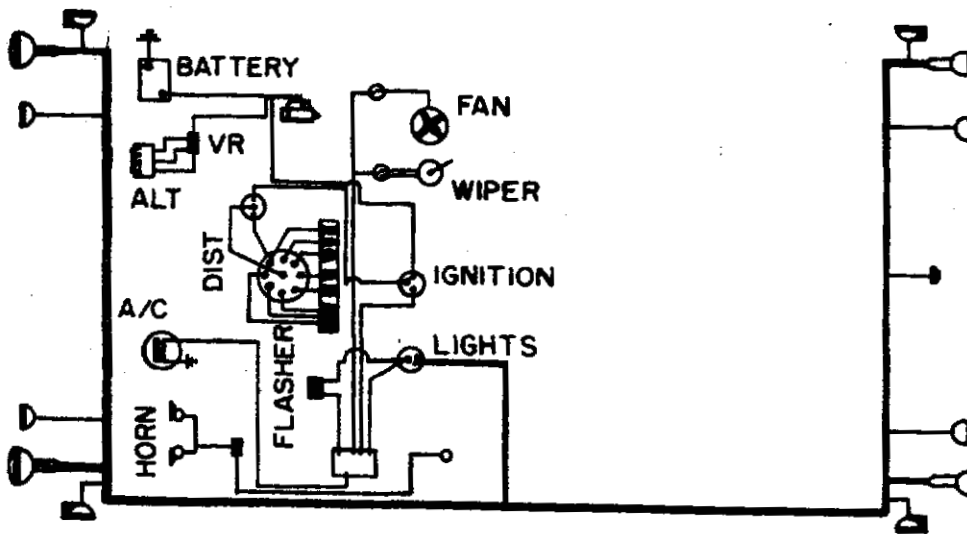
The Society of Automotive Engineers subcommittee on EMI Standards and Test Methods (1974) suggests the use of simulators and presents designs for construction of an alternator-dump transient simulator and field-decay transient simulator in a report of proposed test procedures for electromagnetic susceptibility of vehicle components. An alternator load-dump transient simulator similar to the proposed design (above) was constructed and used to generate the transient waveforms described here. The resultant waveform at the battery cable is that which occurs on a non-repetitive basis when the cable is loose or corroded or when a jumper cable is suddenly disconnected.

The recorded data using the simulator are shown in Figures 2.7 (a), (b), (c), and (d). In each figure, the lower trace is measured at the battery cable. The simulator voltage is allowed to reach 100 V and then it is dissipated into the vehicle power circuit with the battery cable disconnected from the battery. The upper trace in each figure is a coupled signal. The transient decay time is controlled by the simulator and lasts about 300 to 400 ms. The measured transient on the battery cable varies from 50 V to 4 V. These levels depend on the ignition switch load - with a higher measure transient associated with the lighter load. The coupled signal measured in the upper traces varies also with load. The coupled waveform measured at the right front turn-signal wire, recorded in Figure 2.7 (a), reaches a peak voltage of 50 mV. The data in Figure 2.7 (b), (c), and (d) were all recorded on the windshield wiper cable. They show increasing amplitudes with increasing ignition switch loading. The 160 mV level shown in Figure 2.7 (d) was recorded with the ignition, low-beam lights, and fan, all switched on.

2.2.7 Fan Motor

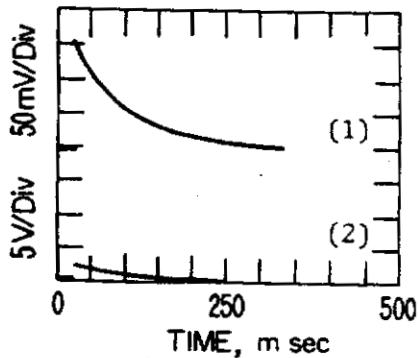
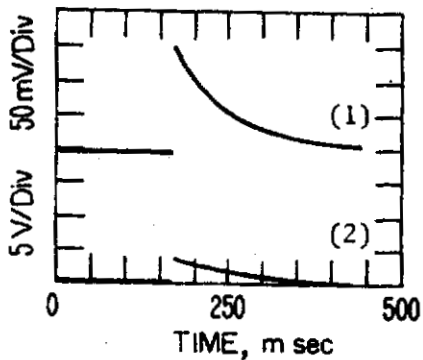
The fan motor drives the fan blade to provide for air circulation in the vehicle. This circulation can be through the air-conditioner, inside only, or air drawn from outside the vehicle. The motor has a high and low speed. The data recorded for this source is of two types. The first is a periodic waveform related to the rotation speed of the motor, and the second describes the transient and decay waveform generated at motor shut-off.

The data in Figures 2.8 (a) and 2.8 (b) show the motor waveform for the high and the low speeds, respectively. The high-speed waveform has a noise amplitude of 0.1 V recorded at the fan switch. The waveform has a basic period of 1.8 ms, which corresponds to a frequency of 555 Hz. The noise during low-speed operation yields a lower amplitude (30 mV) and lower period (3.5 ms), at a frequency of 285 Hz. The waveforms in Figure 2.8 (c) show the high-speed periodic signal recorded at the main power bus and at the right front parking lamp. The light switch was "on" during this recording, which means that the signal at that point



(a) 1 Right front turn-signal wire
2 Battery cable (simulated transient)

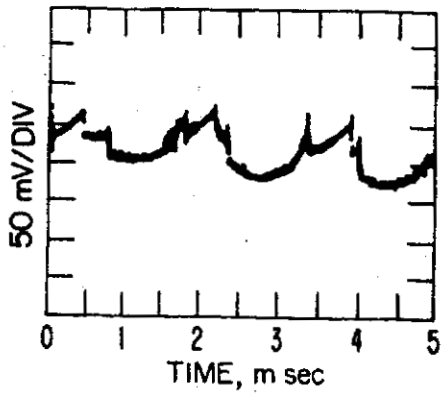
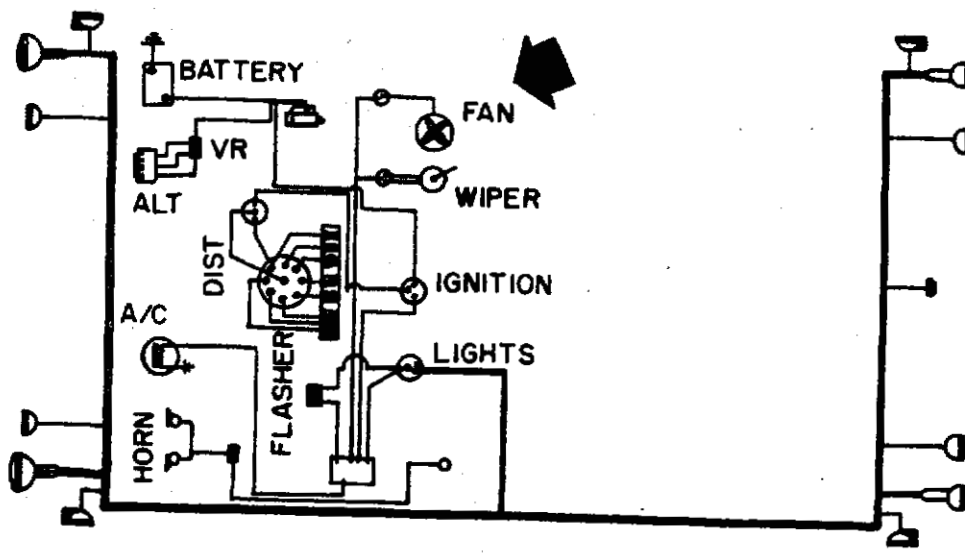
(b) 1 Windshield wiper (ignition on)
2 Battery cable (simulated transient)



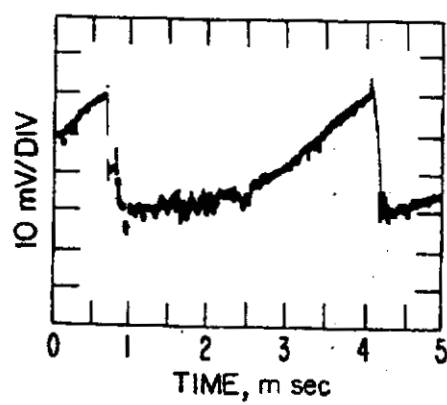
(c) 1 Windshield wiper (ignition and low beams on)
2 Battery cable (simulated transient)

(d) 1 Windshield wiper (ignition, low beam and fan on)
2 Battery cable (simulated transient)

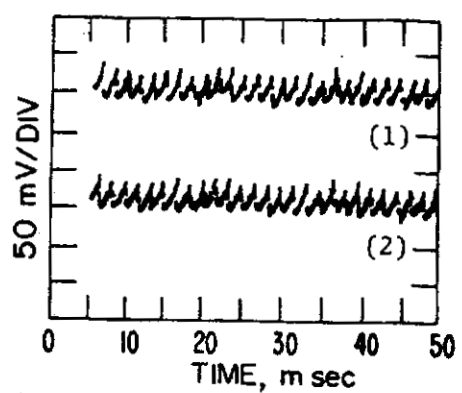
Figure 2.7 Transient Simulator Waveforms



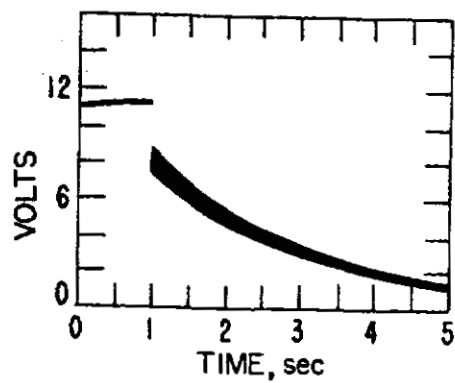
(a) Fan switch
(fan motor high speed)



(b) Fan switch
(fan motor low speed)

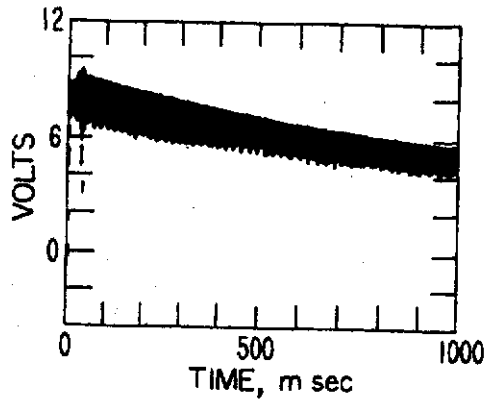
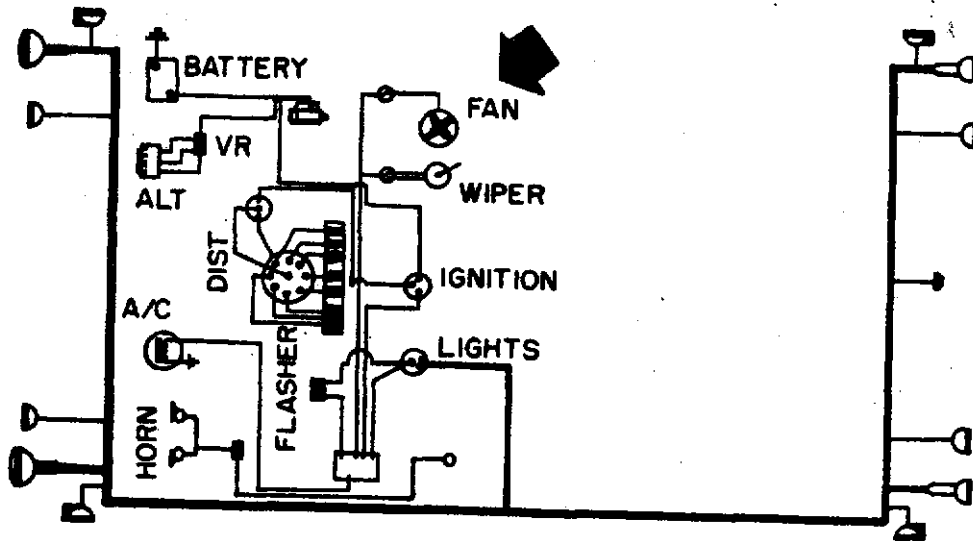


(c) 1 Main bus
(fan motor high speed)
2 Right front parking lamp

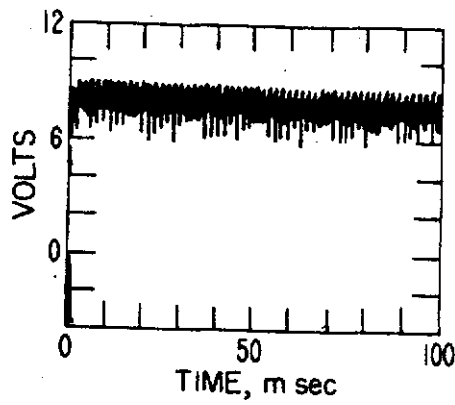


(d) Fan switch
(fan switched off)

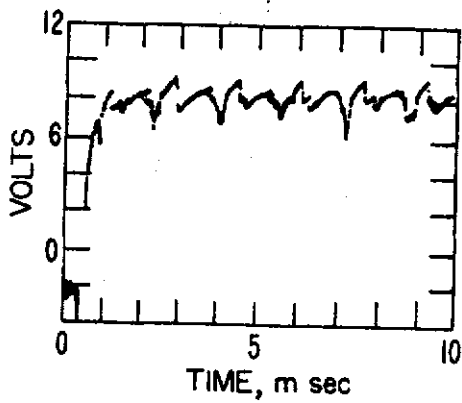
Figure 2.8 Fan Motor Waveforms



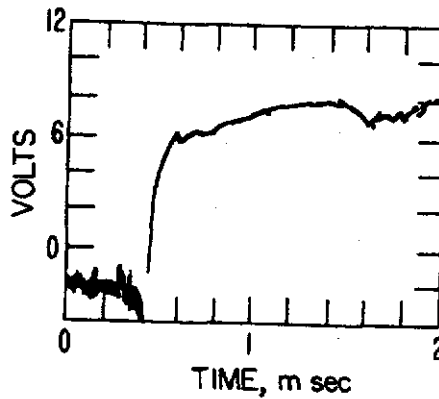
(e) Fan switch
(fan switched off)



(f) Fan switch
(fan switched off)



(g) Fan switch
(fan switched off)



(h) Fan switch
(fan switched off)

Figure 2.8 (cont) Fan Motor Waveforms

was a directly conducted signal rather than an electromagnetically coupled signal. The peak-to-peak amplitude of these signals is approximately 50 mV.

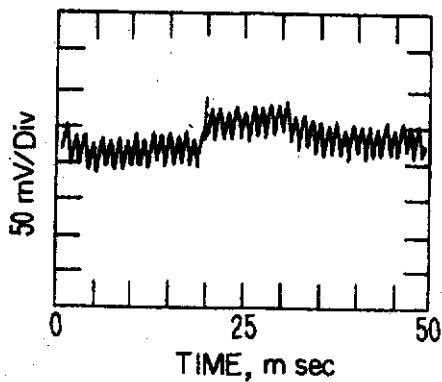
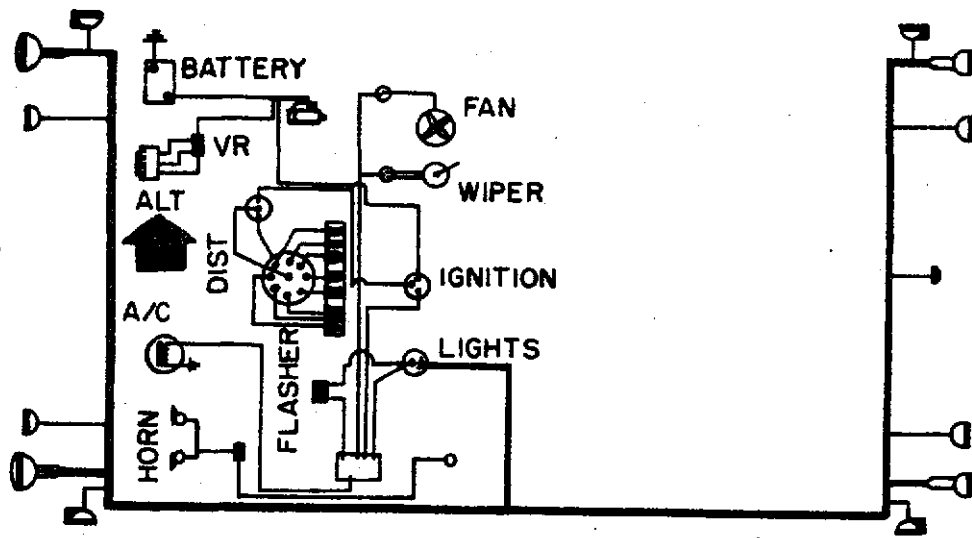
The signals displayed in Figures 2.8 (d) through 2.8 (h) are all related to the fan shut-off transient and stopping waveform. The waveform in Figure 2.8 (d) shows the switching action and a greater than four second slowdown period which follows the motor shut-off. Figures 2.8 (e), (f), (g), and (h) show portions of the decaying waveform, all triggered at shut-off and recorded with decreasing sweep speeds. These speeds are respectively 100 ms, 10 ms, 1 ms, and 0.2 ms per division. The important characteristics to be observed are the amplitude of the periodic waveform (greater than 6 V peak-to-peak) and the initial shut-off transient (-3V to +9V) followed by the slow decay. During the slowdown period, both the amplitude and period are changing. The amplitude decreases to zero and the period increases as the rotation rate (rpm) decreases.

2.2.8 Alternator

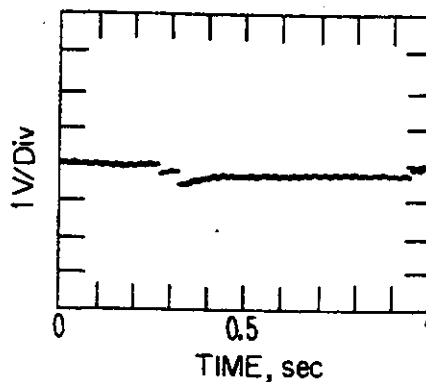
The alternator supplies direct current to the primary power supply, of which the battery is the storage (reserve) element. The magnitude of current supplied is controlled by the regulator and varies according to the load. The alternator is belt driven from the engine drive shaft pulley.

Two data sets recorded with the alternator driven from the drive shaft (engine running) are shown in Figure 2.9 (a) and 2.9 (b). In Figure 2.9 (a), the alternator ripple is of 0.1 V magnitude. Superimposed are ignition pulses at 20 and 50 ms from the beginning of the trace. The data in Figure 2.9 (b) shows the loading effect of switching on the external lights. The total "loading" effect with the lights on is .35 V. The switch goes through two positions when turned "on" and "off." This is evident in the trace.

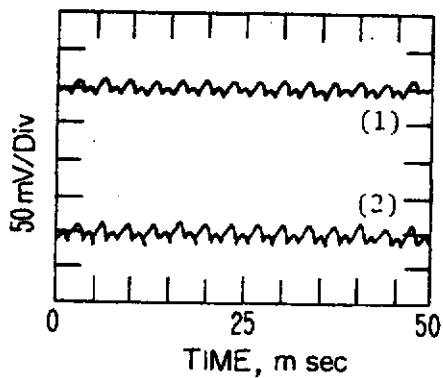
In an attempt to isolate the alternator signals (noise) from other engine related sources, several pictures were taken while driving the alternator with an external motor. These data are shown in Figures 2.9



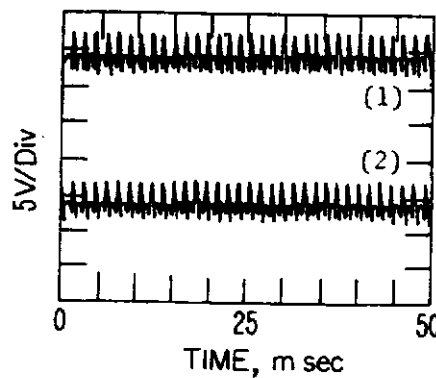
(a) Battery plus terminal (engine idling)



(b) Battery plus terminal (engine idling - light switch on-off)



(c) 1 Battery plus terminal (alternator driven externally)
2 Main bus



(d) 1 Battery plus terminal (alternator driven externally - no loading)
2 Main bus

Figure 2.9 Alternator Waveforms

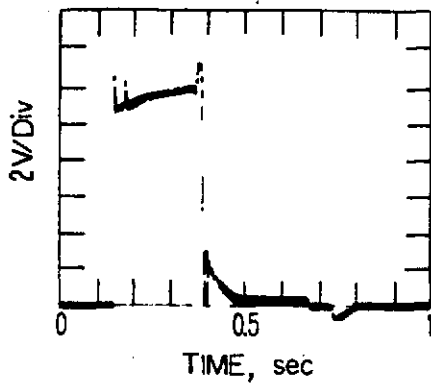
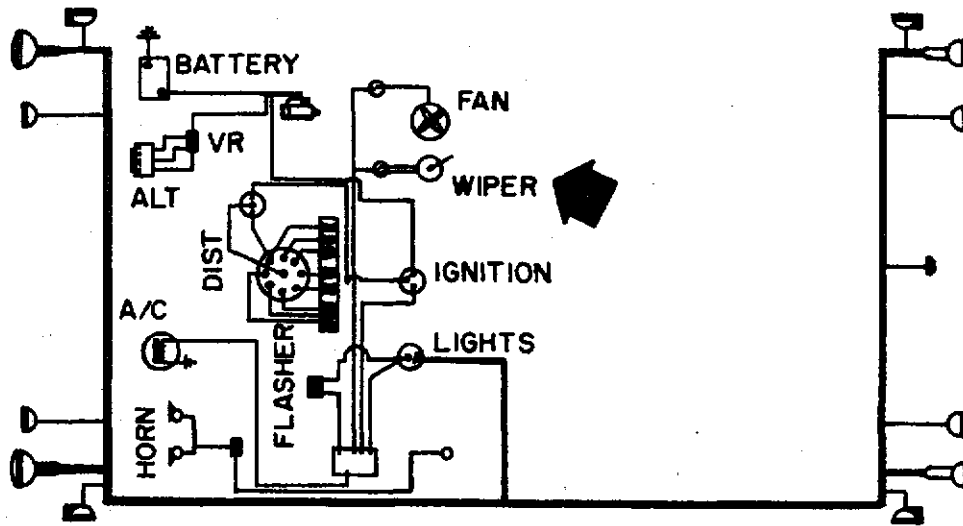
(c) and 2.9 (d). The data in Figure 2.9 (c) is with the alternator charging the battery (under normal loading). Approximately 30 mV of ripple are observed at the battery (+) terminal and on the main bus. Figure 2.9 (d) represents recordings taken during abnormal conditions. These data represent signals generated as a result of a loose battery cable connection. This could occur through improper installation and/or wear or by mishandling. The waveform in Figure 2.9 (d) represents a condition where the field was excited by a momentary contact of the battery cable to the battery post. This created a condition of no appreciable load on the alternator and no filtering effect (which the battery usually provides). This condition is somewhat similar to electrolyte boil-off. In this figure peak amplitudes of 17 V are reached and a peak-to-peak ripple of 6 V is observed.

2.2.9 Windshield Wiper Motor

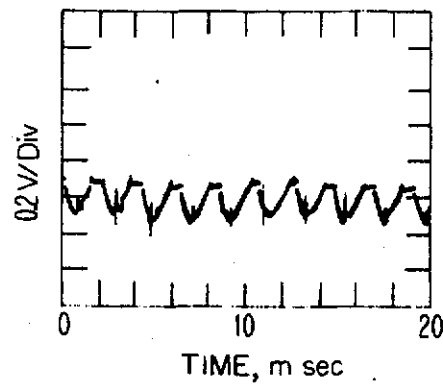
The windshield wiper motor drives the windshield wiper arms. It has a high speed, a low speed, and a motor reverse action to recess the arms when the wipers are turned off. The data in Figure 2.10 (a) show the waveform that appears at the windshield wiper motor when it is switched "on" and then "off." The amplitude scale is 2 V/div and the sweep is .1 s/div. A small transient is generated when the motor is switched "off". The waveform in Figure 2.10 (b) is generated with the motor running at high speed. This waveform has a period of 2.2 ms and peak-to-peak amplitude of about 0.3 V. Short bursts of noise are associated with each period or cycle. The waveforms shown in Figures 2.10 (c) and 2.10 (d) are recorded with the motor running at slow speed. Amplitudes at the battery plus terminal and the ignition main bus are 40 mV and .4 V, respectively.

2.2.10 Horn

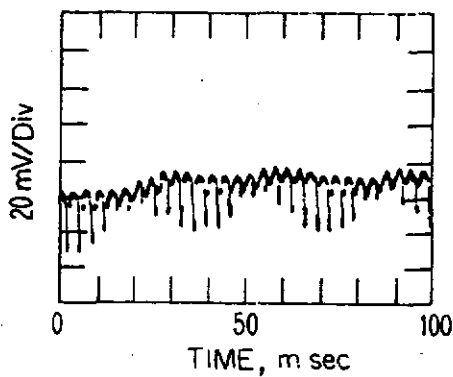
The horn is actuated with a horn ring or button and produces an audio warning or alert signal. The waveforms shown in Figure 2.11 are recorded at the horn itself and on the main bus. The ripple caused by the vibrator circuit as measured at the horn power terminal is shown in



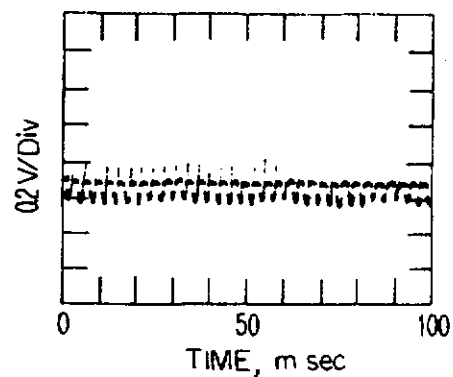
(a) Windshield wiper motor switched on-off



(b) Windshield wiper motor (high speed)

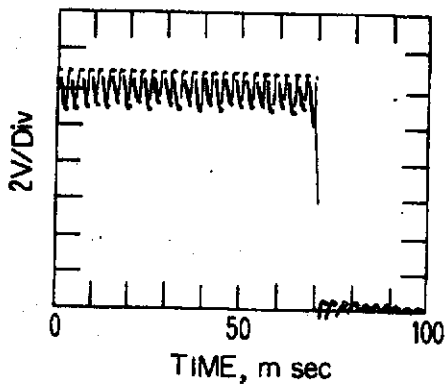
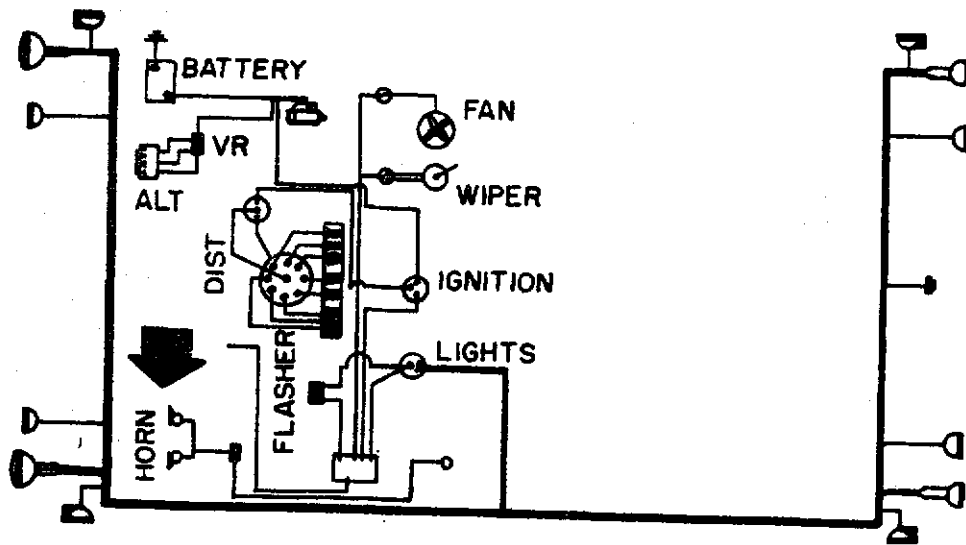


(c) Battery plus terminal (motor slow speed)

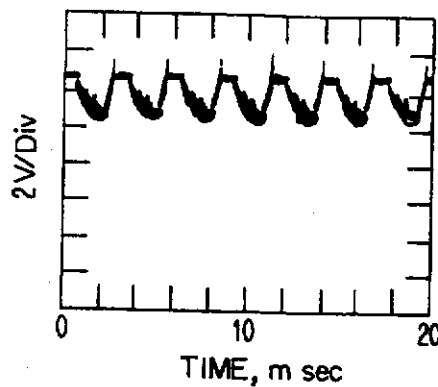


(d) Main bus (motor slow speed)

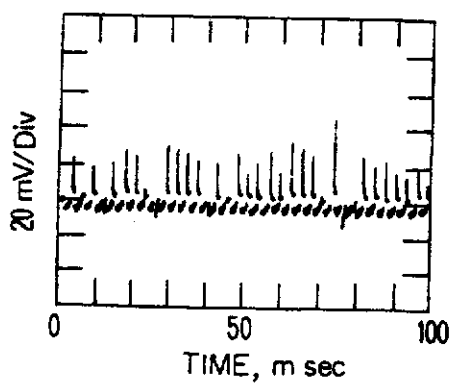
Figure 2.10 Windshield Wiper Motor Waveforms



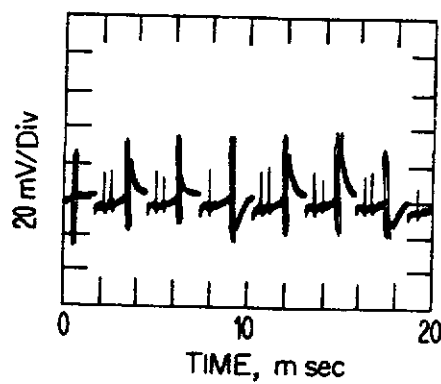
(a) Horn circuit
(on-off)



(b) Horn circuit
(horn sounding)



(c) Main bus
(horn sounding)



(d) Main bus
(horn sounding)

Figure 2.11 Horn Waveforms

Figure 2.11 (a). The magnitude of this ripple is about 2.2 V (p-p) and the repetition cycle is approximately 2.8 ms. An rf noise of 4 V to 6 V is apparent in the waveform of Figure 2.11 (b).

The features of these signals measured at the main bus are shown in Figure 2.11 (c) and 2.11 (d), where rf noise bursts of 60 to 80 mV can be observed.

2.2.11 General Vehicle Noise (Broad-band Noise)

A spectrum analyzer (Model HP 8553) was used to record the spectral intensity of signals emitted from several sources within the test vehicle. The following figures show a calibration and the results of the tests.

Figure 2.12 (a) is the calibration record. The markers are from left to right: 1) zero reference marker, 2) 30 dBm at 30 MHz, 3) 1st harmonic at 60 MHz, and 4) 2nd harmonic at 90 MHz. The frequency scale is from 0 to 100 MHz and the amplitude reference is 0 dBm at the top of the picture. The amplitude scale is logarithmic.

The data in Figures 2.12 (b) thru 2.12 (d) are taken at the main bus for various operating modes.

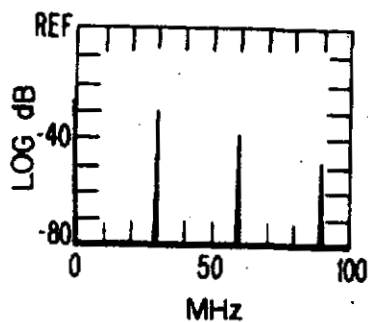
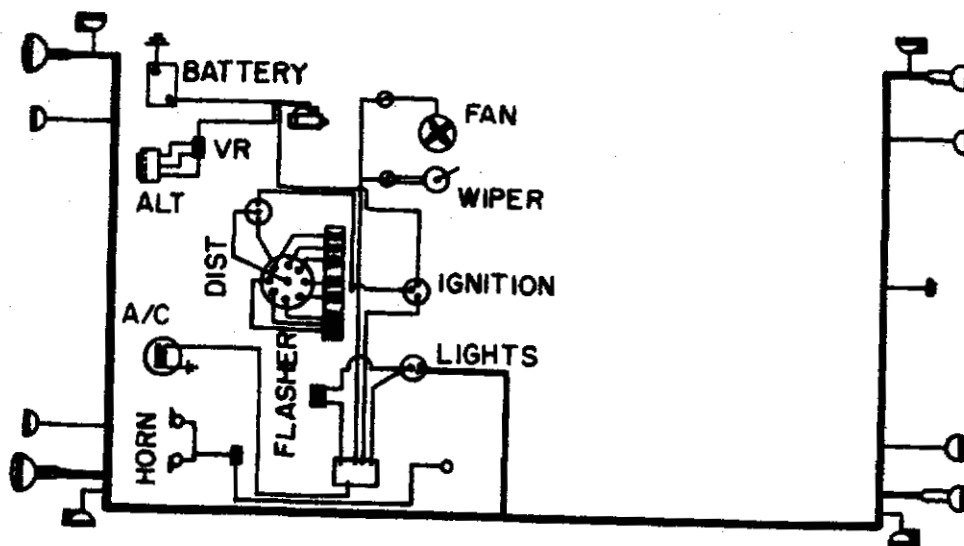
With the ignition key warning buzzer sounding, amplitudes above -50 dBm are recorded across the entire 100 MHz band. Peaks above -30 dBm are observed below 10 MHz. Other strong peaks are at 25 MHz and near 65 MHz. These data are in Figure 2.12 (b).

The amplitude distribution recorded with the horn sounding, in Figure 2.12 (c), shows amplitude levels of about -50 dBm between 15 and 50 MHz. In this record, as was the case for the ignition key buzzer, much energy is spread across the band.

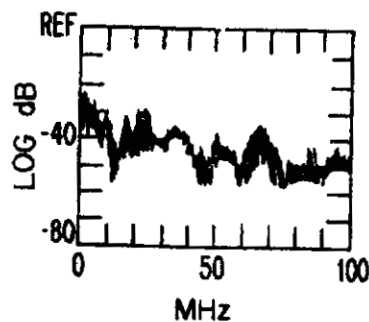
The data in Figure 2.12 (d) are recorded with the engine idling. It is assumed that the principal noise sources are the ignition system and the alternator. A general decrease in amplitude with increasing frequency is observed.

2.3 Power Supply Variations and Severe Transient Characteristics

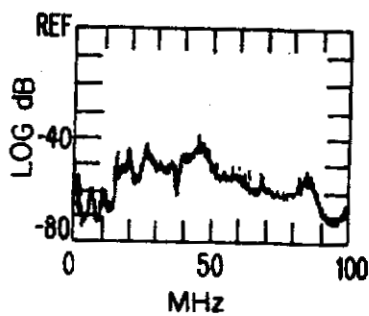
A task in the earlier study (Espeland, et al., 1975) was to assess the internal electrical environment of the motor vehicle. The resultant



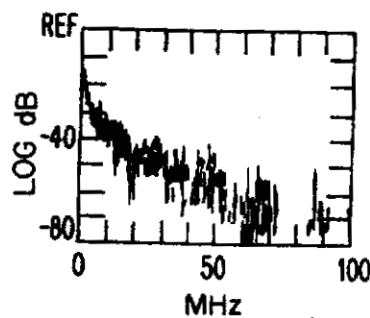
(a) Calibration
(-30 dBmW @ 30 MHz,
30 kHz B and width)



(b) Main bus
(ignition key
warning buzzer)



(c) Main bus
(horn sounding)



(d) Main bus
(engine idling)

Figure 2.12 General Vehicle Noise (Broadband)



search indicated that the information available dealt mainly with variations and regulation of the automotive primary power supply and with determination of expected maximum transients and switching voltages. Certain other data dealing with general noise backgrounds also were available.

Considering that these subjects had been quite well researched, these measurements were not repeated in this study. However, it is considered advisable to include summaries of that study in this report in order that a complete picture of the motor vehicle electrical environment be presented here. The following material is taken from the 1975 study where the references cited are the original data sources.

2.3.1 Voltage Regulation

The normal operating range (McCarter, 1974) of the line voltage for a vehicle is between 10 and 16 V dc. Abnormal line voltages are caused during cold cranking; e.g., at -20 F, the line voltage can drop to 4.5 V dc. Other abnormal conditions occur during jumper starts, when garages and emergency road service facilities often use 24 V and sometimes 36 V sources. These voltages may be sustained for as long as five minutes. They may even be accidentally applied in reverse polarity.

There is another condition which will cause abnormal line voltage; it requires equipment malfunction. Failure of the alternator voltage regulation may cause the line voltage to rise to 17 V. If this condition exists for a long period of time, the electrolyte in the battery may boil away. Voltages of 75 to 130 V have been observed when the electrolyte boiled off. This problem is usually detected and corrected before the extreme voltages are reached.

Table 2.4 summarizes these automotive voltage regulation characteristics.
Table 2.4 Automotive Voltage Regulation Characteristics (After SAE, 1974)

Condition	Voltage
Normal operating vehicle	16 V max 14.2 V nominal 10 V min
Cold cranking at -20 F (-29 C)	4.5 V
Jumper starts	24-36 V for five min. Reverse polarity
Voltage regulator failure	17 V
Battery electrolyte boil-off	75 V - 130 V

2.3.2 Transients

Three principal types of automotive power line transients are encountered. These are the load dump, inductive switching, and alternator field decay.

Load dump transients occur when the alternator load is abruptly reduced. This sudden reduction in current causes the alternator to generate a voltage spike. This creates a worst case situation for two reasons:

- 1) the battery acts like a capacitor and absorbs the transient energy, and
- 2) a discharged battery creates the greatest single load on the alternator, and to abruptly remove it causes greatest possible load change.

Transient voltages as high as 125 V have been reported with rise times of 100 μ s. Decay times of 100 ms to 4.5 s have been reported.

Inductive load switching transients are caused by solenoid and motor fields switching. These occur when an inductive accessory is turned off. The severity is dependent upon the magnitude of the switched load and the line impedance. These transients take the form of a large negative peak followed by a dampened positive excursion.

Alternator field decay transients produce negative pulses which occur after the field is disconnected from the battery when the ignition switch is turned off. The amplitude is dependent upon the voltage regulator cycle at the time of shut down and varies from -40 to -100 V with a duration of 200 ms. Table 2.5 summarizes these three types of transient characteristics.

Table 2.5 Automotive Transient Voltage Characteristics
(After McCarter, 1974)

Type	Max. Amplitude	Rise	Decay	Remarks
Load dump	125 V	100 ms	0.1-4.5 s	Damage potential
Inductive switching	-210/+80 V		320 μ s	Logic errors
Alternator field decay	-100 V	2 ms	200 ms	Occurs at shut-down only

2.3.3 Electrical and Accessory Noise

This noise will normally have a repetition rate which is dependent upon the characteristic of the interfering device or engine. A summary of automotive, electrical, continuous-noise characteristics (including ignition noise) is shown in Table 2.6.

2.4 Chassis DC Resistance Measurements

Grounding and bonding is a topic covered in Volume 3 of this report. It treats the problem of establishing low-impedance paths to a reference within the power and signal circuits of an automobile. Of interest in this regard is an assessment of how well selected vehicle chassis points offer low-impedance paths to the power supply ground. Such a set of measurements was made and a description of the technique used and the results obtained are given below.

A block diagram of the test equipment is shown in Figure 2.13. The instruments used were a power supply, an ammeter, and a digital voltmeter. By setting the power supply to deliver one ampere to the test point, the voltmeter is calibratable to a tenth of a milliohm. The data presented in Table 2.7 has been rounded to the nearest milliohm.

The data in Table 2.7 has been grouped by chassis function such as ground, ground wires, housings, frames, and axles. There is likewise a clustering of the data values within these function descriptions. The results are self-evident. The listed values are averages and are referred to the engine at the ground strap bolt for a ground lead between the engine and the frame. The battery ground (negative post) is tied to another point on the engine.

The significance of these values is that they represent the actual ground value at these several points and indicate the better points at which to establish a ground when adding circuits.

Table 2.6

SUMMARY OF AUTOMOTIVE ELECTRICAL CONTINUOUS NOISE CHARACTERISTICS
(After SAE, 1974)

TYPE	MAX. AMPLITUDE	DURATION	REPETITION RATE	REMARKS
Normal Accessory Noise	1.5 V Peak	Frequency	50 Hz to 10 KHz	Total Pulse Height is 3 V-pp
Normal Ignition Pulses	3 V Peak	10 to 15 μ s	Dependent on engine speed	Total Pulse Height is 6 V-pp
Abnormal Ignition Pulses	75 V Peak	~90 μ s	Dependent on engine speed	
Transceiver Feedback	15 to 20 mV	Carrier	Frequency	Sinusoidal

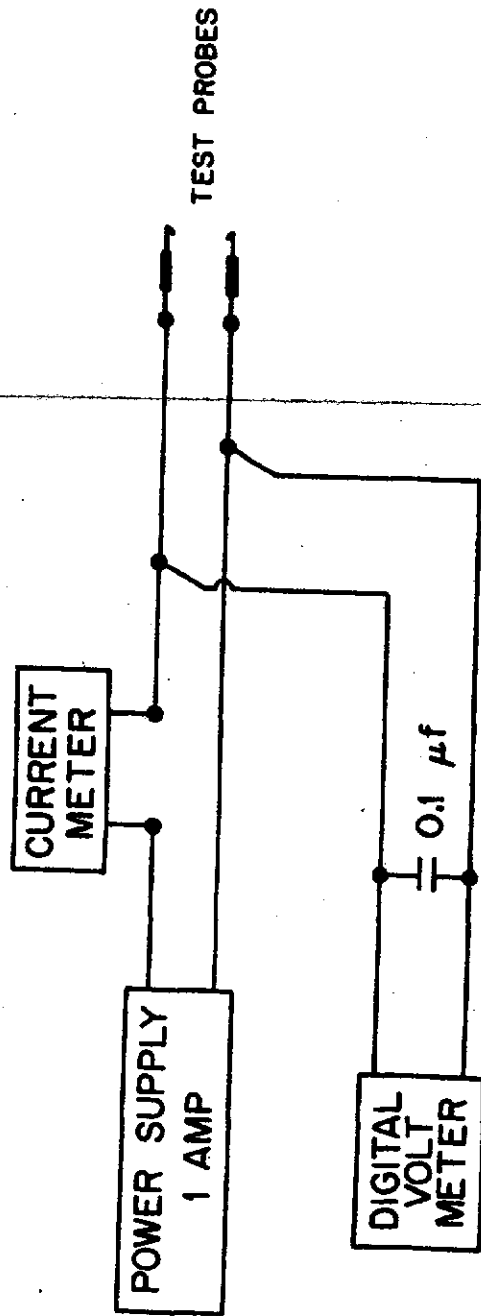


Figure 2.13 Test Equipment

Table 2.7 Chassis DC Resistance Measurement

FUNCTION	LOCATION	RESISTANCE (MILLI-OHMS)
Ground	1.) Starter Solenoid (Right Front Fender)	3
	2.) Battery Post (Negative)	1
	3.) Engine-To-Fire-Wall Cable	2
	4.) Instrument Panel	2
	5.) Hood Grounding Tab	1
	6.) Head Lamp Ground Lug (Left)	3
	7.) Head Lamp Ground Lug (Right)	3
	8.) Tail Lamp Ground Lug (Left)	2
	9.) Dome Light Ground	3
Ground Wires	1.) Tail Lamp Ground Wire (Left)	22
	2.) Tail Lamp Ground Wire (Right)	13
	3.) Park Lamp Ground Wire (Left)	22
	4.) Park Lamp Ground Wire (Right)	43
	5.) Head Lamp Ground Wire (Left)	22
Housing	1.) Tail Lamp Housing (Left)	25
	2.) Tail Lamp Housing (Right)	24
	3.) Cigar Lighter Housing	16
Frame	1.) Alternator	1
	2.) Rear Seat Frame	1
	3.) Front Seat Frame	1
	4.) Front Door (Left)	1
	5.) Rear Door (Left)	4
	6.) Tailgate Door	6
	7.) Hood Hinge	4
	8.) Front Bumper	10
	9.) Rear Bumper	9
Axles *	1.) Rear Axle (Right)	104 (0.104 ohms)
	2.) Front Axle Shaft (Right)	1416 (1.416 ohms)
	3.) Front Wheel (Right)	1440 (1.44 ohms)
	4.) Front Wheel (Left)	1060 (1.06 ohms)

*Vehicle not equipped with a radio - the grounding modification kit (axles) was not installed.

3.0 FIELD-TO-WIRE COUPLING ANALYSIS

An area of concern regarding electromagnetic interference of motor vehicle electronic subsystems is the susceptibility of these devices to external electromagnetic fields. These fields could be generated in external environments such as those described in Section 2 of the earlier study (Espeland, et al., 1975). Identified as sources of potential interference were broadcast stations, radars, mobile radios, power transmission lines, and others. Various internal source fields have also been identified.

As an aid to assessing the potential EMI from fields (external to the subsystem), a Field-to-Wire Coupling Analysis Program (FTWCAP) was used to model motor vehicle subsystem wiring and a specific analysis has been done to assess levels of interference to an Air Cushion Restraint System (ACRS) from transmitted signals typical of a mobile radio unit. The frequency range explored was 100 to 200 MHz and the transmitter is rated at 100 W peak output.

This section describes the computer program, its adaptation to analyze coupling to automotive cabling, and the results obtained from this analysis as a function of frequency, shielding, aperture size, distance from source to aperture, and cable length. Other parameter changes not included could be number of wires and termination impedance.

3.1 The FTWCAP Model

The electromagnetic Field-to-Wire Coupling Analysis Program (FTWCAP) is a modular portion of a computer program developed by McDonnell-Douglas Aircraft Company to predict and analyze electromagnetic interference between avionics systems on aerospace vehicles (Bagdnor, et al., 1971). The program is an analytic tool to aid the user in establishing intravehicle electromagnetic compatibilities and is adaptable to nonavionic systems on land vehicles. The Wire-to-Wire Compatibility Analysis Program (WTWCAP), another modular portion of this same program, was used in the 1975 study to evaluate potential wire-to-wire coupling of conducted signals in automotive cable bundles.

The FTWCAP predicts electromagnetic interference where there is radiative coupling from external electromagnetic fields into internal wiring. The fields usually enter the vehicle through apertures (gaps or openings) in the vehicle metal body and couple into wires immediately adjacent. Thus, this form of interference normally occurs when bundle routing necessitates positioning portions of a wire bundle close to openings in the vehicle skin. Most road vehicles have many such openings. Some of these air gaps occur around the hood, the front grill, and the fenders. Some degree of coupling can occur from reflected signals under the car chassis where cabling may be exposed in the downward direction.

The analysis begins by using an electromagnetic wave propagation model to calculate the rf power density from each radiating antenna at each aperture exposing the bundle. The program then uses WTWCAP for a complete description of the wires with respect to wire routing and types of termination. The induced voltage across or current through the wire terminations are determined using a transmission line model. The interference induced in the wire loads is then compared with the load susceptibility to obtain the EMI margin. The EMI margin is only a relative indicator of potential interference. If the susceptibility level of a receptor is unknown, an arbitrary susceptibility level may be indicated. In this specific exercise, the analysis of the air-cushion restraint system cable, only the received signal data are presented for discussion. The EMI margin levels are not used because the subsystem susceptibility levels were not known.

The input data required by the program include: (1) definition of the three-dimensional grid which describes the geometry of the vehicle; (2) location and bandwidths of transmitters; and (3) aperture data, which includes identification, location, connector locations, and length and width of each aperture. A maximum of ten apertures is allowed for each bundle. The FTWCAP is stored on magnetic tape (or disk file) for easy access to the computer. The input data are punched on computer cards and read by the computer at execution time.

The output of the FTWCAP consists of a summary of the input data,

an rf power density section, and a EMI margin section. The propagation data for each aperture and frequency is given in the rf power density section. This includes the rf power densities in watts per square meter, propagation path code, and shading from wings and fuselage. The EMI margin section provides the information pertinent to the transmission line calculation. For each receptor pin, the EMI margin, total received signal (magnitude and phase), shielding attenuation used, and the susceptibility level are given.

3.2 Program Adaptation

The input data categories defined above indicate the types of data needed to exercise the FTWCAP model. Rules and formats for specifying these data are set forth in the program. Because much of the input data is peculiar to a particular subsystem, a specific example has been chosen to demonstrate the program capabilities and to analyze the coupling that resulted. The candidate subsystem chosen for the adaptation and implementation of the FTWCAP program was an Air Cushion Restraint System (ACRS). The ACRS unit modeled for analysis consists of a bumper impulse detector, two electroexplosive devices (EED's), a monitoring circuit, and interconnecting cables. Upon impact, switches in the series-wired sensors close and provide a low impedance path for current from the battery to the EED's. The EED's fire and inflate the air cushions. The important characteristics of the system for analysis in the model are: 1) the interconnecting cable wire parameters, 2) the routing of this bundle within the vehicle, and 3) the terminating impedances of the individual wires in the bundle. For this FTWCAP example, the bumper sensor can be represented as an impedance. The following paragraphs and figures set the rationale for selecting the input parameters used in this analysis.

Figure 3.1 shows the major components of the system and the placement of the components in a road vehicle. Of particular interest to this program and the analysis of this system is the routing of the approximately 11 foot long interconnecting cable near the hood-to-fender aperture. It is this aperture-to-cable relationship that is analyzed in this example.

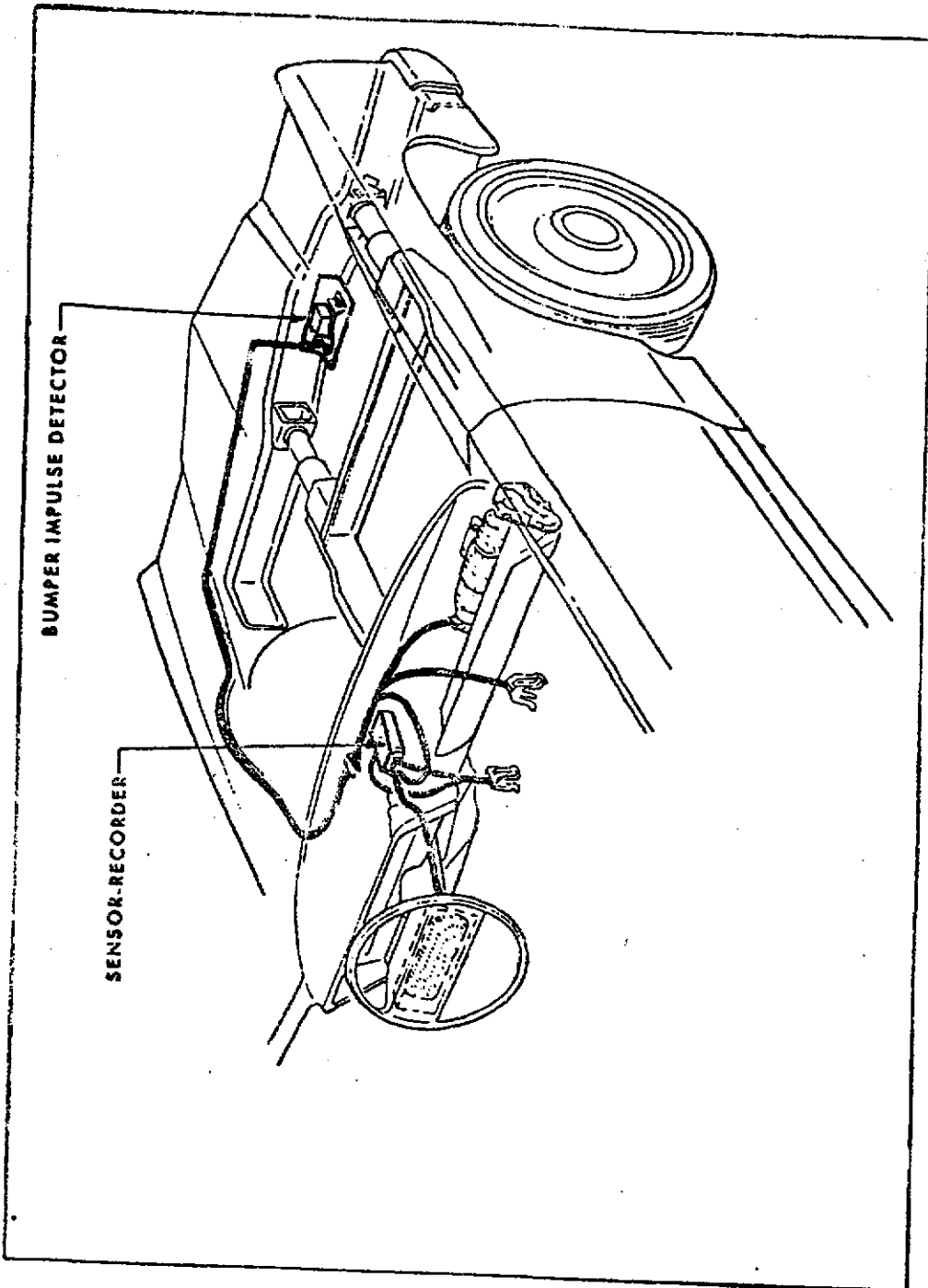


Figure 3.1. Air Cushion Restraint System

A descriptive diagram of the cable bundle is shown in Figure 3.2. It consists of four wires (two each in two shielded cables) that connect the bumper detectors to the EED's. The overall length is set at 132 inches. The wires are designated as A, B, C, and D, and the terminations and interconnections are shown in the figure. The cable end No. 1 is at the sensor-recorder and cable end No. 2 is at the bumper detector. The 1.5 ohm resistor between connector B_1 and C_1 represents the equivalent resistance of the two EED's and series diodes. The 620 ohm and 430 ohm resistors shown at connector No. 2 are the open switch resistances of the two sensors. The .02 ohm resistance at A_1 represents the internal resistance of the battery.

To orient the transmitter, the vehicle aperture, and the cable relative to each other, a three dimensional grid is established. The computer program designates butt line, water line, and fuselage line as distances. Figure 3.3 is used to show references and distances for the vehicle model. The key locations are given as BL, WL, FS, which corresponds to distance in inches along the butt line, water line, and fuselage, respectively. These are convenient terms in the program, reflecting the aircraft usage. Using this notation, (-10, 25, 60) places end No. 1 of the cable at 10.0 inches to the left of the butt line reference, 25 inches above the water line, and 60 inches to the rear from the fuselage reference. The transmitter is placed on an artificial wing, as dictated by the computer model, the tip of which is 100, 1.0, 70. The aperture center is at -20, 25, 40 and the end No. 2 of the cable is at -.7, 0, 0.

3.3 Coupling Analysis

The scenario for this analysis was to assume a transmitter operating in the 100 to 200 MHz frequency range with an output power of 100 W. These values were selected to match the operating frequency range and power output of some mobile radio units. The transmitting antenna which radiates the field is located 60 in. to the right of the vehicle and 70 inches back from the front bumper. In the model, the transmitter is placed at the tip of an artificial wing to represent a source on another vehicle adjacent to the study vehicle.

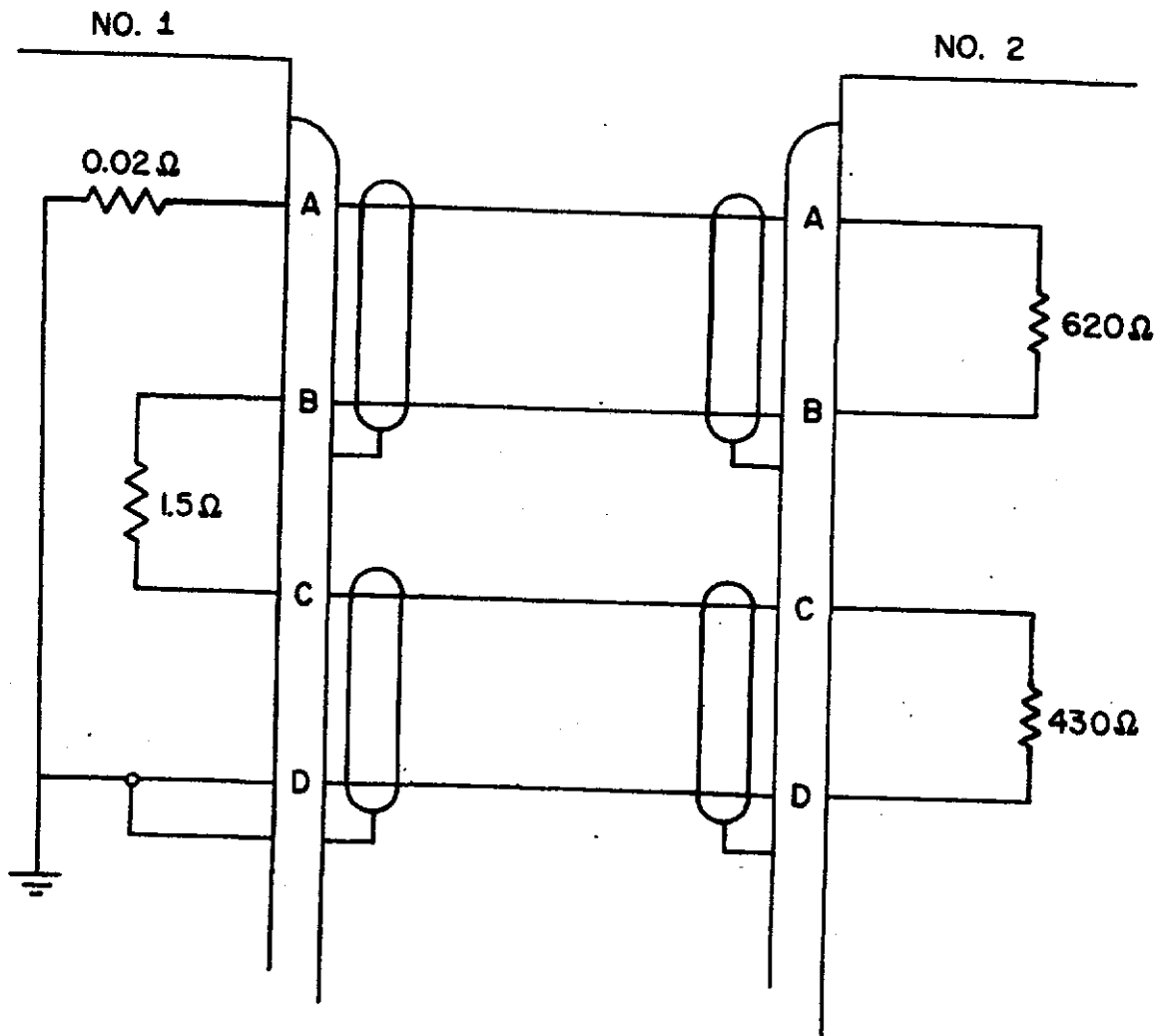


Figure 3.2 Cable Bundle Diagram

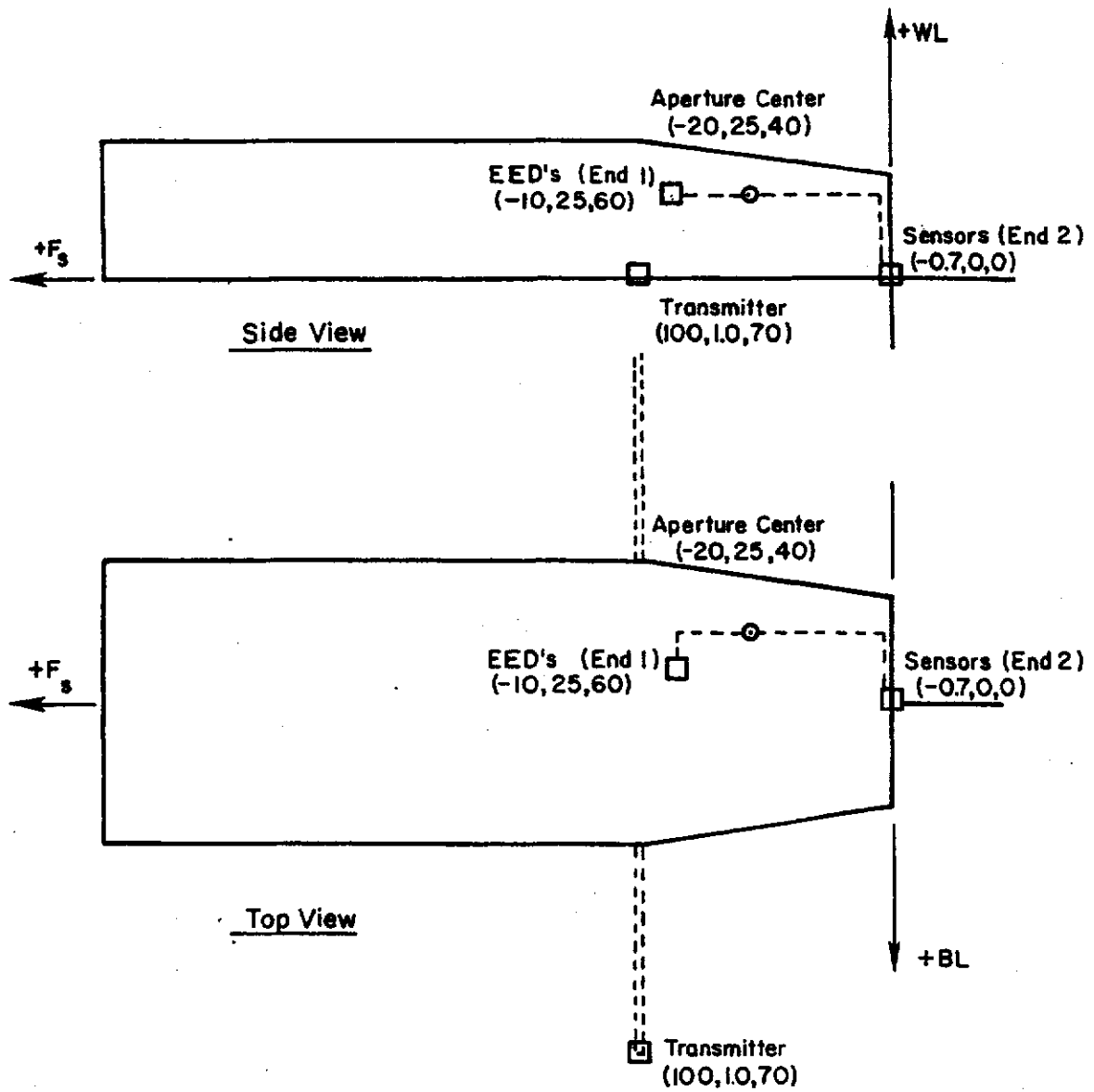


Figure 3.3 Vehicle Model Reference Grid

Only one of the shielded cables in the bundle was analyzed. The load points for which data is calculated were designated as A_1 , A_2 , and B_1 of the upper pair of wires in Figure 3.2. Their respective terminating impedances are .02 ohms, 620 ohms, and 1.5 ohms. The physical locations of the cable ends and the aperture center point were selected to yield (by internal computer program calculation) an overall cable length of 132 inches. This is the approximate length of the bundle. The designated cable ends and aperture center shown in Figure 3.3, produced an overall length of 131.6 inches, placing the aperture center 23.5 inches from cable end 1 and 108.1 inches from cable end 2.

With the aperture center, cable ends, cable length, and impedance parameters fixed as described above, a number of program evaluation runs were made varying the operating frequency and aperture dimensions. The results of these computer runs are listed in Tables 3.1 and 3.2. The following data are included:

- 1) power density at the aperture (W/m^2),
- 2) fuselage (body) shielding effect (dB),
- 3) wire cable shielding effect (dB),
- 4) received signal at the designated load points (dB μ V/MHz).

The first three sets of data (Table 3.1) are functions of frequency only, while the last set (Table 3.2) is a function of frequency and aperture size (dimensions).

For analysis, these data have been plotted in Figure 3.4 through 3.9. The data in the figures show the effect of fuselage shielding on the power density and the effect of cable shielding on the received signal. Also, the received signal variations are dependent on aperture size and dimensions, transmitting frequency, aperture-to-cable end length, and termination.

The two sets of data in Figure 3.4 represent a plot of the rf power density at the aperture as a function of frequency, and the amount of signal attenuation due to body shielding, also as a function of frequency. This shielding is the result of body metal obstructing the direct path between the transmitting antenna and the aperture. Curve

Table 3.1 Power Density, Fuselage Shielding, and Cable Shielding

Frequency (MHz)	Power Density (W/m ²)	Body Shielding (dB)	Cable Shielding (dB)
100	.4895	-3.2	-44.9
112.5	.4682	-3.4	-44.2
125	.4490	-3.6	-43.5
137.5	.4315	-3.8	-42.9
150	.4154	-4.0	-42.3
162.5	.4006	-4.1	-41.8
175	.3868	-4.3	-41.3
187.5	.3740	-4.4	-40.9
200	.3621	-4.6	-40.5

Table 3.2 Amplitude of Received Signal at Designated Load Points (dB μ V/MHz)

Frequency (MHz)	Aperture 4 x .2 (in)		Aperture 4 x 2 (in)		Aperture 40 x 2 (in)		Aperture 40 x 20 (in)	
	A ₁	B ₁	A ₁	B ₁	A ₁	B ₁	A ₁	B ₁
100	71.2	99.5	72.7	100.2	85.2	108.9	90.1	107.5
112.5	68.4	103.6	68.8	104.8	79.9	118.4	77.0	124.4
125	60.8	125.0	61.7	131.9	77.0	122.4	83.0	116.4
137.5	72.1	104.8	73.5	105.3	87.2	116.2	78.5	121.3
150	74.1	107.0	74.2	108.0	79.4	141.6	82.0	117.1
162.5	68.1	114.8	68.8	117.0	88.8	115.1	86.4	115.8
175	72.9	112.0	74.2	111.8	72.8	126.3	74.4	132.5
187.5	74.7	110.4	76.2	111.2	85.2	109.1	92.2	112.0
200	74.7	111.9	75.1	113.2	83.4	118.9	79.4	128.7

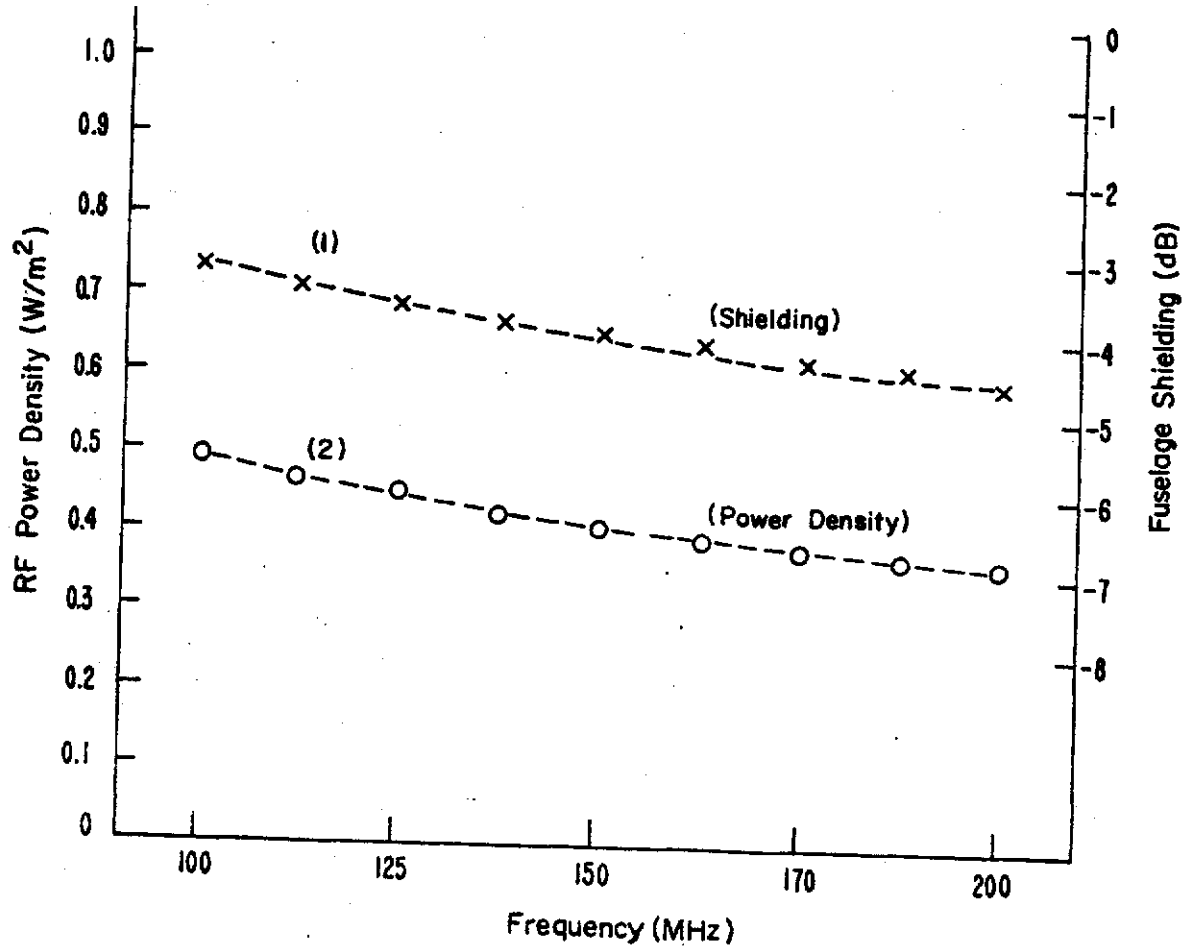


Figure 3.4 Power Density and Shielding Attenuation vs. Frequency

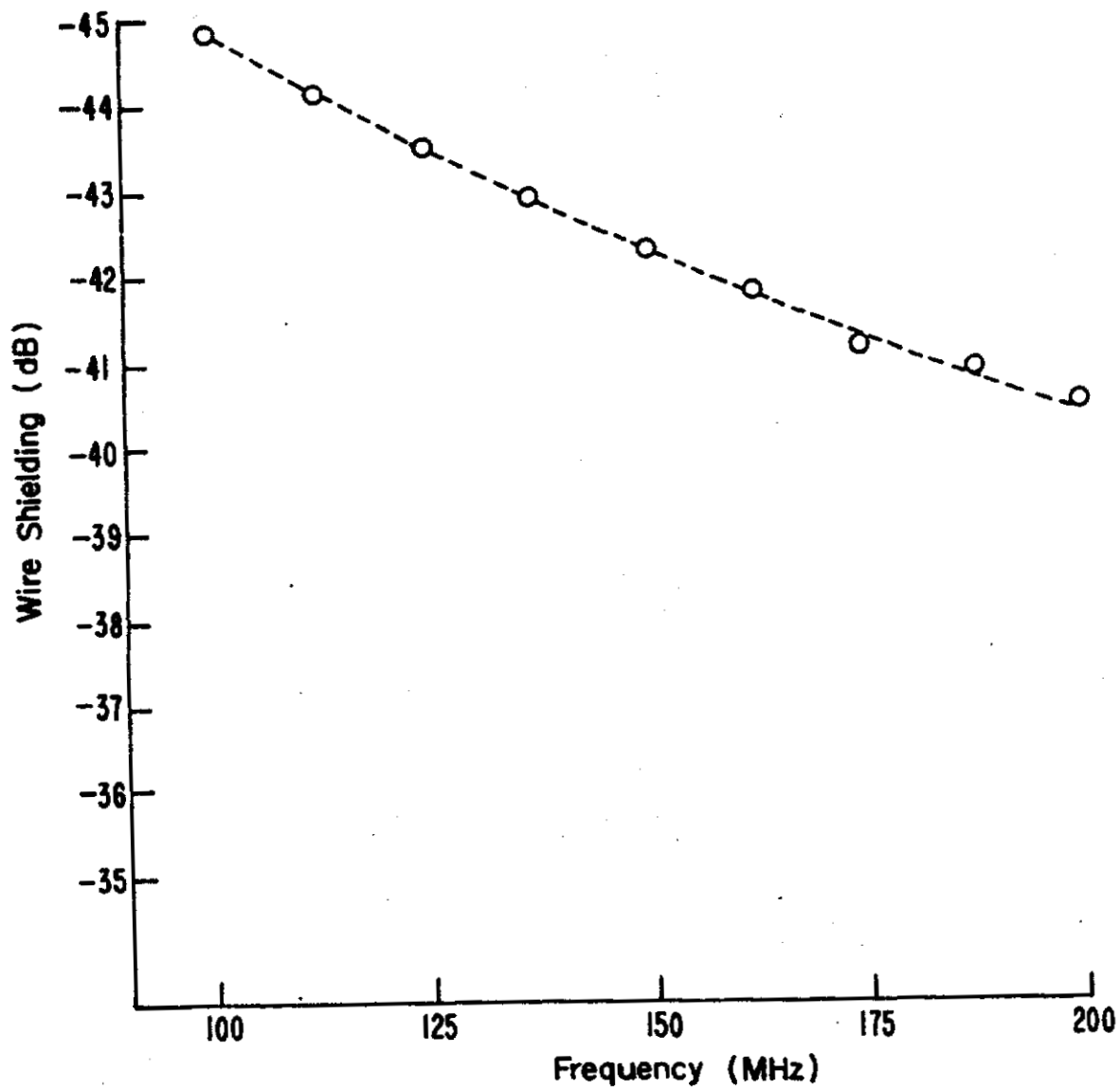


Figure 3.5 Wire Shielding Attenuation vs. Frequency

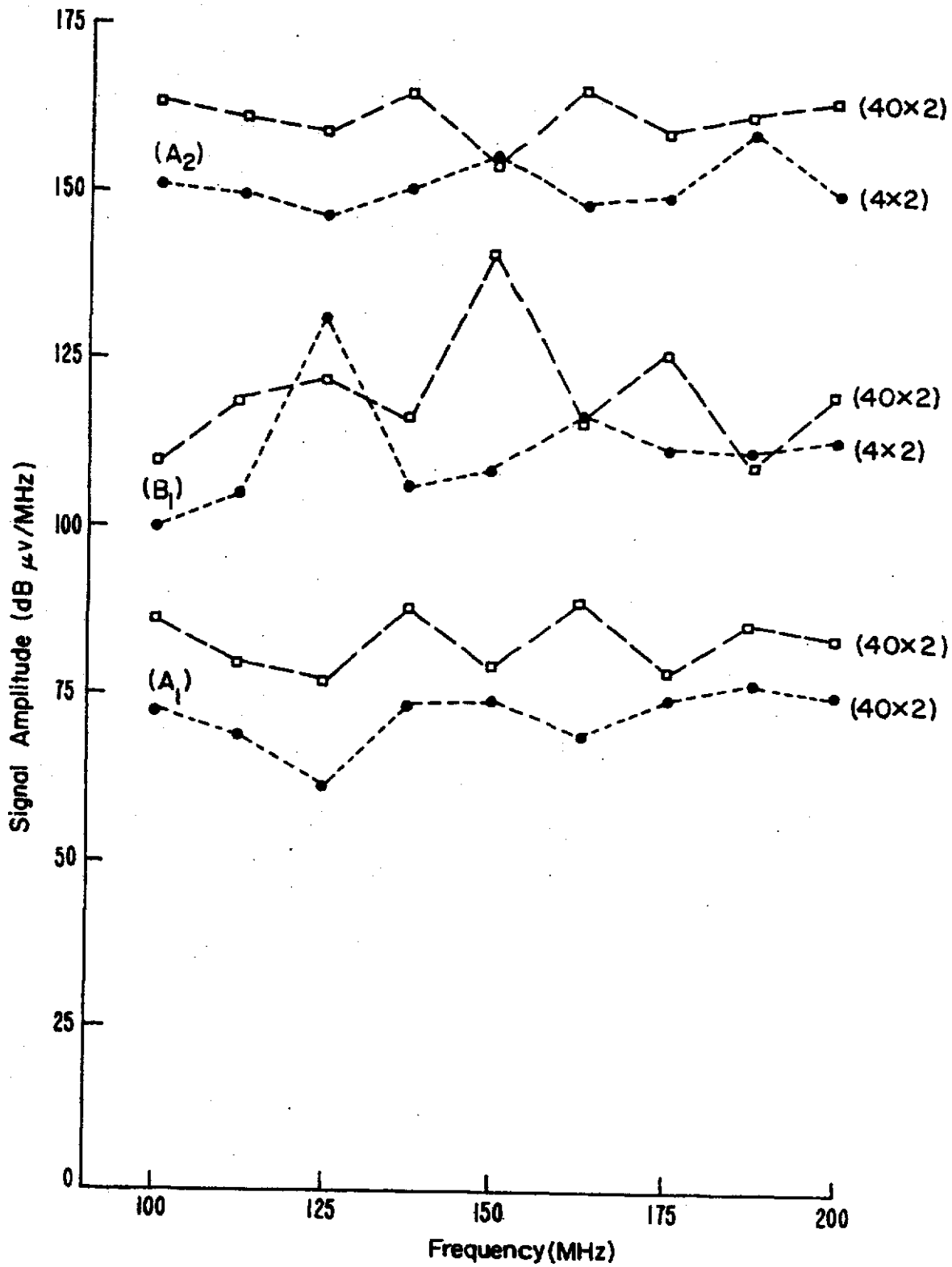


Figure 3.6 Amplitude of Received Signal vs. Frequency (wire ends A₁, B₁, and A₂)

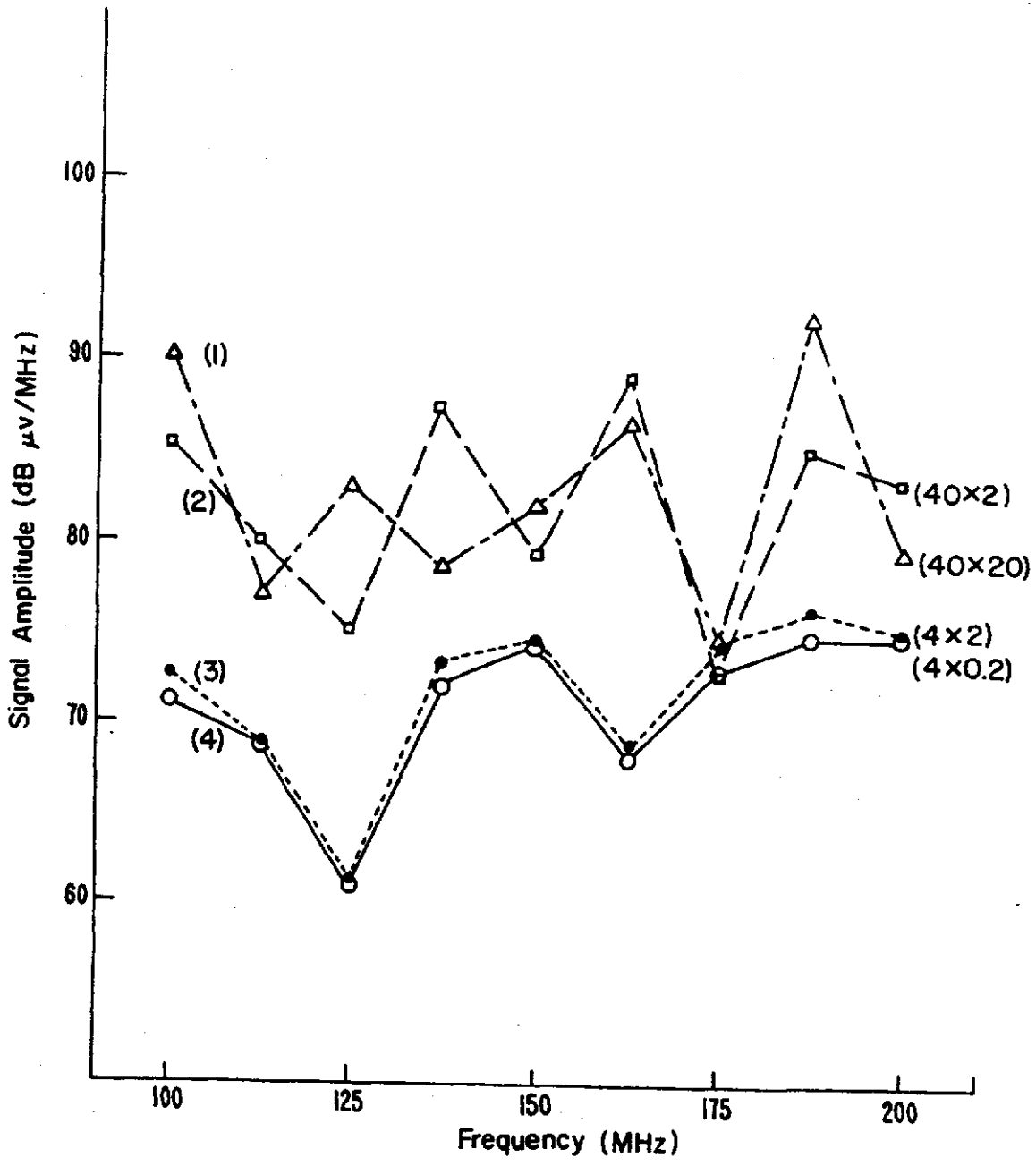


Figure 3.7 Amplitude of Received Signal vs. Frequency (wire end A₁)

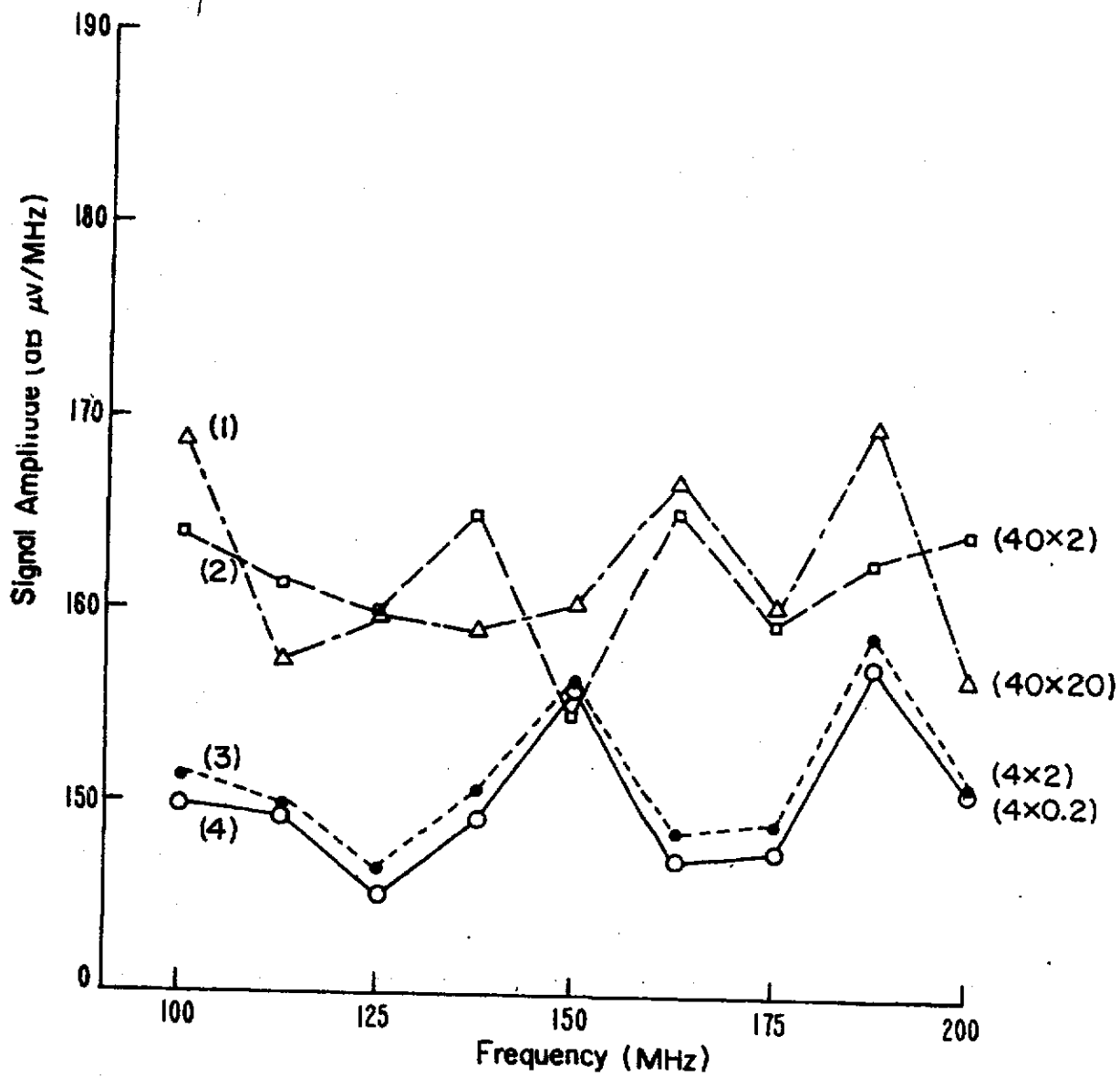


Figure 3.8 Amplitude of Received Signal vs. Frequency (wire end A₂)

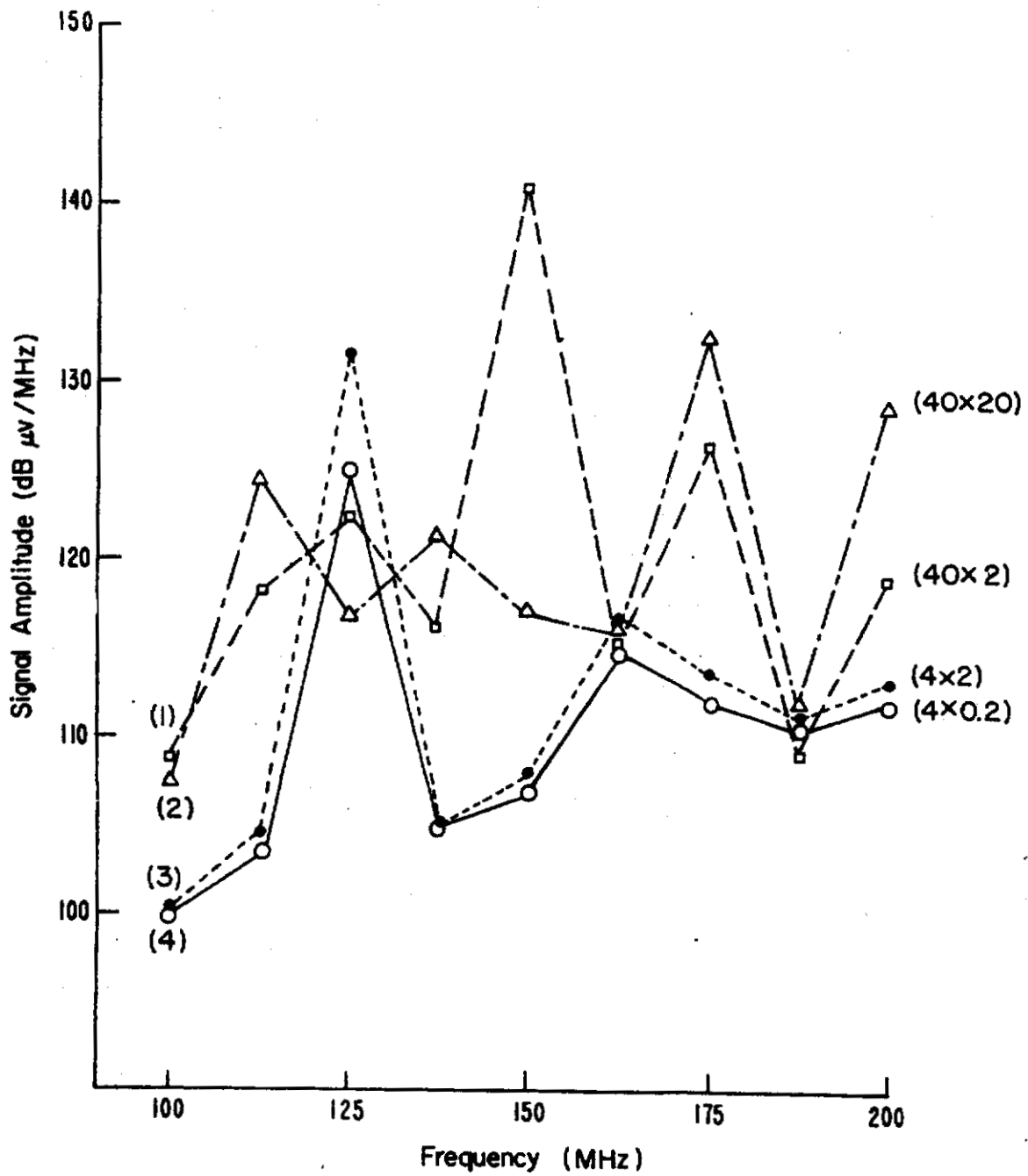


Figure 3.9 Amplitude of Received Signal vs. Frequency (wire end B₁)

number 1 shows the amount of shielding varying from a -3.2 dB to -4.6 dB in the frequency range from 100 to 200 MHz. The change in power density over the same range is from $.4895 \text{ W/m}^2$ to $.3621 \text{ W/m}^2$. The ratio of these two densities is 1.3 dB, indicating that the decrease in power density at the aperture is directly attributable to body shielding.

The curve in Figure 3.5 shows the effectiveness of a shielded cable on the net received signal. The received signal is attenuated by more than 40 dB over that of an unshielded cable. The shielding effectiveness varies slightly with frequency. It is less at the higher frequencies.

The data in Figures 3.6 through 3.9 represent the aperture and frequency dependence of the received signals at the load points A_1 , A_2 and B_1 . (Respective impedances indicated in Figure 3.2.) Figure 3.6 represents received signal in (dB $\mu\text{V}/\text{MHz}$) for aperture sizes (4 in X 2 in) and (40 in X 2 in) at 100, 112.5, 125, 137.5, 150, 162.5, 175, 187.5, and 200 MHz. These data demonstrate variations as a function of frequency and aperture size. These variations will be discussed using Figure 3.7 thru 3.9. The main feature of the data in Figure 3.6, is the apparent grouping of signal level as a function of termination. The smallest received signals are predicted at A_1 (.02 ohms), the next higher at B_1 , (1.5 ohms), and the highest at A_2 (620 ohms).

A second display of the data for A_1 , A_2 , and B_1 on a larger scale along with data for apertures sizes 4 in X .2 in and 40 in X 20 in is shown in Figures 3.7, 3.8, and 3.9. Three effects are apparent. The first is the frequency dependence with as much as 30 dB variation observed across the band. Calculations at frequencies between those for which data was analyzed may reveal even greater variation. A second effect that is apparent from the data is the grouping of results associated with fixed aperture length. This is particularly observable in curves (3) and (4) for which the length was 4 in. If an average level were calculated for a given aperture across the frequency band, the average level of curves (1) and (2) would exceed the average level of curves (3) and (4) by about 10 dB. This effect on signal level is attributable to the increase in size of the larger dimension.

The third observation of the characteristics of the data, and the one most useful for specific application, is the relative signal amplitude as a function of frequency. There is the expected strong interdependence between frequency and aperture size. An example in the data of Figure 3.9 is seen in comparing the signal levels at 125 and 150 MHz for the 4 in X 2 in aperture (curve 3) and the 40 in X 2 in aperture (curve 2). At 125 MHz, the received signal is 131.9 dB μ V/MHz in curve 2 and the received signal in curve 4 is 122.4 dB μ V/MHz. At this frequency, the signal for aperture 4 in X 2 in is 9.5 dB greater than for aperture 40 in X 2 in. At 150 MHz, these relative signal levels are reversed, with the signal for 40 in X 2 in being 33.6 dB greater than for aperture 4 in X 2 in.

One additional program evaluation run was made to demonstrate the effect of overall cable bundle length on signal coupling. This evaluation was for only the 4 in X 2 in. aperture. The results are shown in Figure 3.10, where the coupled signal levels of a 100 in cable are compared to the coupled signal levels of the 132 in cable (the 132 in length was used in all the previous analyses). The 110 in length of cable represents a one-sixth reduction in overall cable length. This data shows the expected definite frequency dependence of coupled signal on the cable length.

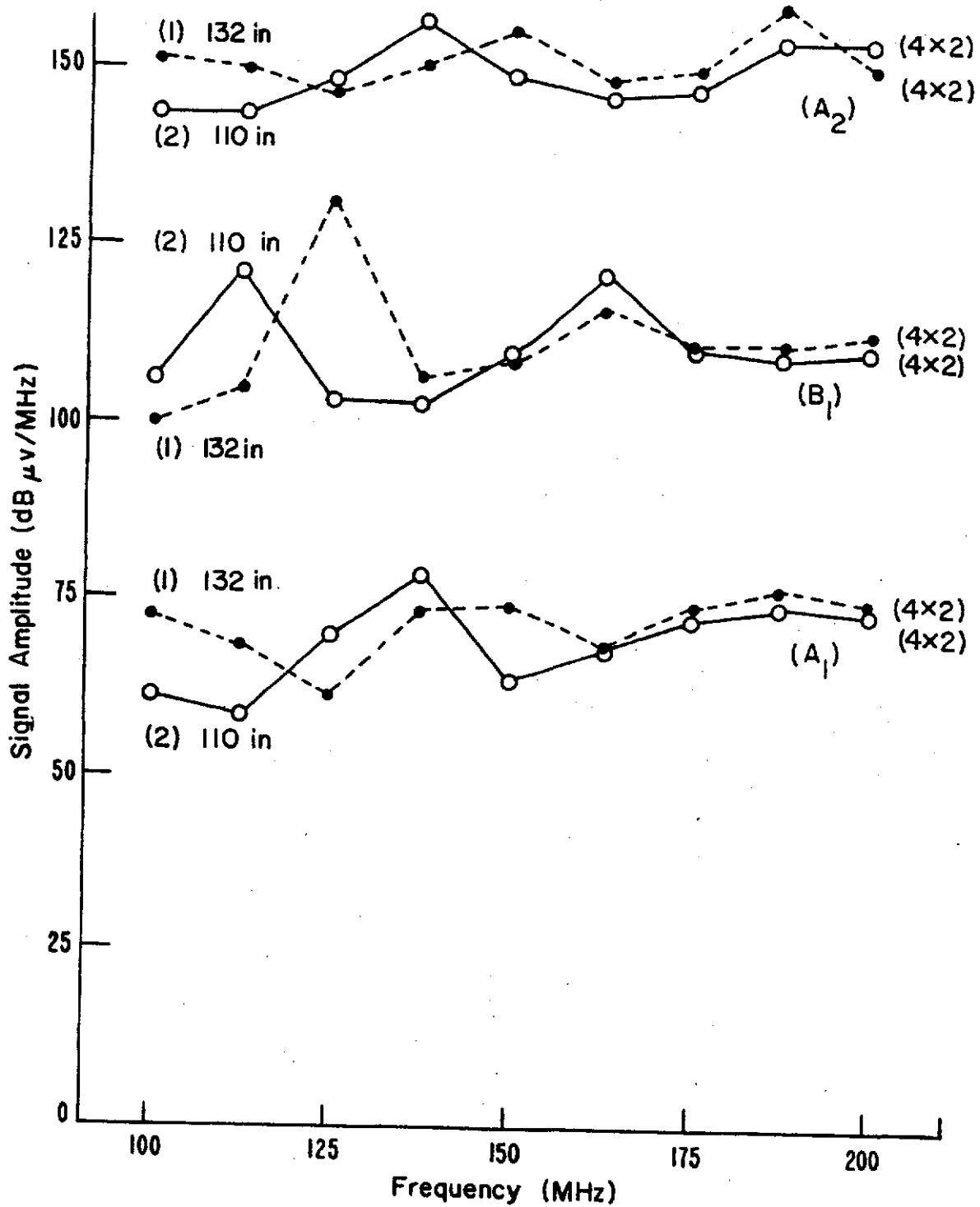


Figure 3.10 Amplitude of Received Signal vs. Frequency (132 in. and 110 in.)

4. SUBSYSTEM SUSCEPTIBILITY TESTING

The circuit analysis models, electromagnetic coupling analysis programs, and component specification surveys used in the earlier study (Espeland et al., 1975) established device sensitivity and noise immunity ranges for various types of electronic components. This information is very useful in the selection of devices and components for design, but does not address performance criteria of subsystems in the automotive environment. It was for this reason that a subsystem susceptibility testing effort was included in the present program. This testing effort is directed toward conducted interference only.

Conductive susceptibility tests were performed on a speed control subsystem and an antiskid braking module. Interference signals used in the tests included rf pulses and dc pulses (square wave and exponential transients). Potentially susceptible points were selected for interference signal injection and appropriate upset points were monitored to determine system performance degradation resulting from the injected interference signals. Normal system operating modes were simulated for the tests.

This section reports the preparation and procedures required for this type of susceptibility evaluation, on the test plans and methodology used, and the results obtained.

4.1 Testing Preparation and Procedures

Most present day automotive electronic subsystems are either factory installed or are sold as add-on devices in kit form. Because some of these devices are in a developmental stage of application to automobiles, the functional diagrams and schematics which are normally available for most electronic equipment are proprietary and unobtainable. Consequently, much searching and many contacts were required to obtain the modules, subsystems, and support literature necessary to prepare properly a subsystem for susceptibility testing.

4.1.1 Procurement of Equipment and Descriptive Documentation

The modules and subsystems can often be obtained directly through automobile dealers, whose repair and maintenance departments may have these items in stock or can order them. Some equipments are available only as factory installed items and others are prototypes and are unavailable through normal purchase channels.

Documentation and information about any specific system to support the test planning and equipment preparation necessary to interface with the test facilities and to conduct useful tests is not generally sold with the equipment. This information must be obtained through special request to the manufacturer, through a search for articles in the open literature, or by tracing schematics and functional diagrams from the equipment itself. Even this last approach is not always feasible because of coded identification of components.

4.1.2 Preparation of Subsystems for Interface and Operational Synthesis

There are two ways to test subsystems. One method is to evaluate performance and degradation during normal operation in a vehicle. This technique requires considerable preparation of portable test equipment, both to sense malfunctions and to determine the cause and evaluate the severity of these malfunctions. A second technique is to place the subsystem in an available test facility where well-controlled tests can be made. The second technique, however, requires a means for operational synthesis. The modules and subsystems that are being tested must be made to function in those modes for which tests are desired. In each of these modes, the test facility generates the desired interference signals and records the degree of functional performance obtained from the unit under test. In the case of the speed control unit, a vacuum pump was used as substitute for the manifold vacuum. Also, it is necessary to provide external power and to simulate any initializing and control functions. Such equipment as power supplies, signal generators, pumps, etc. are used to provide the simulated conditions for bench testing.

4.1.3 Test Series

Two further steps leading to subsystem testing are the interface with the facility and the preparation of the computerized control program. The interface should in most cases be straightforward, because the necessary requirements have been planned for in the preparation for interface activity described above. The Direct Drive Facility at AFWL in Kirtland, N. M. used in the evaluation of the subsystems described below has provision for computer control of the actual test runs. A short computer program was prepared, debugged and then used to control the test cycle and the recording of the results. This program controls the sequence of events, the levels, duration, and range of the various test parameters used. A diagnosis is provided in the computer printed documentation of the data and associated test and control values (Greaves, et al., 1975).

4.2 Test Activities (Speed Control System)

Two subsystems were selected for testing: a speed control subsystem and an anti-skid brake control module. These particular devices were chosen on the basis of availability of both the devices and documentation. The following paragraphs describe the preparations, procedures, and results of testing.

4.2.1 Speed Control System

The electronic speed control unit selected for testing was a 1974 Philco speed control system used on 1974 Ford, Mercury, and Lincoln passenger cars. This electronic automatic speed control system is comprised of four major items: driver control switches, vehicle speed sensor, amplifier or electronics module, and servo unit or throttle actuator. The electronics module and the throttle actuator were purchased from a local Ford Motor Company dealership. A laboratory box was constructed as substitute for the driver control switches and a signal generator was used to simulate the vehicle speed sensor.

The documentation obtained and used as reference material for writing the test plan and preparing the unit for the test facility

interface was a 1974 Car Shop Manual (Ford Motor Co., 1974) and a detailed paper (Follmer, 1974) which describes the design implications, and component function and system operations. The determination of test signal characteristics to be used was based on a knowledge of the expected electrical environment to be encountered and the capabilities of the test facilities.

4.2.2 Speed Control System Test Plan

The speed control concept is illustrated in the block diagram shown in Figure 4.1. An initial speed is set by the driver and stored in a memory. This speed is compared to the actual speed signal from the speed sensor. Any error signals are amplified and applied to the servo unit. The servo unit responds by opening or closing the throttle thus changing the engine torque to compensate for the effect of road grade, wind, etc. on the vehicle which caused the speed change.

4.2.2.1 Electronic upset testing

The remainder of this test plan defines the rationale for selecting specific circuit points to be tested, the character of test signal to be used in the test, and an outline of the test activities.

Signals chosen for interference (upset) testing of the speed control system were rf pulses and dc pulses.

These types of signals are indicative of the potential internal and external interference signals determined from the survey of the automotive electrical environment (Espeland, et al., 1975) and the measurements made for section 2 of this report.

Individual test plan tables were prepared for each of the types of interference listed above. The tables specify the injection points, signal characteristics, monitor locations, and module status. Some rationale is given to explain the choice of parameters and further explanation is given in the discussion of the test results.

4.2.2.2 RF pulse tests

In the test preparation stage, to interface the speed control subsystem assembly with the AFWL test facility, certain laboratory

Reproduced from best available copy.

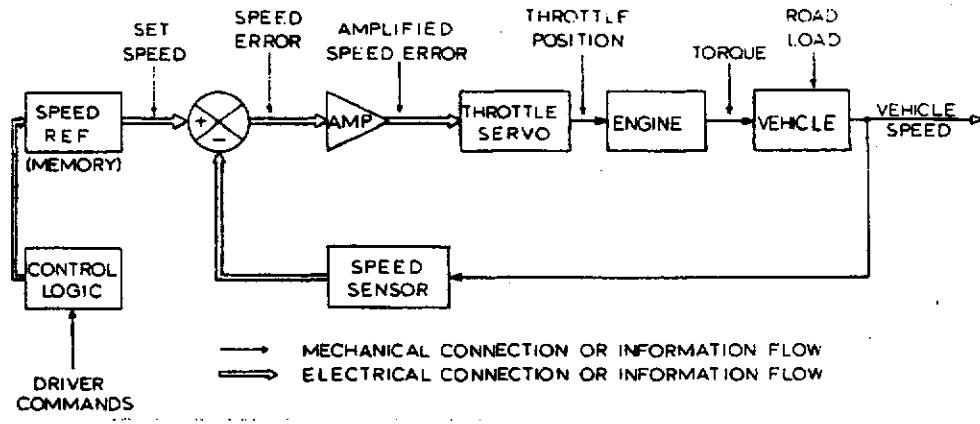


Figure 4.1 Speed Control Electronics (Follmer, 1974)
 (Reprinted with permission, "Copyright © Society of Automotive Engineers, Inc., 1974, all rights reserved.")

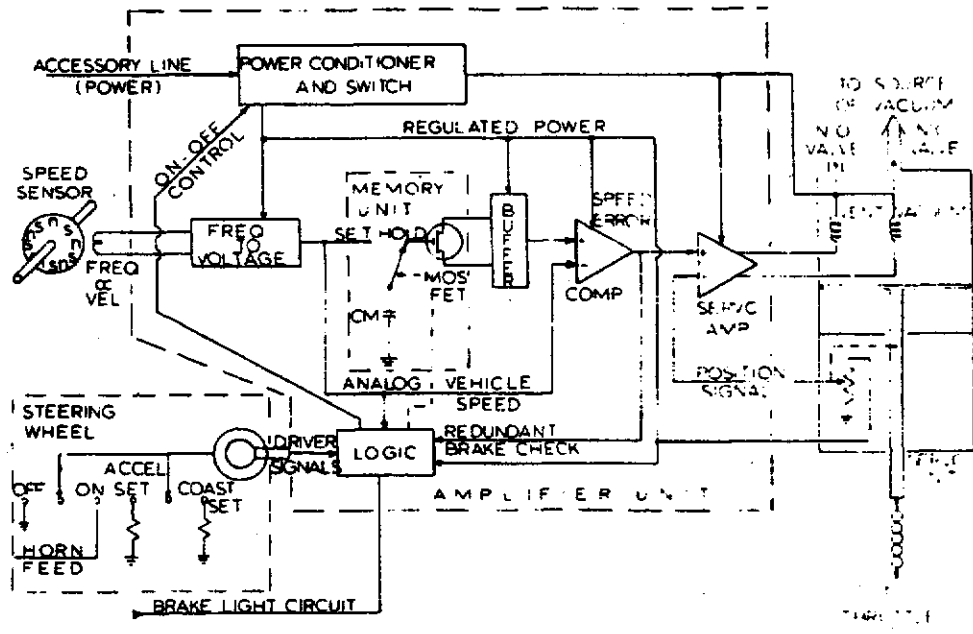


Figure 4.2 Speed Control Electronics (Follmer, 1974)
 (Reprinted with permission, "Copyright © Society of Automotive Engineers, Inc., 1974, all rights reserved.")

equipments are substituted for the automotive devices that perform the same or similiar functions or provide equivalent signals. The following bench equipment was used: an oscillator to simulate the speed sensor, a small control box to simulate the driver command signals, a vacuum pump to simulate the manifold vacuum, and a power supply in place of the battery. A road test showed that the frequency from a speed sensor was 2.5 Hz/mph. Using the 2.5 Hz/mph ratio required oscillator settings of 100, 125, and 150 Hz to simulate the 40, 50, and 60 mph test speeds. Small variations in the settings simulated small variations in vehicle speed. The frequency oscillator signal was input to the frequency-to-voltage converter shown in Figure 4.2.

The driver command switches mounted in the steering wheel crossarm were simulated by the control box, which contained simple combinations of switches and resistors. This box was connected to the control logic circuit.

The laboratory vacuum pump was connected to the vacuum port on the throttle actuator and the power supply (+12 V) was connected to the power accessory line to provide power normally available from the car battery.

These substitutions permitted normal functioning of the subsystem. The rf pulse tests outlined in Table 4.1 were performed with the module functioning to control vehicle speed at 40, 50, and 60 mph. The injection points (for interfering signals), injected signal characteristics, and the monitor locations used in the series of tests were determined from a knowledge of potential interference, the capabilities of the test facilities, and the most susceptible points in the circuit.

The input control signals for this system are set by the driver. The pulses are generated by the application of powerline voltages or resistive shunts to ground. If a 12 V positive pulse should appear on the driver signal line, the system could be turned on without a driver command. If the system is operational under driver command, negative pulses on the same line could activate the acceleration set, coast set, or turn the system off.

Table 4.1 RF Pulse Test (Speed Control Unit)

Injection Points

Power Line
Sensor Input
Control Line

Injected Signals (Characteristics)

Sinusoidal pulse at $f = 3.7, 7.1, 14, 21, 30, 44, 52,$
75 MHz.
Pulse length - 10 ms
Pulse rise and fall time - fixed at 50 ns
Pulse amplitude - attenuation range of 120 dB in - 10 dB steps
Pulse repetition rate - 25 Hz asynchronous
Pulse train duration - 1.2 s

Monitor Location

Position Signal

Module Status

Simulated operation at 40, 50, 60 mph

An interfering signal on this line could result in three possible system upsets:

- 1) the wrong speed could be set in memory if the interference and "on" command are simultaneous,
- 2) the vehicle could speed up if the unit is activated, and
- 3) the vehicle could slow down if the unit is activated.

Interfering signals on the vacuum and vent lines are not likely to cause any serious problems because the resistance of the solenoids is relatively low (90 ohms).

The position signal line could be susceptible to interference, causing the throttle position to change through the differential action of the servo amplifier. However, this action must remain in harmony with the memory and speed sensor for any action other than servo hunting to take place.

The power line is susceptible to all interference produced within the vehicle as well as that which may be produced by external sources. The abnormal transients produced by a vehicle that could appear on this line during the course of normal operation would be caused by alternator load dump and possibly other inductive load dump.

The selection of frequencies for rf pulse testing was made to represent the type of interference signals that could be produced by equipment used in the Amateur Mobile, Citizens Band, or Motor Carrier Radio Services. The frequency bands for these services lie between 3.5 and 160 MHz. Fortunately, the majority of the radio services of interest lie below 100 MHz, the maximum frequency of the AFWL facility. The mobile transceiver frequencies of interest which are covered by the AFWL facility are listed in Table 4.2:

Table 4.2. Mobile Radio Frequencies

Amateur	Motor Carrier	Citizens Band
3.7 MHz	31.00 MHz	27 MHz
7.1	43.80	
14	44.00	
21	44.54	
28	72.50	
52	75.70	

The close spacing of some of the above frequency bands implies that it is probably unnecessary to test all the frequencies listed above. The frequency range is probably adequately covered by test frequencies of 3.7, 7.1, 14, 21, 30, 44, 52, and 75 MHz.

The mobile transceivers will emit a waveform with an initial appearance of a cw signal until the operator starts his communication. During a period of communication, the shape and frequency content of the emitted waveform will depend upon the type of modulation employed (AM, FM, SSB, etc.). The initial choice was pulses 10 ms long at a repetition rate of 25 Hz and a pulse train duration of 1.2 s.

The pulse amplitude was controlled by an attenuator (range 120 dB to 0 dB). A maximum or high attenuation was set at the start of a test and then decreased in uniform 10 dB steps. Details of amplitude control are given in the section describing the results. Maximum input voltage levels greater than 100 V(p-p) were used in the tests.

An upset for these tests was defined as a significant change in the level of the position feedback signal from that observed during unperturbed operation. A level change of 0.1 Vdc, which corresponds to approximately a 4 mph speed change, was considered significant.

4.2.2.3 DC pulse test

The dc pulse tests were planned according to the details of Table 4.3. The test configuration remained the same as for the rf pulse tests.

The selection of pulse amplitudes and duration was based on the information available from the measurements tests of motor vehicle electrical signals. The range of injected signals should compare to those measured.

4.3 Speed Control Test Results

The test data presented in this section resulted from tests conducted at AFWL, Kirtland, NM. Except for the passive circuit impedance measurements, all the tests were performed under simulated operation modes as discussed in the Speed Control System Test Plan (4.2.2). The rf pulse tests (Table 4.1) and the dc pulse tests (Table 4.3) were

Table 4.3 DC Pulse Tests (Speed Control Unit)

Injection Points

Sensor Input

Control Line

Signal Injected

Pulse amplitudes - Both positive and negative (0-to-peak)

120 dB to 0 dB - 10 dB steps,

Pulse duration - 0.03, 0.3, 3.0 ms

Pulse rise and fall time - 25 μ s

Pulse repetition rate - 500 pps at 0.03 ms

50 pps at 0.3 ms

5 pps at 3.0 ms

all asynchronous

Pulse train duration - 1.2 s

Monitor Location

Position signal

Module Status

Simulated operation at 40, 50, 60 mph

followed except when results indicated redundant testing or circuit characteristics dictated unrealistic interference conditions. These discrepancies are described with the presentation of data.

Prior to the direct-drive conductive interference testing, impedance measurements were made of the designated drive points on the circuit to be tested. These measurements were made with the HP 8543A Automatic Network Analyzer. During these tests, the circuit was passive (unpowered). The results are discussed in Section 4.3.1.

The direct-drive conductive interference testing was performed using the Programmable Universal Direct Drive (PUDD) system. This system places under computer control the source generators, functional monitors, and computer peripheral elements. The pre-programmed commands cycle the test parameters (frequency, amplitude, duration), monitor upset conditions as they occur, and print out the results.

Upset conditions resulting from rf and dc pulse interference are reported below for three circuit injection points.

4.3.1 Circuit Impedances

The data in Figures 4.3 through 4.5 show the magnitude of input impedance at the three injection points. These are, respectively, the sensor line, the control line, and the power line. The range of measured values is generally below 250 ohms, except for the lower frequency data from the sensor input whose values run to about 2000 ohms at 1 MHz. The impedances are highly variable within the frequency range from 1 MHz to 100 MHz. Lowest measured values are about 5 ohms in the 20-80 MHz region. This information is useful in setting up the test experiment and in interrupting the upset results.

4.3.2 RF Pulses Testing

The speed control system upset tests were conducted using the PUDD system to control the injected signals and to monitor upset levels. The block diagram in Figure 4.6 shows the interface of the circuits under test and the testing facility. The test unit in the diagram identifies

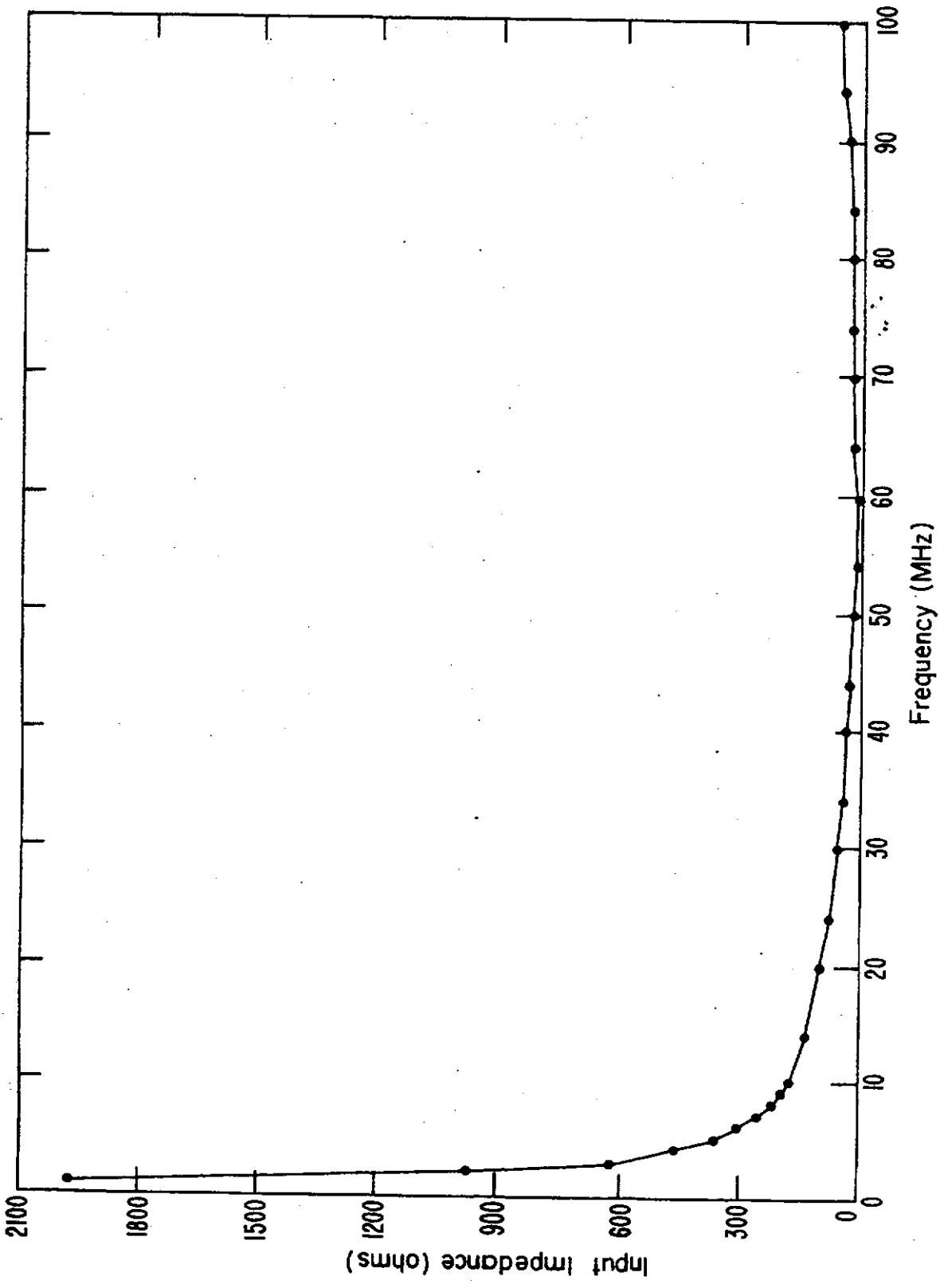


Figure 4.3 Speed Control Sensor Input Impedance

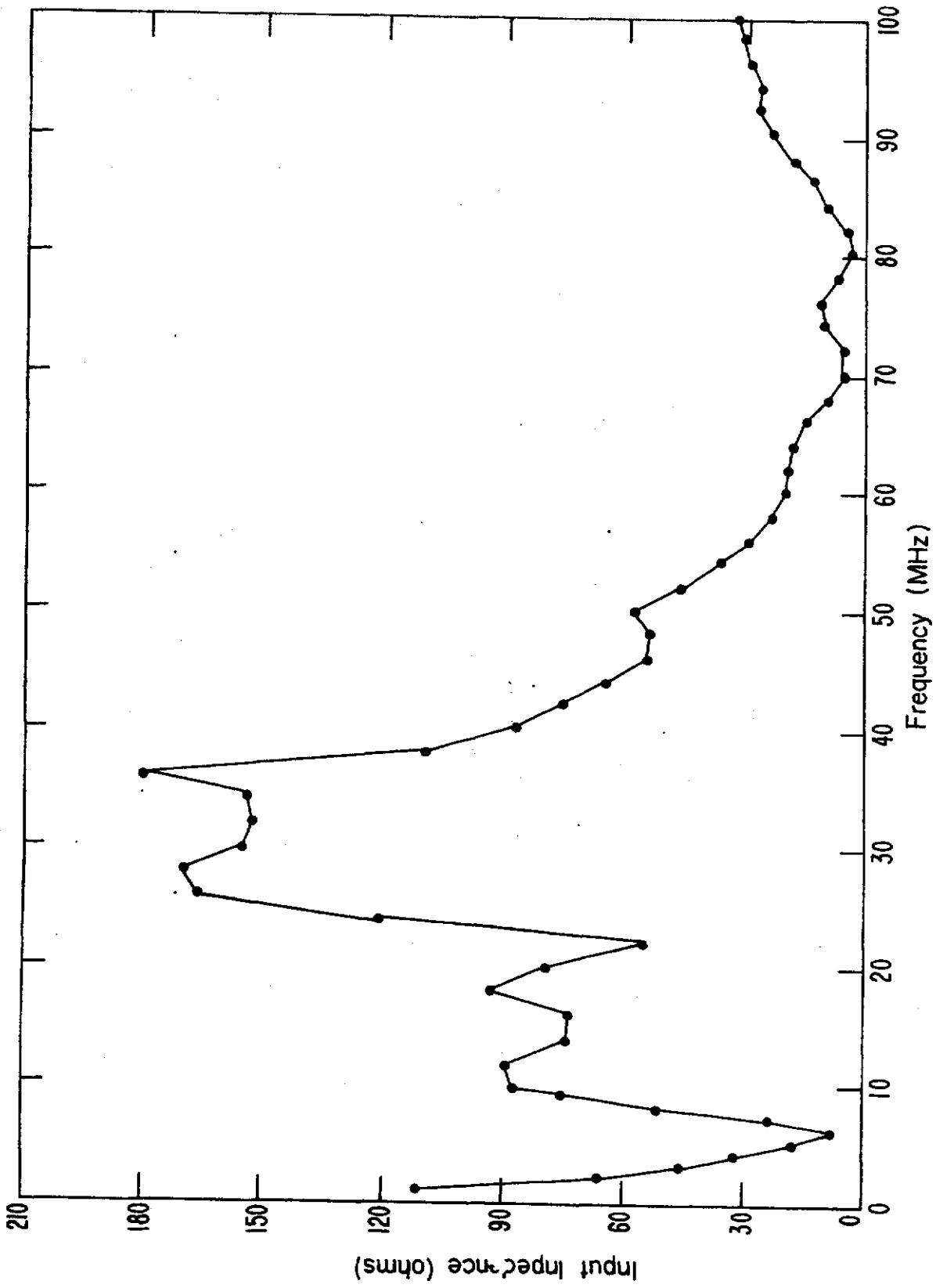


Figure 4.4 Speed Control Power Line Input Impedance

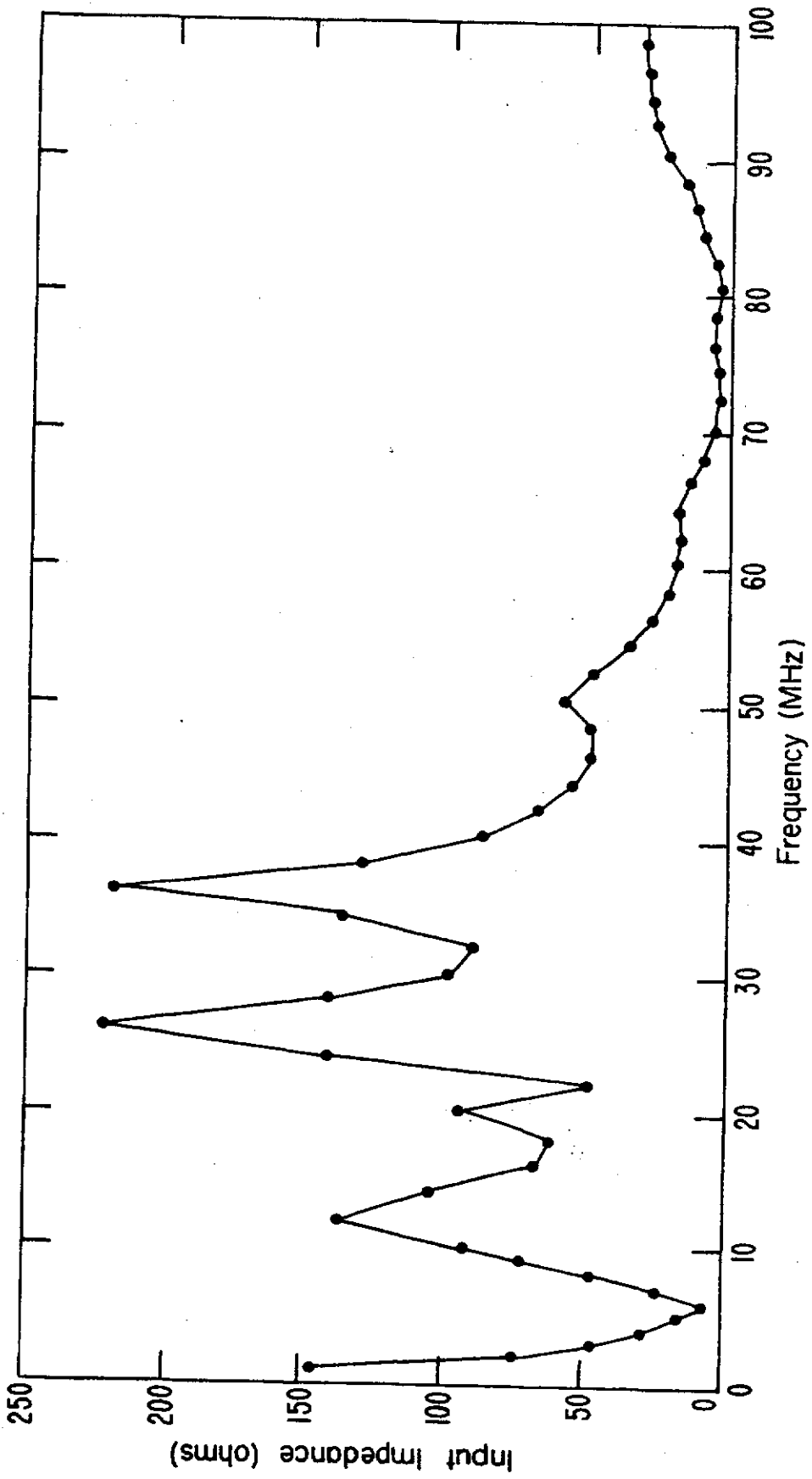


Figure 4.5 Speed Control Line Input Impedance

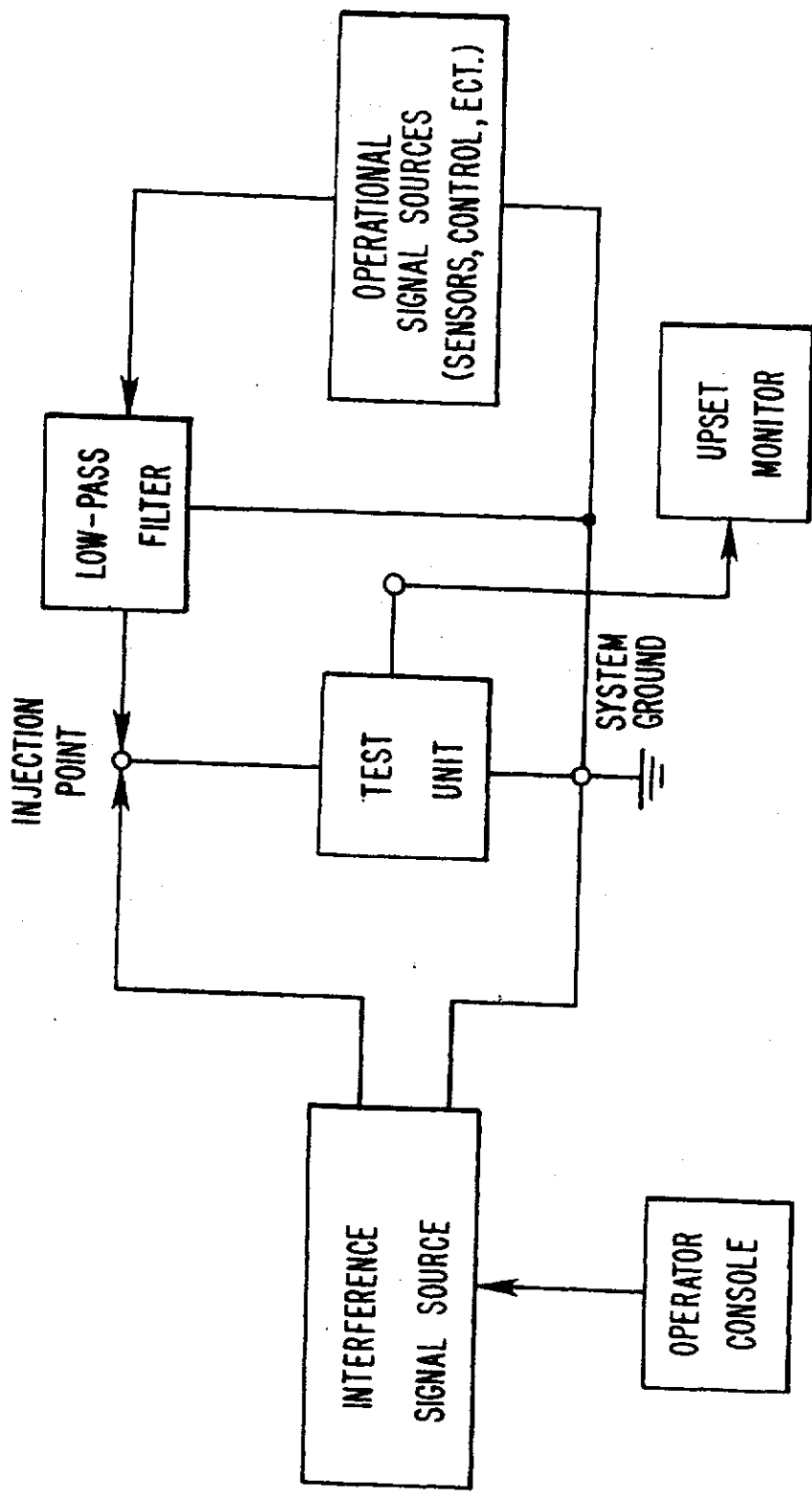


Figure 4.6 Test Configuration

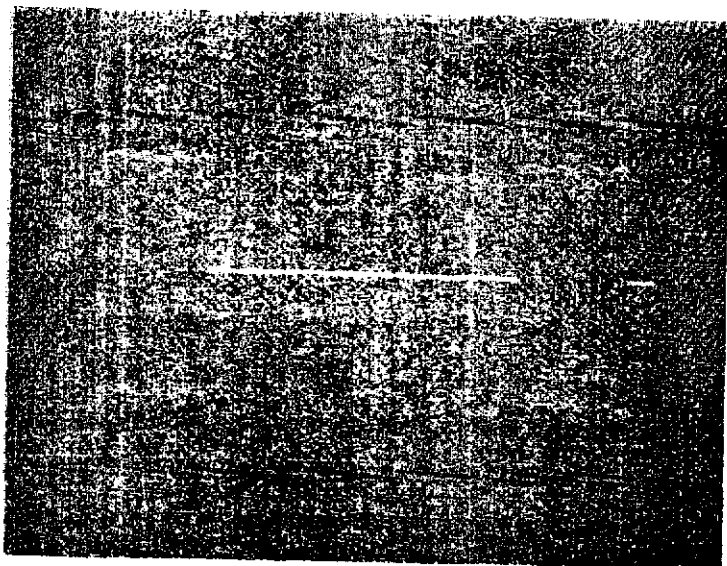
the injection and monitor points. The interference signal source and operator console represent the PUDD drive amplifier and interference signal control. The low-pass filter isolates the normal signal source at the injection point from the interference source. The upset monitor measures a reference voltage, which is set under a no-interference condition. When this reference voltage varies by a predetermined amount, an upset has occurred.

The detailed test procedure for the rf pulse tests was as follows:

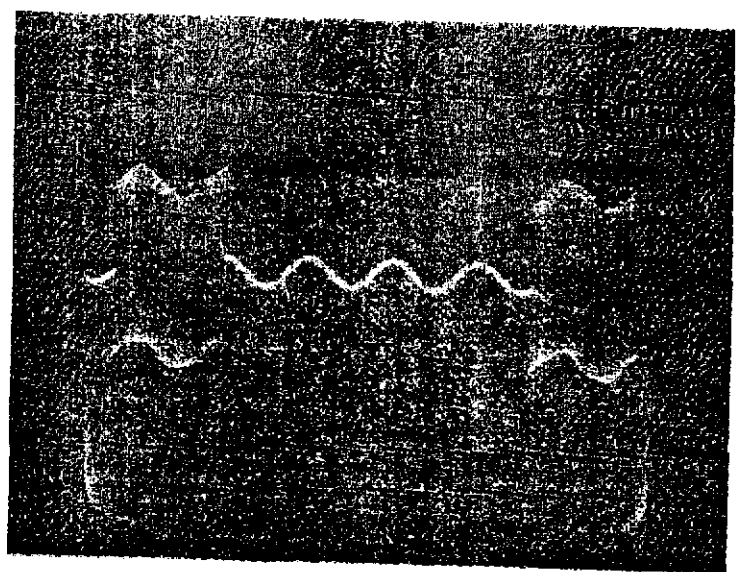
- 1) check power supply, vacuum setting, and the simulated speed,
- 2) initialize the equipment (let the cruise speed control stabilize),
- 3) type in the interference test frequency, and
- 4) type a run message.

With this input information, the system automatically runs through a test sequence. It drives the test point with rf pulses (bursts) that are 10 ms wide and occur at a pulse repetition rate of 25 Hz, which yields a 25% duty cycle. The pulse train duration is set for 1.2 seconds. A representative picture of these signals is shown in Figure 4.7. The rf pulse at the drive line termination is shown in Figure 4.7(a), and this same signal mixed with the sensor input is shown in Figure 4.7(b). This signal is at 7.1 MHz with 24 dB attenuation. The signal amplitude starts at 120 dB below a maximum level that the system will deliver to the test port. This level is frequency dependent. The amplitude of the injected signal is increased in 10 dB steps, and the circuit is tested for an upset condition during each cycle. An upset is defined as a change that is greater than 0.1 V in the signal measured at the position signal potentiometer in Figure 4.2. This corresponds to a vehicle speed change of 4 mph. If no upset is encountered, the circuit is allowed to stabilize and the next higher level (10 dB) signal is injected. If an upset occurs, the injection signal is reduced by 10 dB and a rerun is made at that level. Then the level increments are increased by 3 dB until upset again occurs. This permits finer testing resolution and rechecks that the upset was due to interference and not to other system disturbances.

Reproduced from
best available copy.



(a)



(b)

Figure 4.7 Interference Pulses (rf)

If no upset is encountered, the test cycle continues until maximum signal (0 dB attenuation).

The information in Table 4.4 shows the data produced during a test cycle with signals injected at the sensor line input at 7.1 MHz. This table is typical of the data produced during a test run.

4.3.2.1 Sensor input interference

A data table similar to Table 4.4 (sensor input as injection point) was produced for each of eight test frequencies at simulated operating speeds of 40, 50, and 60 mph. The results of these tests are plotted in Figure 4.8. These curves show the rms upset voltage (or maximum drive voltage with no upset) as a function of test frequency. All points indicate upset, except for the 40 and 60 mph data at 44 and 52 MHz and for all speeds at 75 MHz.

We observed that:

- 1) at all speeds, the upset sensitivity decreases with increasing frequency;
- 2) results were not dependent on speed; and
- 3) this test point is not a highly susceptible circuit point.

The lowest injection signal level for which upset was recorded occurred at a frequency of 3.7 MHz. The input level was 1.5 V (rms).

4.3.2.2 Control line input interference

Tests similar to the sensor input tests were made using the control line as the injection point. These tests were conducted at simulated operating speeds of 40 and 50 mph. The results from these tests are shown in Figure 4.9. This is a plot of data (upset voltage vs. test frequency) similar to Figure 4.8. For these injection points, all data shows upset except at 1 MHz.

The following comments regarding this data are in order:

- 1) the lowest injected signal level for which upset was observed occurred at 2.85 V (rms) at the test frequency of 14 MHz,
- 2) there was a difference in the data record for the two operating speeds,

Table 4.4 Upset Test Date (rf pulses)
Sensor Line

<u>Position Voltage (V)</u>	<u>Attenuation (dB)</u>
4.327	120
4.326	110
4.326	100
4.326	90
4.326	80
4.326	70
4.326	60
4.324	50
4.318	40
4.286	30
4.026	20
4.271	30
4.254	27
4.216	24

REF. POSITION VOLTAGE IS 4.328

TEST FREQUENCY IS 7.1 MHz

UPSET OCCURRED DURING PULSING SEQUENCE

PULSE LEVEL = 24 dB

POSITION VOLTAGE - 4.216

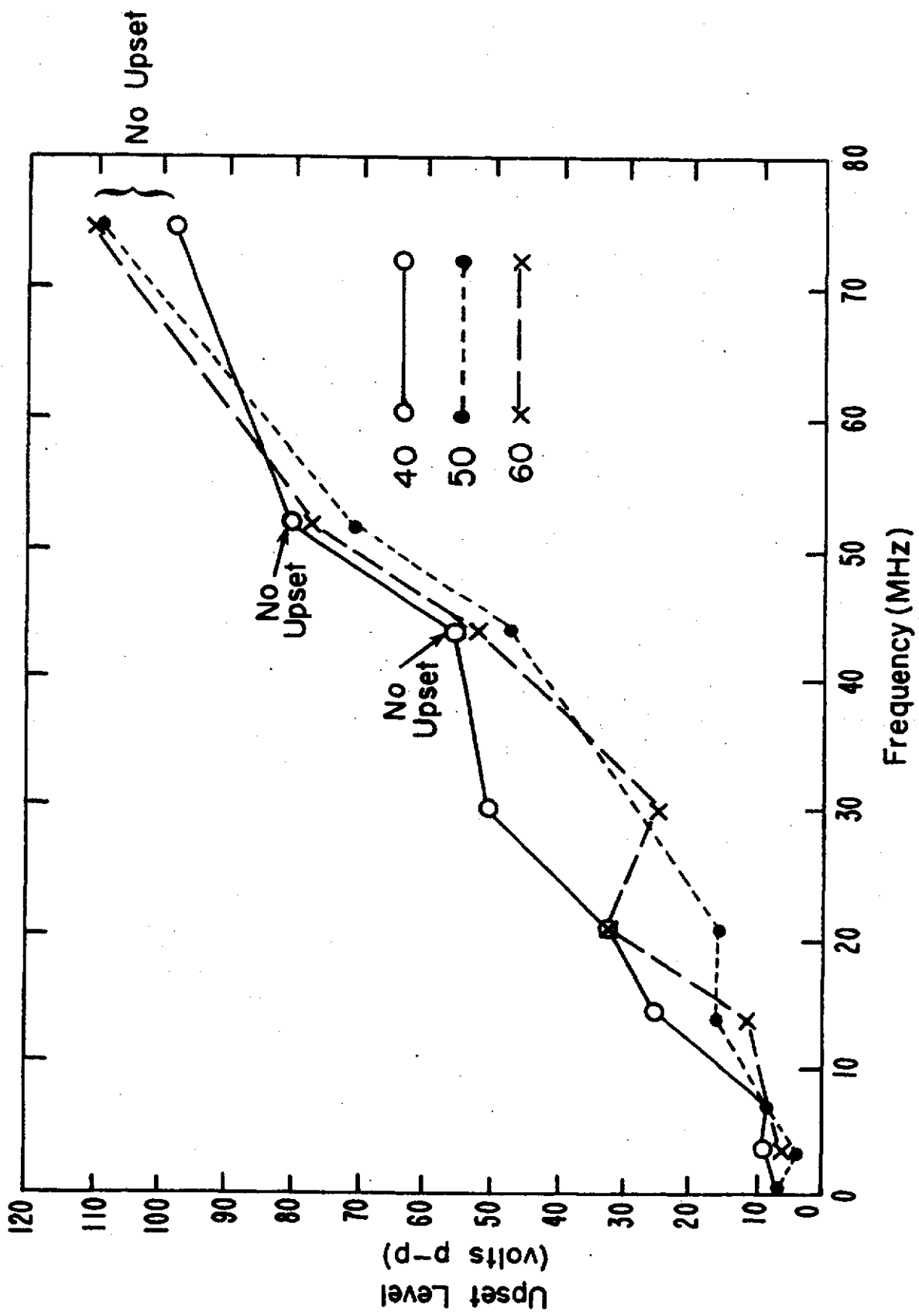


Figure 4.8 Sensor Line Test Results (Speed Control System)

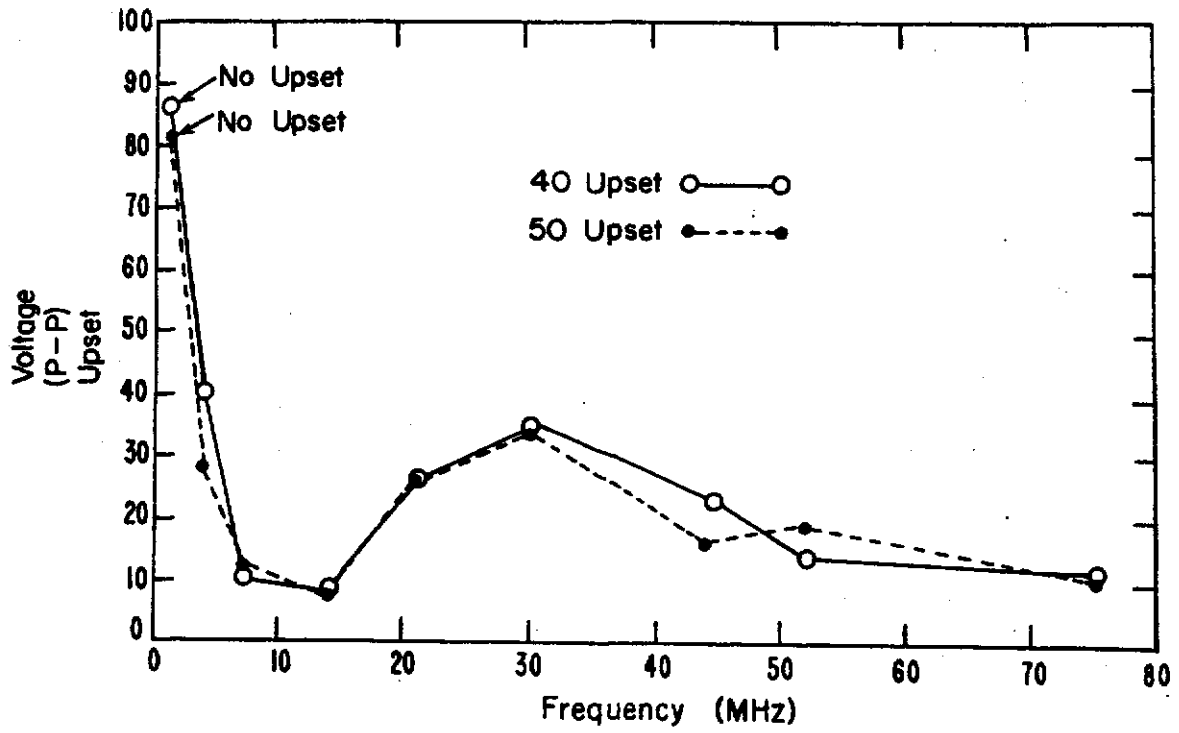


Figure 4.9 Control Line Test Results (Speed Control System)

- 3) the frequency range of 20 MHz to 40 MHz is less susceptible than at frequencies immediately above and below this range, and
- 4) this test point is not a highly susceptible point.

4.3.2.3 Power line interference

The third circuit point selected for rf pulse interference tests was the power line. Tests at this point were conducted at the simulated 40 mph operation only. The results of this test are shown in Figure 4.10. No upset was reached at 7.1 MHz and at 30 MHz. The lowest upset injection levels were 4.28 V (rms) at 44 MHz and 3.92 V (rms) at 75 MHz. Only limited tests were made at this point, because it is not considered a vulnerable circuit point.

4.3.3 DC Pulse Testing

Similar test procedures were followed to conduct the dc pulse testing of the speed control system as were used to conduct the rf pulse tests. The rf signal synthesizer used in the rf pulses was replaced by a dc source, and the dc pulses were defined as either positive or negative polarity, and in terms of a pulse repetition rate (PRR) and pulse width or duration. The pulse train duration remained at 1.2 seconds. Using the same upset criteria as described for the rf pulses and the initial 120 dB amplitude setting, a series of tests were conducted to test the speed control system for susceptibility at the sensor line and the control line. The results of these tests are discussed below.

4.3.3.1 Sensor input interference

The outline for dc pulse tests in Table 4.3 was followed for these tests. The diagnostic print-out format includes the injection point, initial upset reference voltage, simulated vehicle speed, PRR, pulse width, attenuation setting, and corresponding monitor voltage. If upset occurred, this information is also printed out. Typical run data are shown in Table 4.5.

The composite results of these test runs are shown in Table 4.6. Tests were made at 40, 50, and 60 mph. Upset was obtained for each of the three positive and three negative pulse conditions at all three simulated speeds. Furthermore, there is only a small difference in the

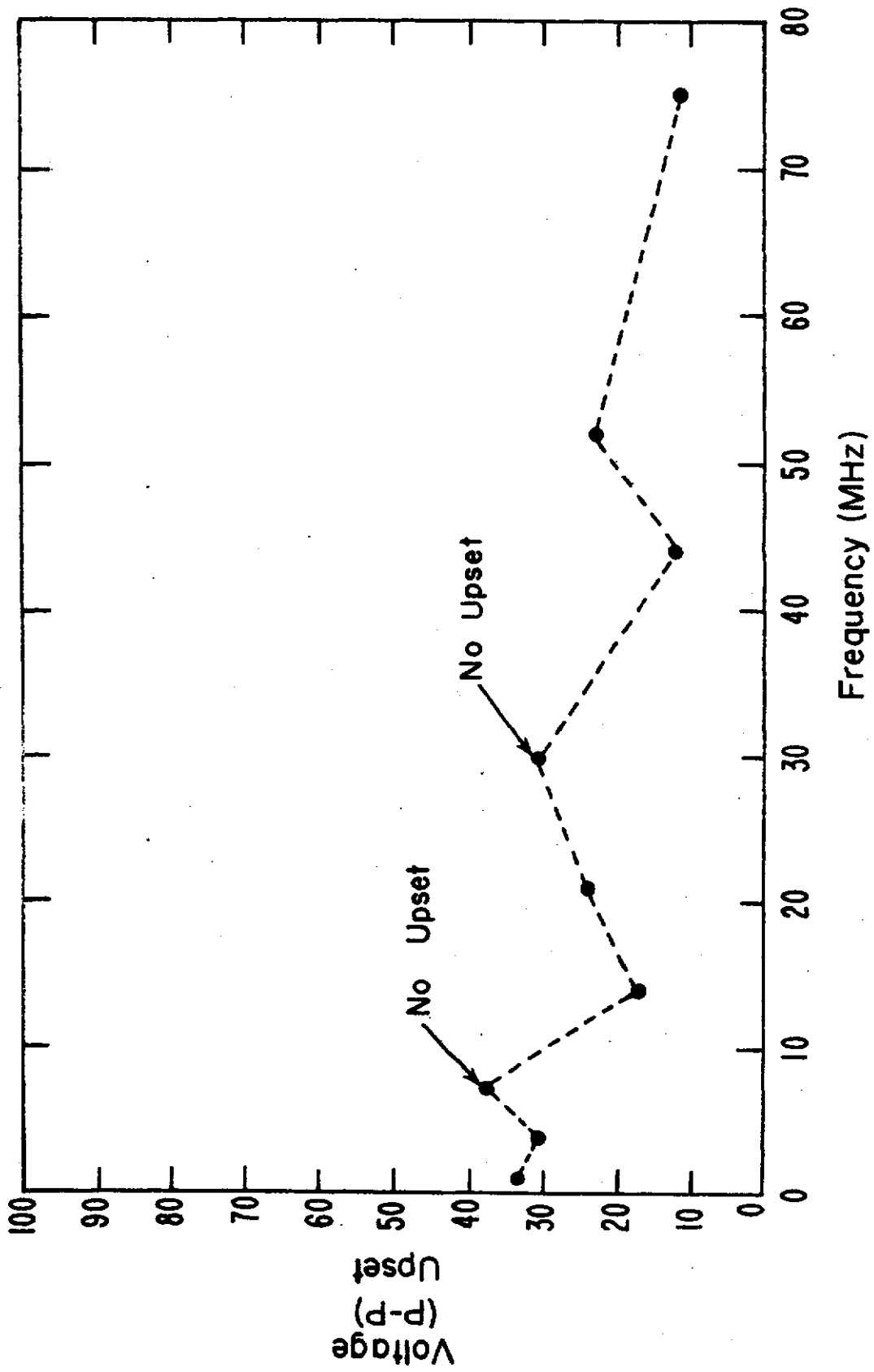


Figure 4.10 Power Line Test Results (Speed Control System)

Table 4.5 Upset Test Data (dc pulses)
Sensor Line

<u>Position Voltage (V)</u>	<u>Attenuation (dB)</u>
4.255	120
4.256	110
4.256	100
4.256	90
4.257	80
4.256	70
4.257	60
4.256	50
4.257	40
4.257	30
4.041	20
4.249	30
4.147	27

REF. POSITION VOLTAGE IS 4.254

REPETITION RATE = 50 Hz

PULSE WIDTH = 0.0003 sec.

UPSET OCCURRED DURING PULSING SEQUENCE

PULSE LEVEL = 27 dB ATTENUATION

POSITION VOLTAGE = 4.147

Table 4.6 DC Pulse Tests (velocity sensor line)
Speed Control System

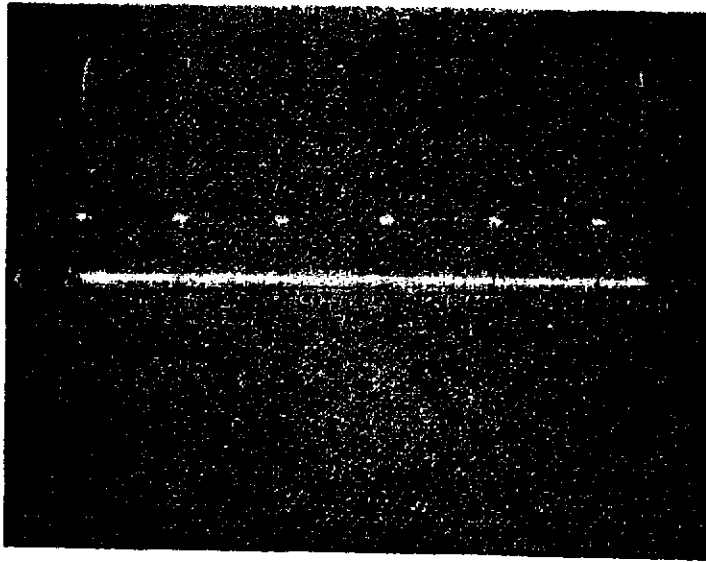
Voltage			Upset Level (volts)		
Polarity	PRR	Width (ms)	40 mph	50 mph	60 mph
POS	25	3.00	1.6	1.6	1.6
POS	50	0.30	1.1	1.6	1.6
POS	500	0.03	1.2	0.9	1.7
NEG	25	3.00	1.9	1.1	1.7
NEG	50	0.30	2.4	1.1	1.2
NEG	500	0.03	1.1	1.1	1.6

upset values, ranging from 0.9 V to 1.7 V for the positive going signals and 1.1 V to 2.4 V for the negative going pulses. The average zero-to-peak value for the 18 tests is 1.44 V. Also, there appears to be negligible correlation of the results as a function of simulated vehicle speed and as a function of the pulse characteristics (such as PRR and pulse width). One conclusion that is noteworthy is that the average upset level (1.44 V) is almost equal to one-half of the simulated sensor peak-to-peak voltage. This indicates that as the interference level approaches in amplitude equal to the zero-to-peak amplitude of the sensor output the added pulses simulate an increased velocity and the servo action tends to slow the vehicle down. As the position signal potentiometer moves outside the 0.1 V limit, an upset is sensed.

The waveform pictures in Figure 4.11 show both the sensor output signal and the interference pulses. The signal in Figure 4.11(a) is the dc interference pulse only and in Figure 4.11(b) is the combination of the sensor output and the interference pulses. Amplitude and sweep settings for both pictures are 1 V/div and 20 ms/div. The PRR is 25 Hz and pulse duration is 3 ms. The sensor frequency was set at 125 Hz.

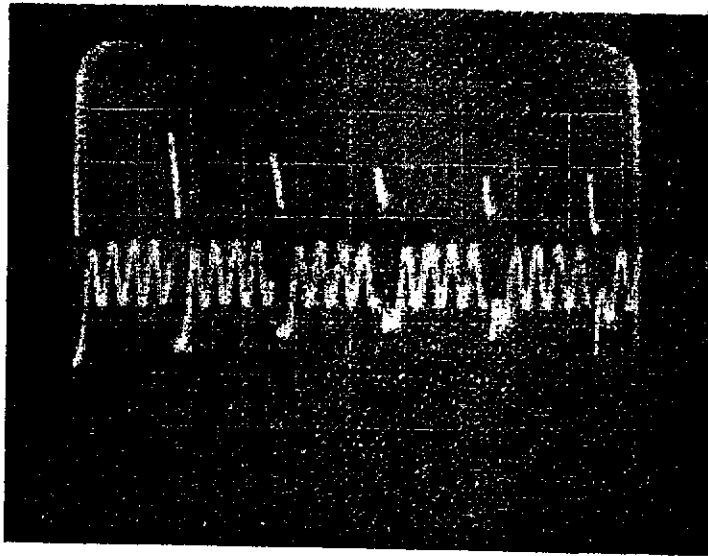
4.3.3.2 Control line input interference

The results of the tests injecting dc pulses onto the control line are shown in Table 4.7. The same pulse characteristics were used as for the sensor input tests. Simulated vehicle speeds of 40 and 50 mph were used. This circuit point is less susceptible to this type of interference than was the sensor line. Maximum levels of 21 to 25 V (zero-to-peak) were injected without upset. The data does show, however, that the control line is more susceptible to negative pulses than to positive pulses. This result can be expected because the control line is used to change the system operating mode. When the system is turned on (power on), the control is at +12 V. To "accelerate-set," a control button is pressed that lowers this voltage to approximately 9 V, and to "coast-set," a control button is pressed that lowers this voltage to approximately 6 V. The hypothesis that negative pulses at the control point



Reproduced from
best available copy.

(a)



(b)

Figure 4.11 Interference Pulses (dc)

Table 4.7 DC Pulse Tests (control line)

Voltage			Upset Voltage	
Polarity	PRR	Width (ms)	40 mph	50 mph
POS	25	3.00	+ 8V, -3V	No upset (+26,-10)
POS	50	0.30	No upset (+25 V)	No upset (+23V)
POS	500	0.03	No upset (+21 V)	No upset (+21V)
NEG	25	3.00	-8V,+3V	+2V,-8V
NEG	50	0.30	-14V	-7V
NEG	500	0.03	No upset(-21V)	No upset (-21V)

enhance an upset condition is that the pulse train reduces the average level at this circuit point until the 9 V level is reached and the system is inadvertently put in the "accelerate-set" mode, causing the upset monitor level to exceed the prescribed limit.

The recorded upset voltage for the plus and minus signals at PRR=25 and width=3 ms (Table 4.7) show both a positive and negative amplitude. This amplitude designation was used to identify the exponential waveforms that resulted from capacitive coupling of the source to the control line. This mode of coupling was used to prevent source loading. Such loading would cause a shut-off condition at the control line.

The picture in Figure 4.12 shows the differentiation of the leading and falling edges of the input pulse to produce an exponentially shaped interference signal. This shape is typical of those encountered in the measurements tests discussed in Section 2 of this report. The amplitude and sweep settings were, respectively, 5V/div and 10ms/div.

4.4. Test Activities (Antiskid Brake System)

The second subsystem for which test activities were planned was the anti-skid brake system. The following paragraphs describe the preparations, procedures, and results of testing.

4.4.1 Anti-Skid Braking System

The electronic anti-skid braking controller module selected for testing was a Kelsey-Hayes M26 Sure Track Anti-Skid System used on luxury-class Ford Motor Company cars. The anti-skid system is comprised of three major components: a mechanically driven electromagnetic sensor at the rear axle drive pinion, an electronic control module, and a vacuum powered actuator to modulate the brake pressure as skid conditions are approached. Only the electronic control module was purchased for these tests. The electromagnetic sensor signals are simulated using a voltage controlled oscillator and the vacuum powered actuator load is simulated with a resistor load. A 3A, 12V power supply replaces the battery function. In the test configuration, the electronic control module is made to cycle through a series of accelerate-

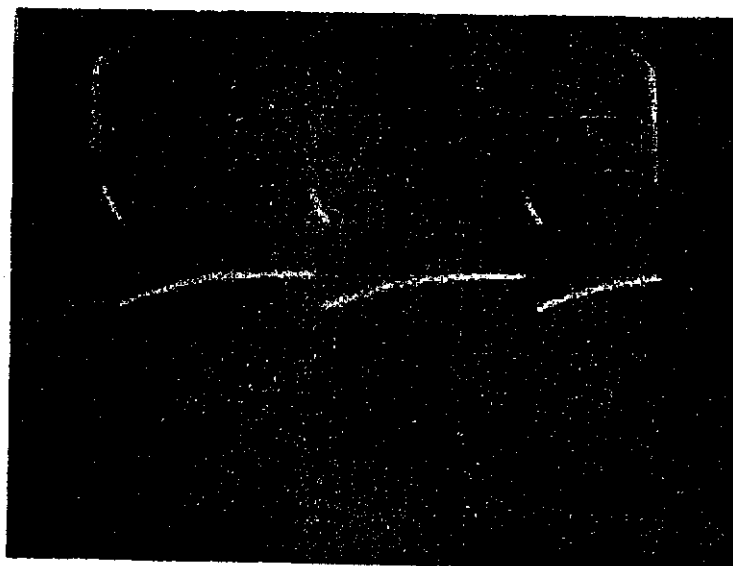


Figure 4.12 Interference Pulses (exponential shaping)

decelerate actions, where a portion of the decelerate cycle is at a sufficient rate to cause output signals for brake modulation.

The documentation used as reference material for writing the test plan and preparing the unit for the test facility interface was a 1974 Car Shop Manual (Ford Motor Company, 1974), an article by Lapidus (1973), and a schematic diagram on which some of the component identification had been removed. The diagram proved very useful for identifying connector inputs and outputs, however.

4.4.2 Anti-Skid Brake System Test Plan

A generalized block diagram of an adaptive feedback controller which is representative of the anti-skid systems in production is shown in Figure 4.13.

4.4.2.1 System operation

The ac tachometer senses wheel speed and sends audio frequency information to an electronic control module. The frequency-to-voltage converter generates a dc voltage proportional to wheel speed. When the wheel deceleration approaches a lock-up condition, the negative rate detector uses this information as a necessary condition for removing (or reducing) the brake pressure from the wheels which are starting to lock up. An estimate of vehicle velocity can be obtained from the wheel speed by using peak detecting circuits. The vehicle velocity estimate, detected negative rate, and solenoid drive status are combined to generate the enabling signals at the AND gate indicating that excessive slip has occurred. The solenoid driver is then allowed to actuate the modulator which momentarily removes brake pressure from the wheels starting to lock. For the sake of simplicity and power efficiency the modulators are on/off in controlling brake pressure with a pulse rate of the order of 4 Hz.

The relationship between the wheel and vehicle velocities is shown in Figure 4.14. The graph is a plot of relative velocity vs time. When the driver applies the brakes, the wheel velocity decreases according to the curve indicated as wheel speed in the figure. As the deceleration

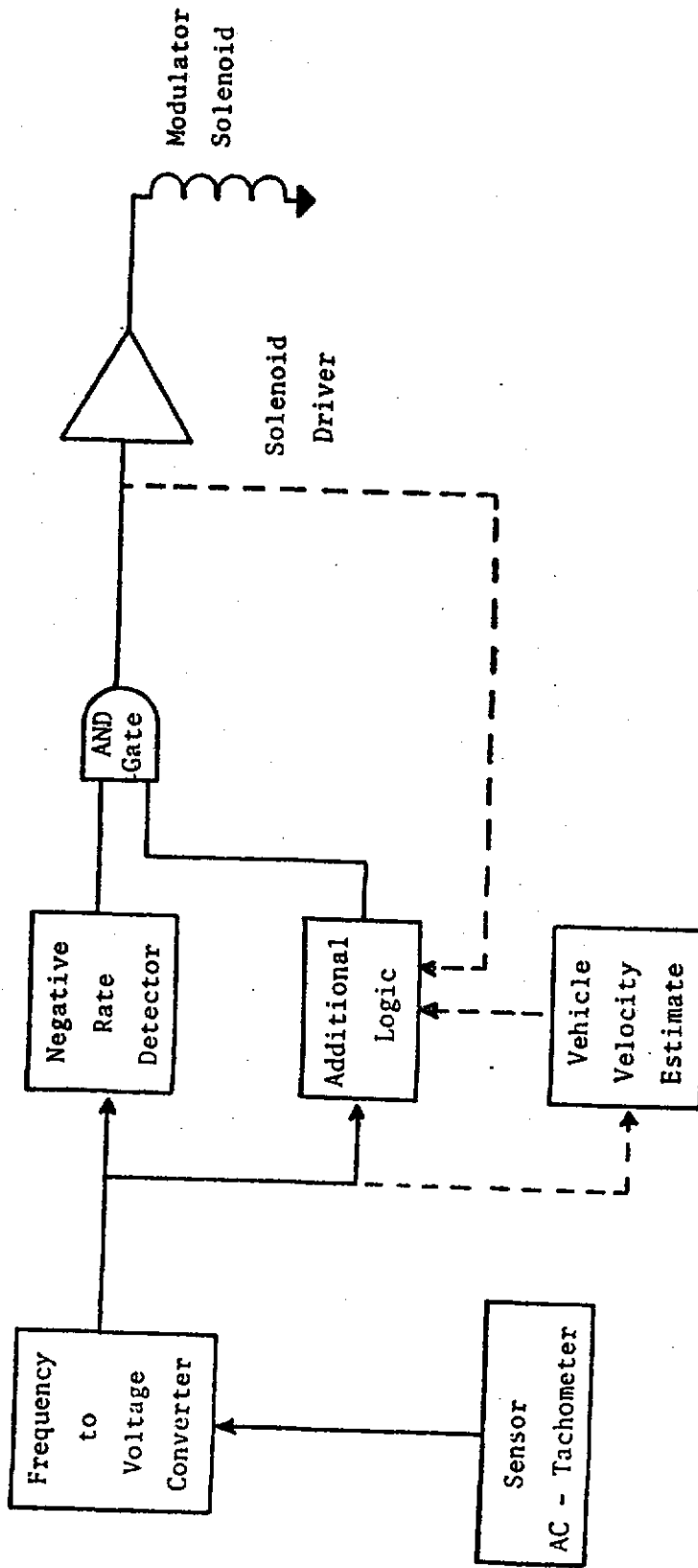


Figure 4.13 Generalized Block Diagram of Anti-skid Brake Controller (Lapidus, 1973)
 (Reprinted by permission, IEEE Spectrum, Vol. 10, No. 3, March, 1973,
 pp. 26-30. Copyright 1973 by the Institute of Electrical and
 Electronics Engineers, Inc.)

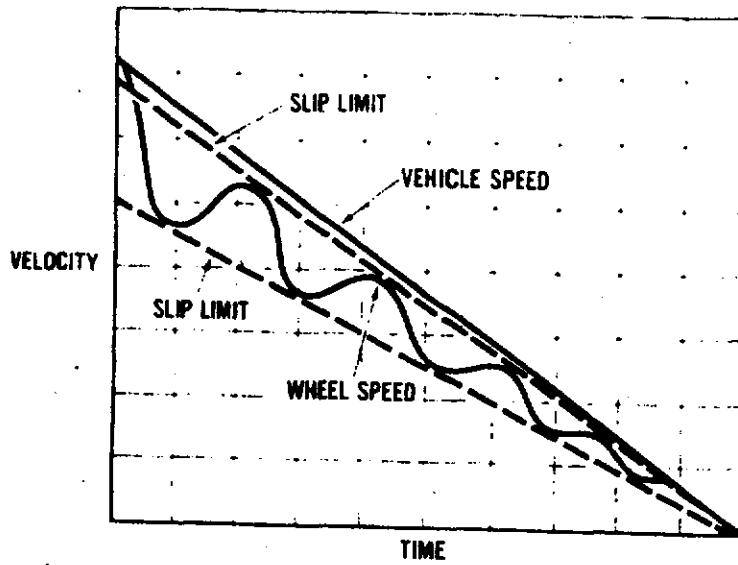


Figure 4.14 Wheel and Vehicle Velocity Relationships (SAE, 1975) (Reprinted with permission, "Copyright © Society of Automotive Engineers, Inc., 1974, all rights reserved.")

rate approaches the slip limit, the anti-skid modulator momentarily releases the pressure. This causes the actual brake pressure at the wheel to cycle through a range that is near maximum without a skid condition occurring. This range is maintained until the vehicle is stopped or until the master brake pedal pressure is released.

Anti-skid systems are installed in vehicles in a variety of configurations. Some passenger vehicles have only rear wheel implementation while others have four wheel implementation. Heavy trucks use both wheel-by-wheel and axle-by-axle implementation. Where axle-to-axle configurations are used the number of anti-skid modules required is reduced.

4.4.2.2 Electronic upset testing

The rationale behind the plans for this testing procedure is the same as for the speed control unit. The three signal types chosen for testing of the anti-skid module were rf pulses, cw signals, and dc pulses.

The individual test plan tables prepared to test the types of interference are specified in Tables 4.8, 4.9, and 4.10. These tables specify the injection points, signal characteristics, monitor locations, module status.

4.4.2.3 RF pulse tests

As stated earlier, the module being tested is the electronic control unit. A diagram showing the laboratory equipment used in the synthesis of the anti-skid system operation is shown in Figure 4.15. The circuit board input pin identifications were taken from a circuit diagram obtained from a Kelsey-Hayes representative. The voltage oscillator set at .066 Hz controls the acceleration-deceleration cycle used during the test period. The sine wave drives the voltage-controlled-oscillator (VCO) output frequency through a range from approximately 50 Hz to 3400 Hz and back to 50 Hz. These output frequencies from the VCO simulate the wheel sensor output over a velocity range of 2 mph to 136 mph. During the deceleration portion of this cycle, a rate is reached that approaches the slip limit (Figure 4.14). The negative rate detector in the control module senses this rate and activates the

Table 4.8 RF Pulse Tests

Injection Points

Sensor Hi-Lo (pins 2 & 3)

Fused B+ (pin 12)

Signals Injected

Sinusoidal pulse at $f = 3.7, 7.1, 14, 21, 30, 44, 52, 75$ MHz.

Pulse length - 10 ms

Pulse rise and fall time - 10 μ s

Pulse amplitude - attenuation range of 120 dB - 10 dB steps

Pulse repetition rate - 25 Hz asynchronous

Pulse train duration 5 seconds

Monitor Locations

Solenoid (pin 6)

Module Status

Deceleration (maximum to zero)

- a) interference
- b) non-interference

Table 4.9 CW Tests

Injection Points

Sensor Hi-Lo (pins 2 & 3)

Fused B+ (pin 12)

Signals Injected

Sinusoidal signals at $f = 3.7, 7.1, 14, 21, 30, 44, 52, 75$ MHz.

Signal amplitude - attenuation range 120 dB - 10 dB steps

Signal duration 5 seconds

Monitor Locations

Solenoid (pin 6)

Module Status

Deceleration (maximum to zero)

a) interference

b) non-interference

Table 4.10 DC Pulse Tests

Injection Points

Sensor Hi-Lo (pin 2 & 3)

Fused B+ (pin 12)

Signal Injected

Pulse amplitudes - Both positive and negative (0-to-peak)
attenuation range of 120 dB - 10 dB steps

Pulse duration - 0.03, 0.3, 3.0 ms

Pulse rise and fall times - 25 μ s

Pulse repetition rate - 500 pps at 0.03 ms

50 pps at 0.3 ms

5 pps at 3.0 ms

all asynchronous

Pulse train duration - approximately 5 seconds

Monitor Locations

Solenoid (pin 6)

Module Status

Deceleration (maximum to zero)

- a) interference
- b) non-interference

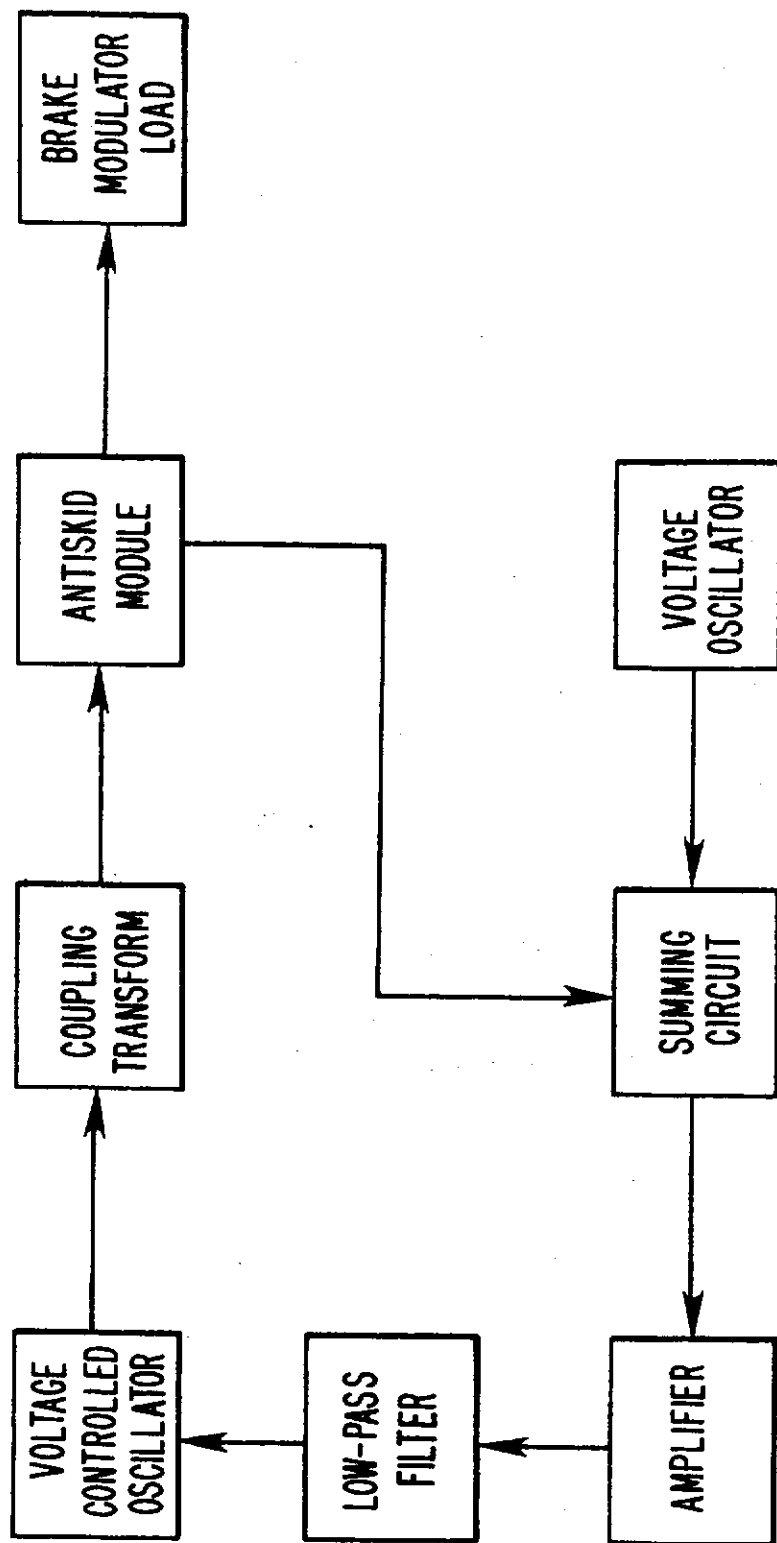


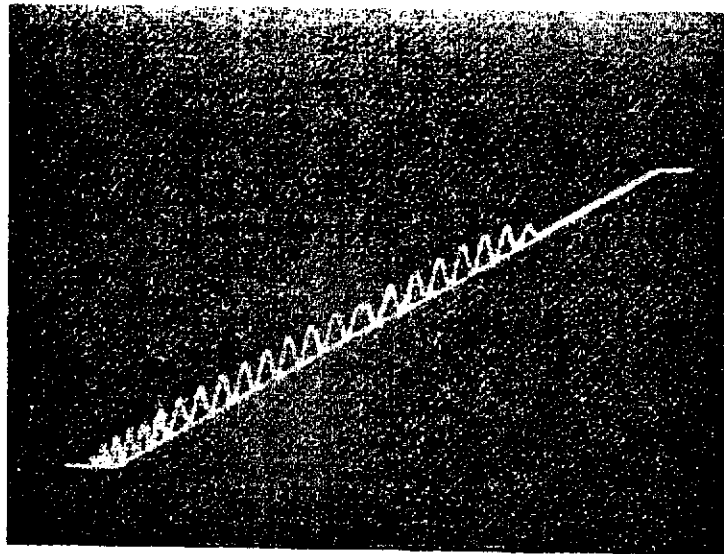
Figure 4.15 Antiskid Module Test Diagram

solenoid driver. The solenoid output on the control module drives the modulator solenoid. In the test set-up, this solenoid load is simulated with a resistor-lamp combination. The lamp is lighted during each solenoid driver command. In an actual vehicle operation, the solenoid releases brake pressure to the wheel and the wheel accelerates to the vehicle velocity at which time the driver cycles through a braking condition again and the wheel decelerates. This on-off rate is controlled by the inertia of the wheel, allowing for about 4 cycles per second. In the test set-up, a signal is feed-back from the anti-skid module to the summing circuit to simulate the wheel velocity increase normally derived from the wheel sensor. The wheel inertia is simulated by the low-pass filter in the feed-back loop. The VCO thus controlled does simulate this velocity variation. This anti-skid control action is maintained until the vehicle is slowed to a near stopped condition or until the master brake pressure is released. The complete accelerate-decelerate cycle simulation occurs in about 15 seconds and the anti-skid control module modulation action is for only a portion of the decelerate part of the cycle.

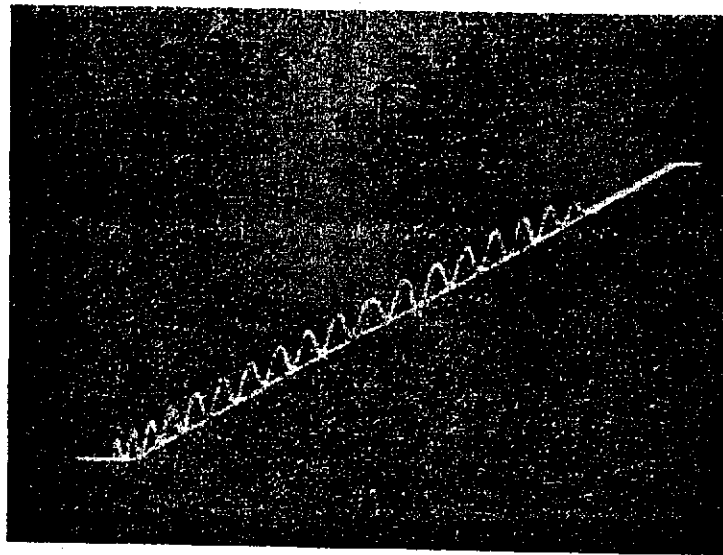
The pictures shown in Figure 4.16 are of oscilloscope tracings in the X-Y mode. The Y-axis input is the output from the low frequency oscillator in Figure 4.15 and the X-axis input is the frequency-to-voltage converter output (a part of the control module). The lower straight line trace in each picture represents the frequency-to-voltage output as the oscillator which simulates wheel velocity accelerates from about 50 Hz to 3400 Hz.

The horizontal lines at each end of the traces represent the cut-off limits of the circuitry. The upper line represents the decelerate portion of the cycle. This line is nearly a retrace of the acceleration portion (due to symmetry of the controlling sine wave) until the negative rate detector senses a slip limit and the brake modulation commences. The remainder of the deceleration trace as shown represents the wheel velocity variation as converted by the frequency-to-voltage con-

Reproduced from
Best available copy. ©



(a)



(b)

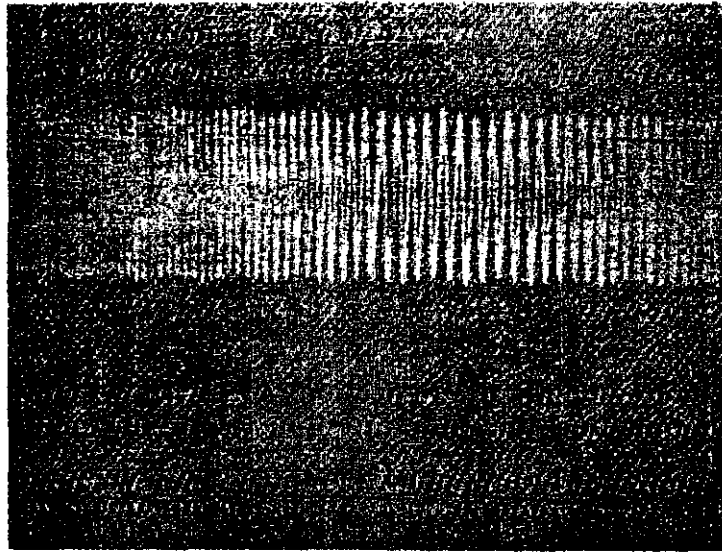
Figure 4.16 Waveforms Representing the Acceleration-
Deceleration Cycle of an Anti-skid Control
Module

verter. This modulation continues until the lower limit of the circuitry is reached. The data in the pictures of Figure 4.17 show the sensed frequency due to a simulated wheel velocity variation. The trace in Figure 4.17 (a) starts with a wheel sensor output frequency of 450 Hz at the left, decreasing to a low of 225 Hz, and then increasing again. This represents a brake pressure modulation showing a pressure release, a pressure increase, and then a release again. These frequencies convert to wheel velocities at about 18 mph and 9 mph. The data in Figure 4.17 (b) is similar to Figure 4.17 (a), representing wheel velocities of 10 mph and 5 mph.

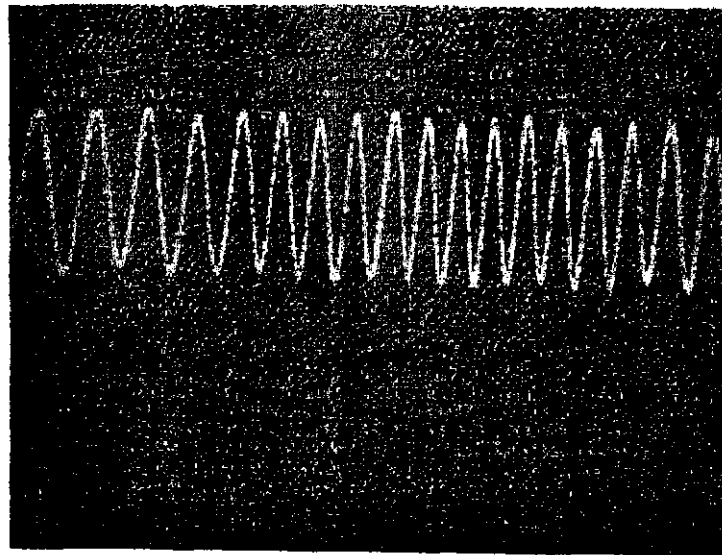
The coupling transformer in Figure 4.15 provides a balanced input to the anti-skid module, and the amplifier provides gain in the drive circuit for the VCO. The low-pass filter eliminates any high frequency components from the VCO and simulates wheel inertia. This is compatible with the 4 Hz brake actuator modulating rate.

The most likely source of externally generated upset signals are pickup and conducted signals on the interconnecting cables of the anti-skid system. Figure 4.18 shows the typical component placement for a skid control system on a Lincoln Continental. Interconnecting wires are used between the wheel velocity sensor mounted at the rear axle and the control box in the glove compartment. Also, control wires run between the control box and the actuator. A typical anti-skid installation on heavy tractors is shown in Figure 4.19. The length of the interconnecting cables, ranging from 5 to 30 feet, combined with inadequate shielding would make the computer module very susceptible to RF radiation.

A schematic of a Kelsey-Hayes passenger car brake control module was used to identify the control board input contacts. Table 4.11 lists the printed circuit board contact numbers, function, and estimated dc impedance at the opposite end of the connecting wires.



(a) Vertical = 0.5 V/DIV
Horizontal = 20 ms/DIV



(b) Vertical = 0.5 V/DIV
Horizontal = 10 ms/DIV

Figure 4.17 Wheel-Sensor Type Signals Showing the Effect of Brake Modulation

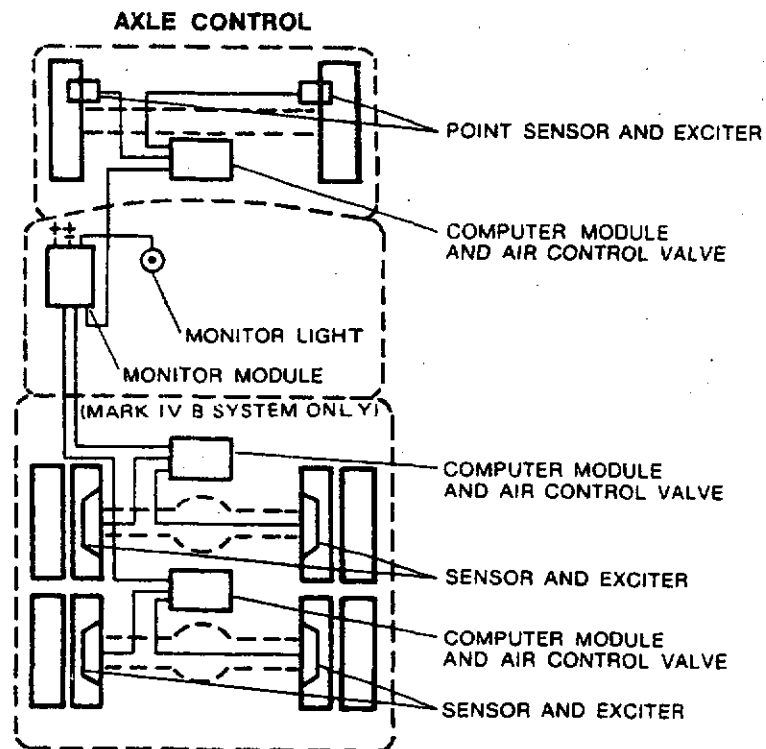
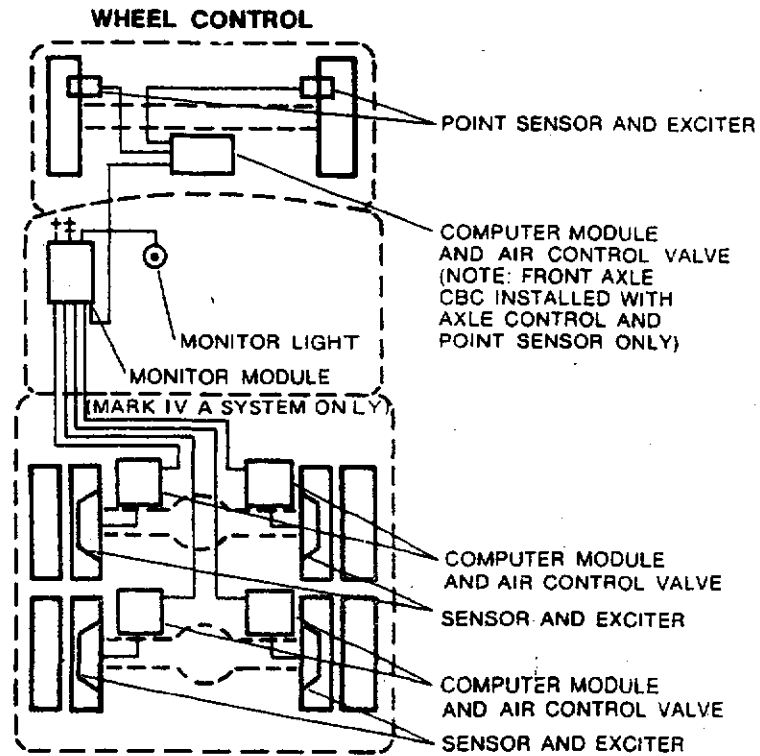


Figure 4.19 Wheel and Axle Control Schematics (Kelsey, 1974)
 (Reprinted by permission, Kelsey-Hayes, June 1974
 Weatherly Index 148, CBS Skid Control Brochure,
 Kelsey Products Division, Kelsey-Hayes Co.,
 Romulus, MI.)

Table 4.11 Control Board Pin Connections

Contact Number	Function	Impedance
1	Not used	---
2	Sensor Lo	2500 ohms*
3	Sensor Hi	2500 ohms*
4	Ground	0 ohms
5	FSM switch	0 ohms*
6	Solenoid	5 ohms
7	Not used	---
8	FSM switch	0 ohms*
9	Not used	---
10	Lamp	5 ohms
11	Lamp	5 ohms
12	Fused B+	0 ohms

* Impedance as seen from the paired contacts 2, 3 and 5, 8.

The rf pulse tests are outlined in Table 4.8. The same frequencies are used as were selected for the speed control tests. Amplitude steps and durations are changed to accommodate the differences in subsystem functioning. The sensor input and B+ are selected for interference signal injection, and the solenoid drive was used as a monitor. System upset is based on a measure of the performance under interference conditions as compared to non-interference conditions.

4.4.2.4 CW and DC pulse tests

The cw tests are identical to the rf pulse tests, with the exception that the signal duty cycle is increased from 25% to 100%. The test details are outlined in Table 4.9. The dc pulse tests are detailed in Table 4.10. These tests are very similar to the rf pulse tests.

4.5 Antiskid Brake System Test Results

There are many similarities between the upset testing conducted on the antiskid brake module and the speed control unit described in

Sections 4.2 and 4.3. The same test equipment was used to generate the interference signals and the units were tested over the same frequency range. The principle difference was the upset criterion, which, of course, must be determined as a meaningful function of each system operations.

Prior to conducting the upset tests using the PUDD system, input impedance measurements were made of each proposed injection point. These measurements were made with the HP 8543A Automatic Network Analyzer. The results are presented in Section 4.5.1.

The same test point interface configuration (see Figure 4.6) was used as in the speed control tests. The test outlines for the rf pulse tests, the cw signal tests, and the dc pulse tests are shown, respectively, in Tables 4.8, 4.9, and 4.10.

4.5.1 Circuit Impedances

The data in Figures 4.20 and 4.21 show the magnitude of input impedance at two injection points of the antiskid circuit. These are one side of a balanced input from the velocity sensor (pin 2) and the power line (pin 12). The other side of the balanced input from the sensor (pin 3) has an identical input impedance. The impedance at the sensor input varies from 800 ohms at 1 MHz to below 10 ohms at 64 MHz and then goes to about 50 ohms at 100 MHz.

The measured impedance at pin 12 (the 12 power line connection) is 30 ohms at 1 MHz, increasing to greater than 300 ohms at 25 MHz. There is a dip to 160 ohms at 30 MHz, with another peak at 32 MHz. From that point, the impedance reduces to a low of less than an ohm at 75 MHz and then increases to approach 25 ohms at 100 MHz. These impedances were measured with the circuit unpowered. The transformer circuit used to simulate the sensor input signals (see Figure 4.15), however, was in place.

4.5.2 RF Pulse Testing

The circuit upset results obtained by injecting rf pulse signals at the wheel sensor inputs are shown in Figures 4.22 and 4.23. These data

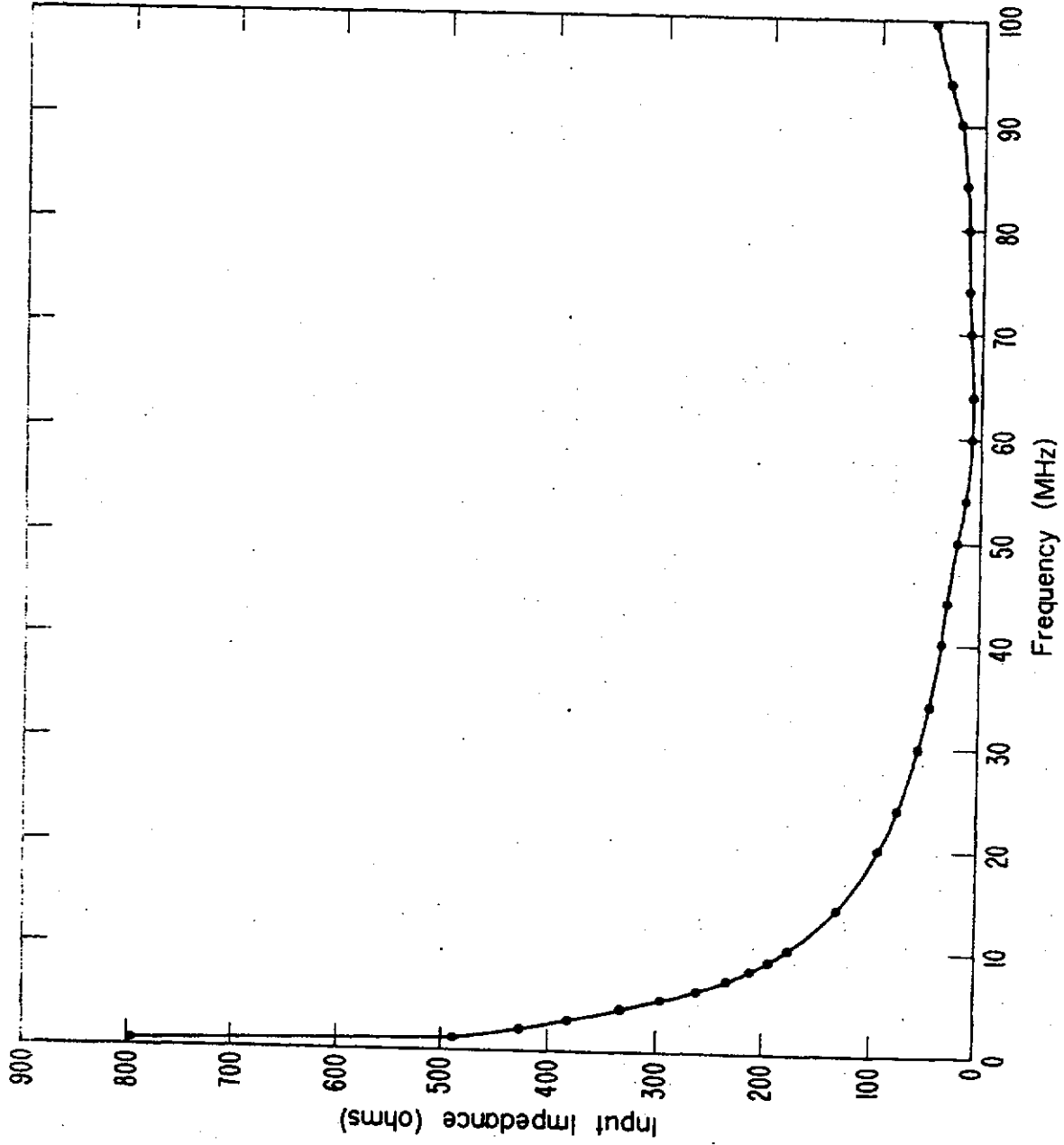


Figure 4.20 Antiskid Sensor Input Impedance

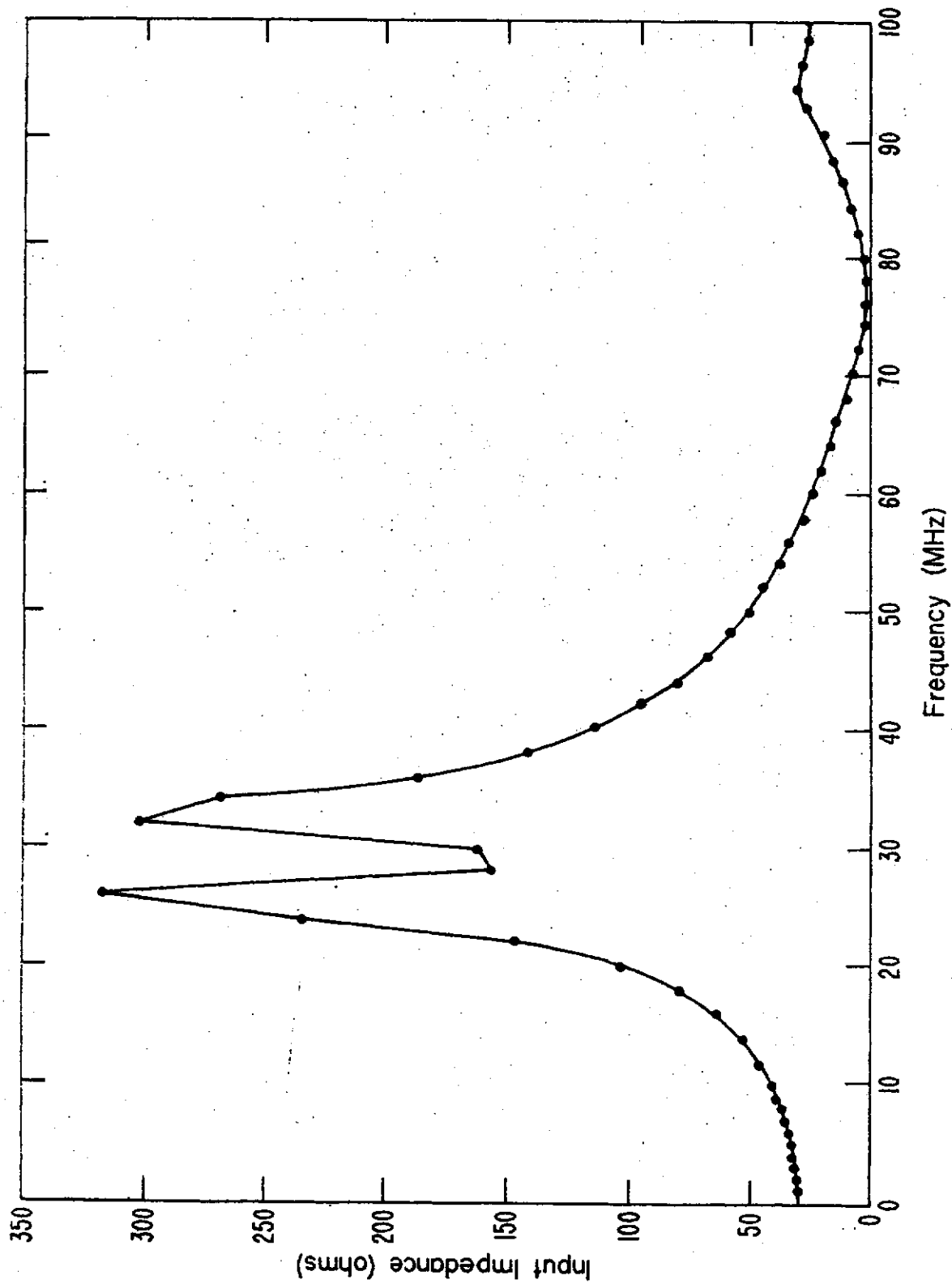


Figure 4.21 Antiskid Power Line Input Impedance

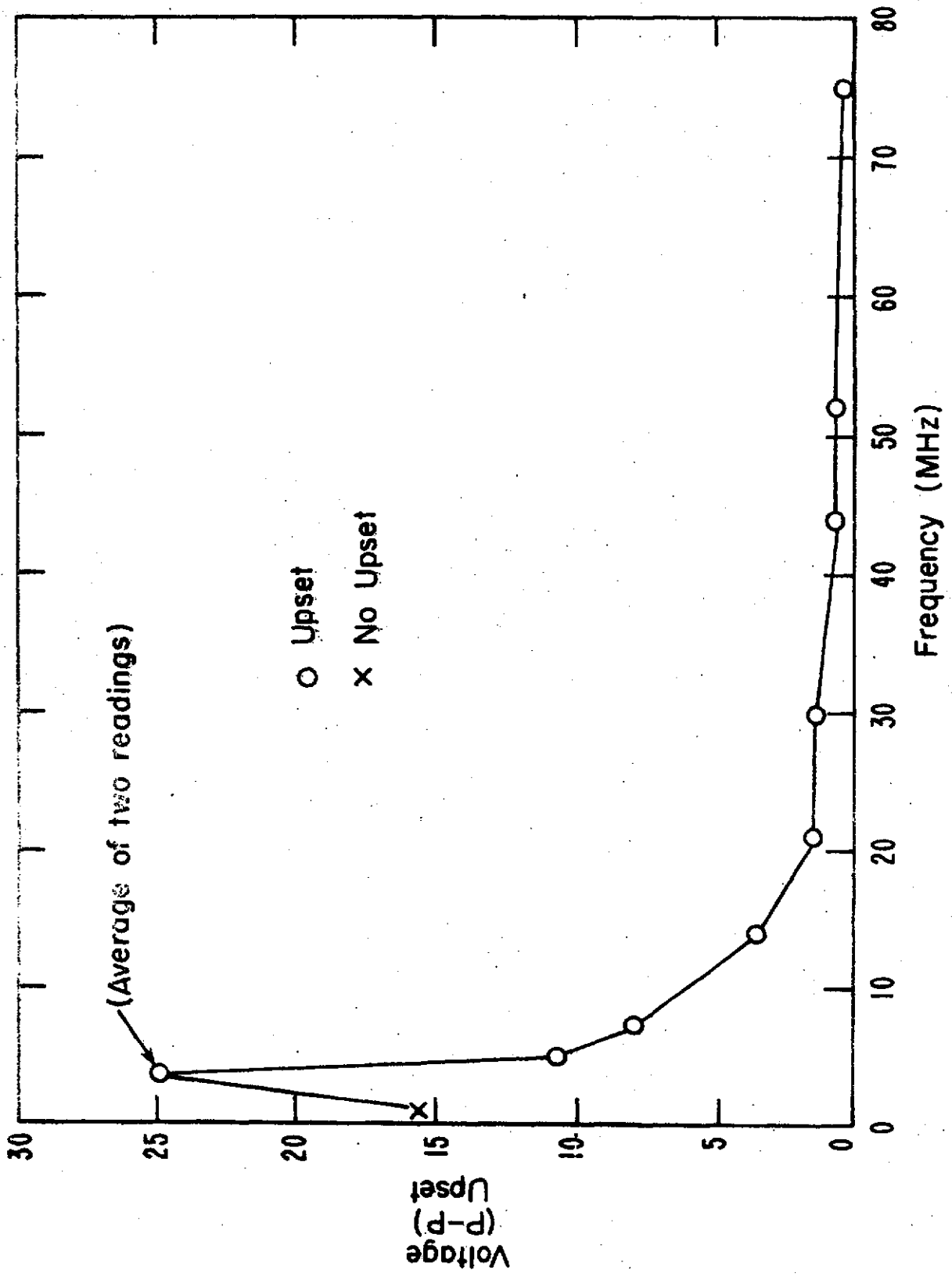


Figure 4.22 Antiskid Sensor Line Test Results (single point-rf pulse)

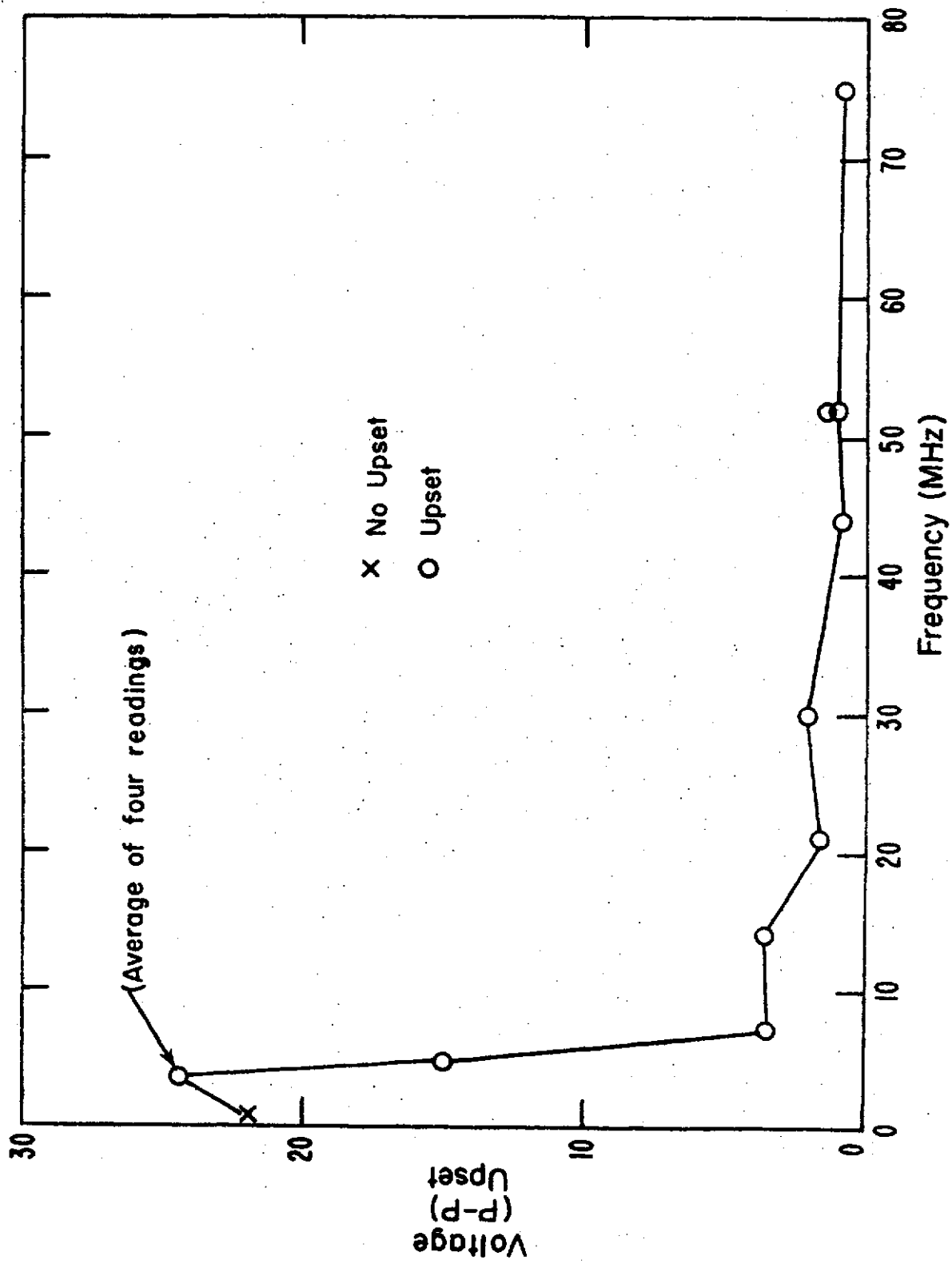


Figure 4.23 Antiskid Sensor Line Test Results (dual input - rf pulse)

are respectively with injection at the sensor "Hi" input (pin 3) and at both sensor inputs (pins 2 and 3). The results obtained using these two modes of injection are quite similar. No upset and/or high-level upset was obtained at frequencies below 20 MHz. Above 20 MHz, low level upset was obtained, with measured levels below 1 V (peak-to-peak) above 40 MHz.

The systems operation simulation, test set-up, and upset criterion are all explained in section 4.4.2. The operations simulation set-up cycles the system through acceleration-deceleration in a carefully controlled and repeatable manner. During each deceleration, the skid rate was approached at exactly the same time and a precise number of brake modulations were counted before the vehicle was "stopped." The criterion for upset was to count the number of modulations obtained during a normal (non-interference) cycle, which was then compared with the number obtained during the interference cycle. If the count difference was three or more, an upset was obtained. A margin of three difference assured that a real disturbance to the system had been obtained. The data in Table 4.12 shows a typical test record. The injection point was pin 3; the test frequency was 14 MHz. The table shows the reference count (14) measured for each new attenuation setting and the count during interference for the same attenuation setting. The attenuator changes in 10 dB steps until an upset is obtained. After the first upset, the attenuator is increased by 10 dB and the advance (decreasing attenuation) continues in 3 dB steps until upset is again obtained. Several upset modes were observed during the testing of this device. Distinction is not made between these modes in the results shown in Figures 4.22 and 4.23. The data in those figures is merely a plot of the results obtained from the printouts such as Table 4.12. Additional monitoring confirmed the upset criteria and showed further details of the system malfunction. Three distinct types of upset are observed.

The data in Figures 4.24 through 4.26 represent the various modes of upset cause by rf pulse signal injection at the sensor inputs. These

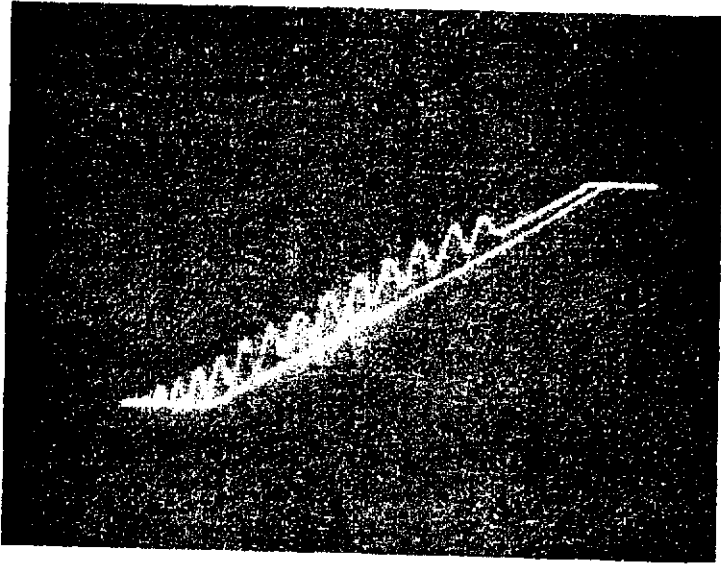
Table 4.12 Antiskid Module Test Record

<u>REFERENCE MODULATION COUNT</u>	<u>TEST MODULATION COUNT</u>	<u>ATTENUATION (dB)</u>
14	14	60
14	14	50
14	14	40
14	14	30
14	17	20
14	14	30
14	16	27
14	15	24
14	17	21

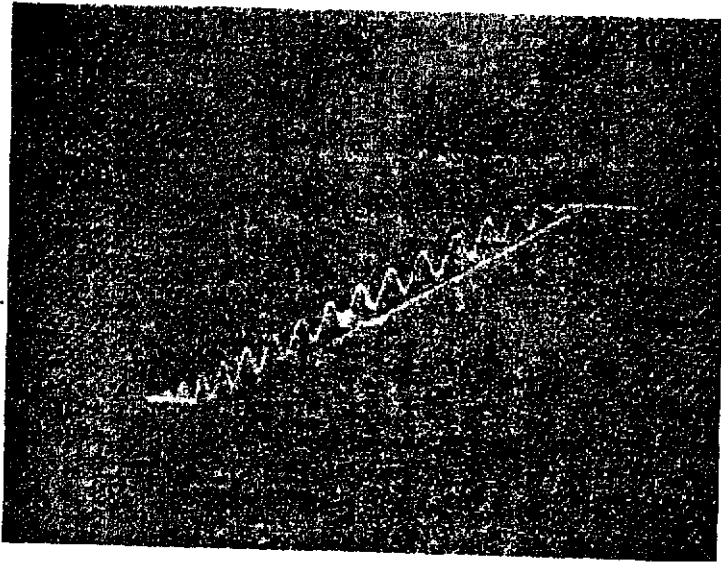
TEST FREQUENCY IS 14 MHz

UPSET OCCURRED DURING PULSING SEQUENCE

PULSE LEVEL = 21 dB

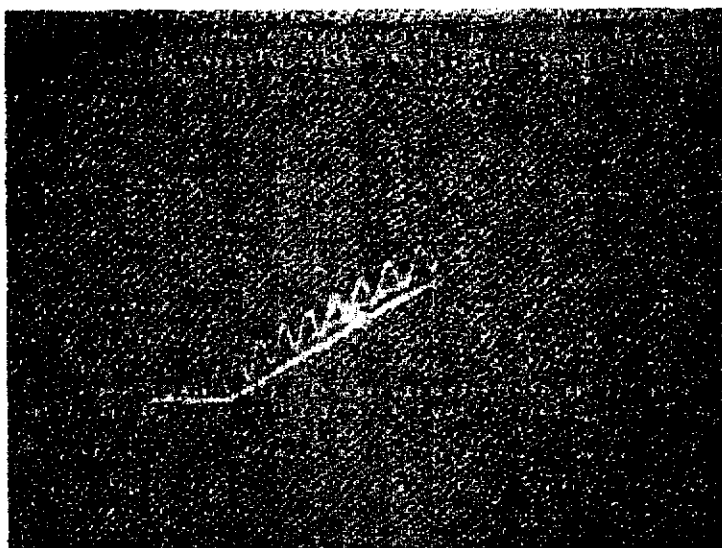


(a)

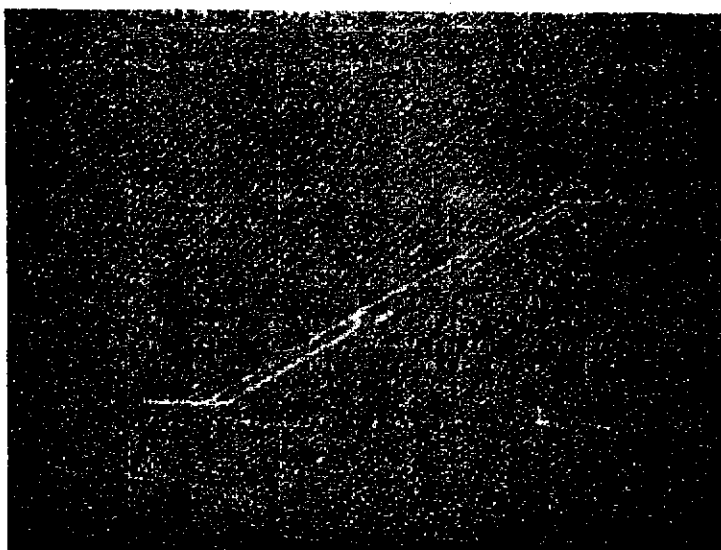


(b)

Figure 4.24 Anti-Skid Accelerate-Decelerate Cycles with Brake Modulation

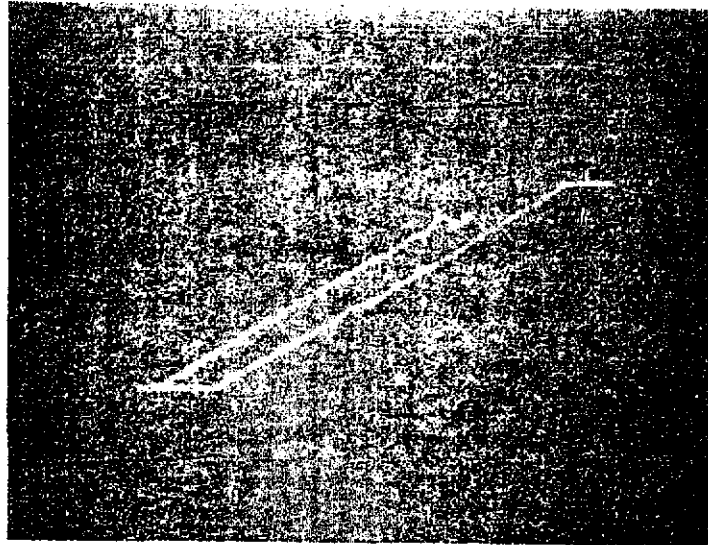


(a)

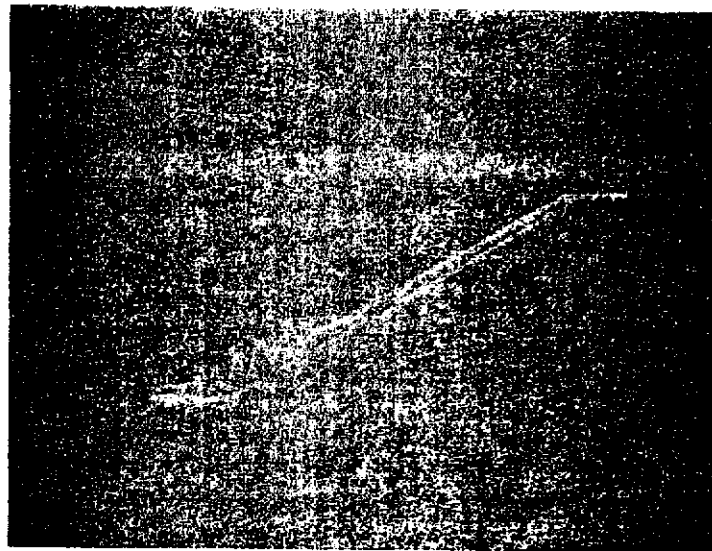


(b)

Figure 4.25 Anti-Skid Accelerate-Decelerate Cycles Showing System Upset Conditions



(a)



(b)

Figure 4.26 Anti-Skid Accelerate-Decelerate Cycles with System Upset Conditions

are displays similar to Figure 4.16, depicting the acceleration-deceleration cycle discussed above. The trace in Figure 4.24(a) shows a normal (non-interference) cycle. The normal number of counts (14) is observed. The trace in 4.24(b) shows additional modulation pulses, indicating skid conditions even though the wheel deceleration was not sufficient to warrant it. This condition of upset may not represent a serious safety hazard, but does indeed represent circuit malfunction due to interference.

The data in Figure 4.25 further represents circuit malfunctions during interference conditions. The data in Figure 4.25(a) is similar to Figure 4.24(b). The upset in Figure 4.25(a) is characteristic of an early onset of brake modulation which occurred with an interference signal of 1.5 V (p-p). The upset in Figure 4.25(b) occurred with an interference signal level of 3.0 V (p-p), causing a condition of no modulation. This upset condition would mean that the deceleration rate was sufficient to require modulation, but that the interference prohibited modulation from occurring and the wheels could go into a skid. This test was conducted with an interference frequency of 21 MHz.

The pictures in Figure 4.26 show two additional types of malfunction caused by interference signal injection at the sensor inputs. The trace in Figure 4.26(a) shows an early onset of brake modulation followed by a lock-up in the released pressure state. This is a serious malfunction manifest in temporary loss of brakes. This occurred with 1.5 V (p-p) injected signal at a frequency of 75.0 MHz.

The data in Figure 4.26(b) shows a skid condition malfunction similar to Figure 4.25(b), but with a recovery near the end of the braking cycle. This condition resulted from a 11V(p-p) injected signal at 5 MHz.

The data in Figure 4.27 is representative of the rf pulse injected waveforms. The composite data in the figure is the 1.3 kHz sensor input mixed with a 5 MHz rf pulse. The amplitude of the sensor signal is slightly more than 2 V (p-p), and the peak-to-peak amplitude of the rf pulse is about 10.5 V. This interference signal did cause an upset at

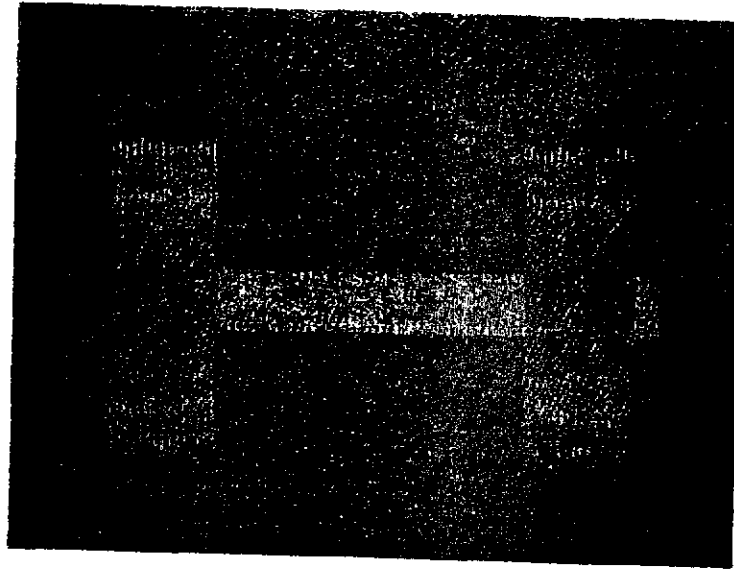


Figure 4.27 Anti-Skid Sensor Waveform with RF
Pulse Signals Superimposed

that frequency.

A second port selected for rf pulse injection was the 12 V power supply pin. This point proved to be quite susceptible to rf pulse interference. The results of this test series are shown in Figure 4.28. The circuit showed an upset at all frequencies for levels below 1.5 V (p-p). This electronics module has been designed to operate over the voltage range of 11-18 volts and has built-in protection against large transients. These precautions apparently have little effect in immunization to rf pulse interference.

4.5.3 CW Testing

The rf pulse tests described above were conducted using a pulse duty cycle of 25%. A second series of tests were conducted using the same interference source, but with the duty cycle increased to 100% creating a continuous wave (cw). The test plan outline in Table 4.9 was followed. The results from this series are shown in Figures 4.29 and 4.30. Figure 4.29 gives the results with injection to both input points (pins 2 and 3), and the data in Figure 4.30 resulted from injection into pin 2 only, the "lo sensor" port.

The results of these tests were very similar to the results obtained injecting rf pulse data into these ports. Basically, the circuit shows high immunity at the lower test frequencies and lower immunity as the frequency increases. The variability of upset amplitude in the frequency range between 10 and 50 MHz was more pronounced than for the rf pulse tests.

4.5.4 DC Pulse Testing

Difficulty was experienced in effective coupling between the dc pulse source and low impedance or impedance critical circuits, without severe signal reduction or circuit upset due entirely to coupling. This problem was apparent in coupling the dc pulse to the control circuits and to the power supply of the speed control module, and similarly was experienced in attempts to couple to both the power supply and to the sensor of the antiskid module. No tests were conducted using dc pulses at the power supply port (pin 12). Adequate levels were injected to the "lo sensor" port to cause upset, and the results of that test are shown

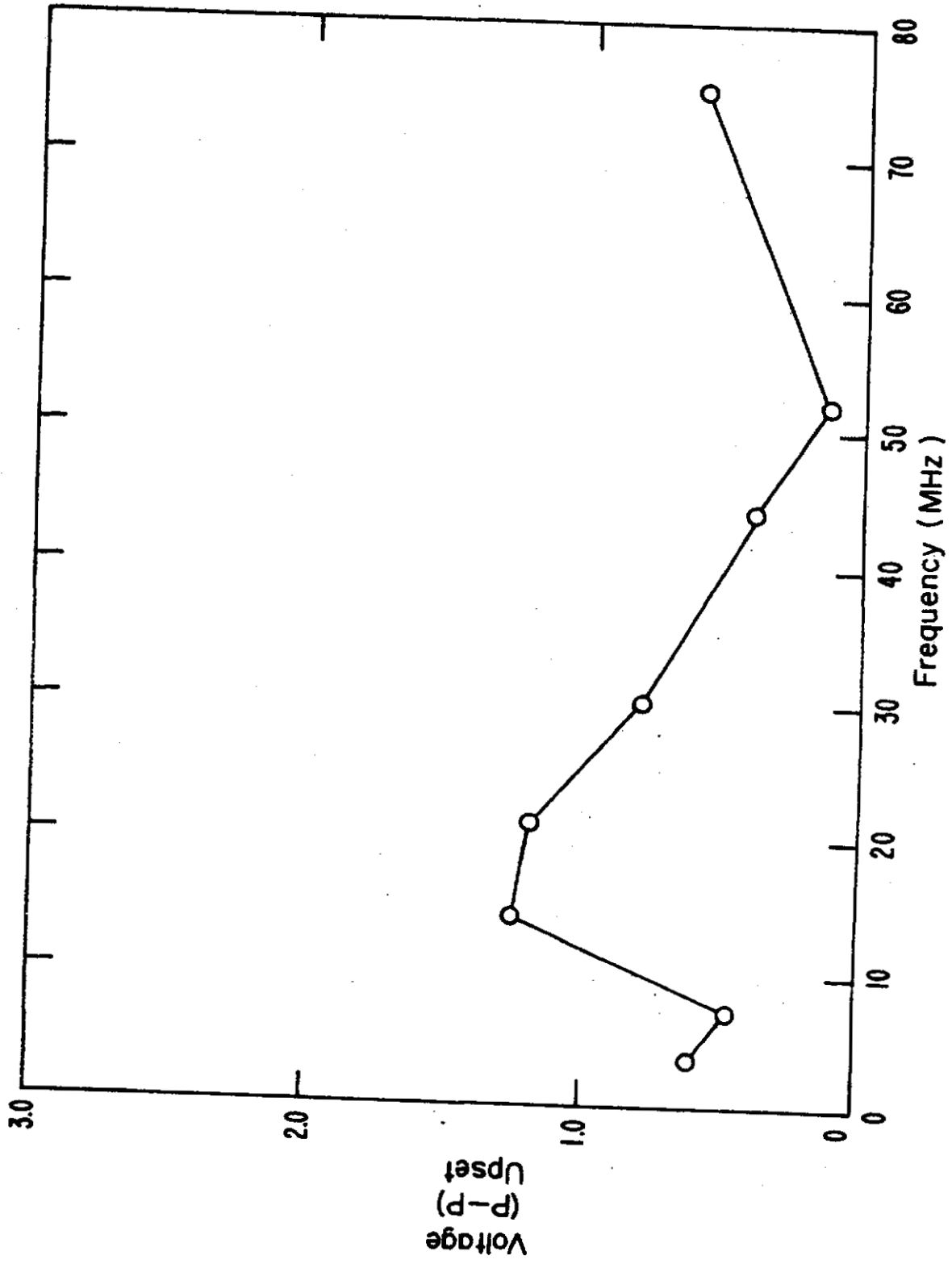


Figure 4.28 Antiskid Power Line Test Results

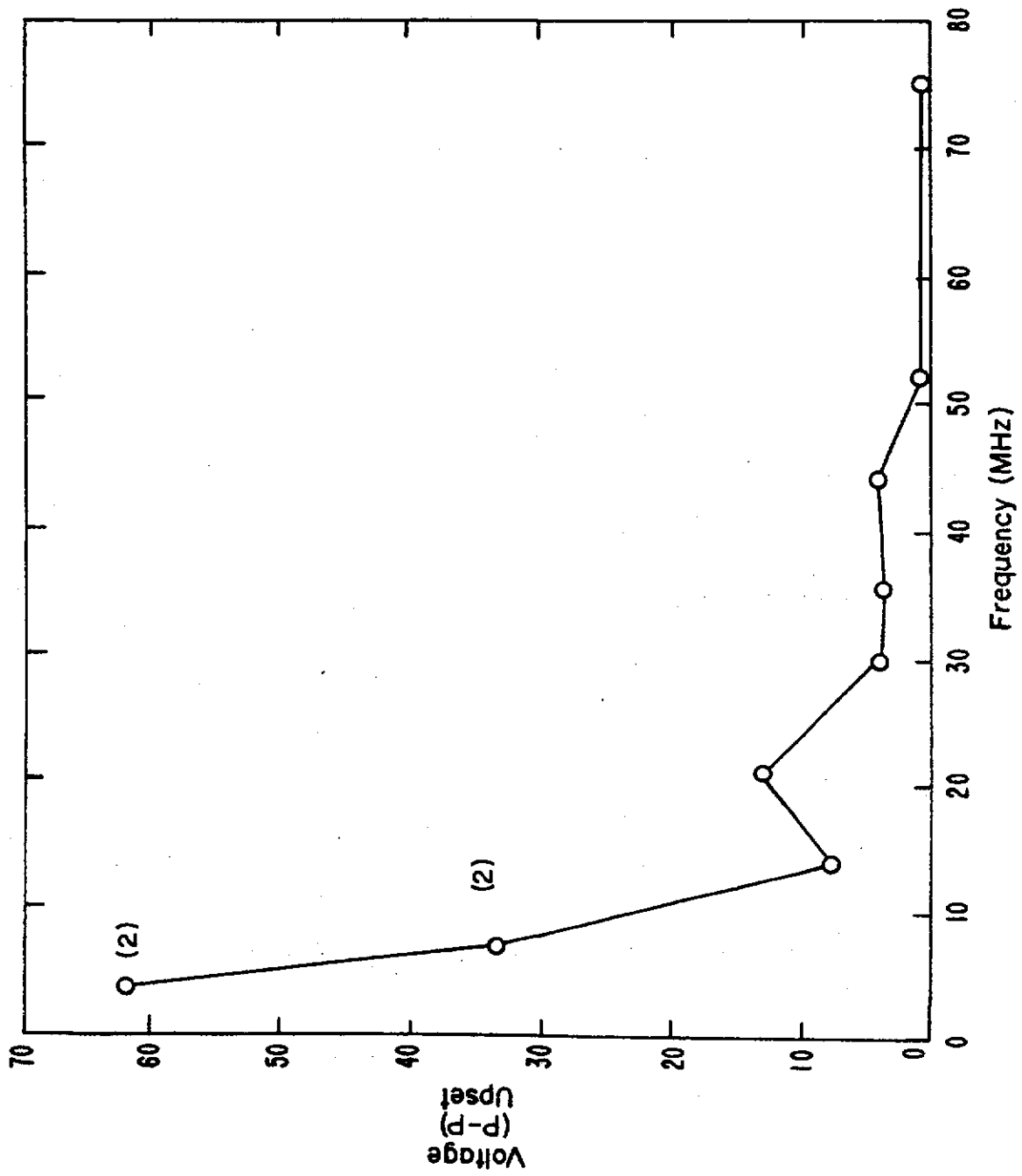


Figure 4.29 Antiskid Sensor Line Test Results (dual input - cw)

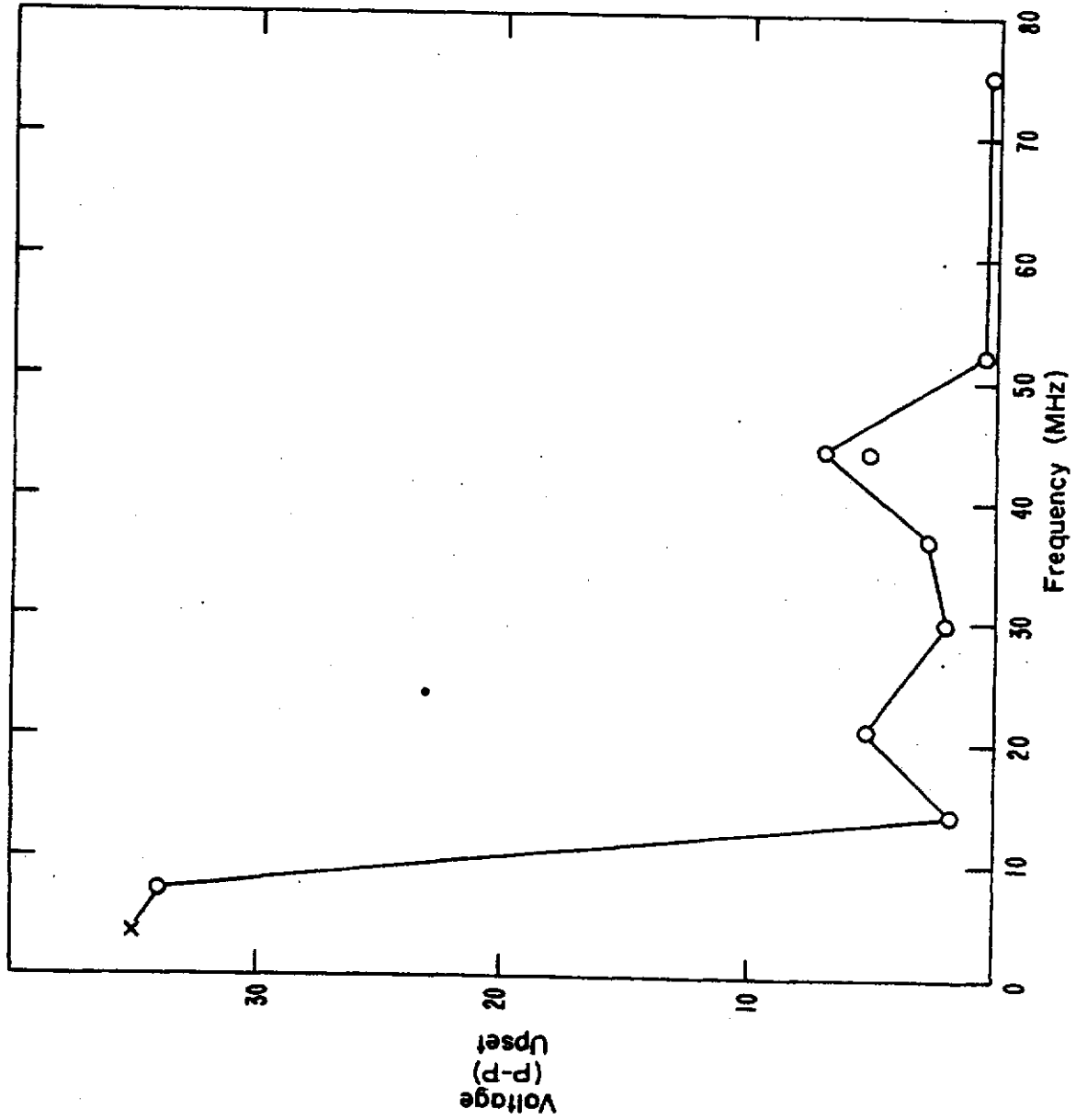


Figure 4.30 Antiskid Sensor Line Test Results (single point - cw)

in Table 4.13. Also, tests were conducted injecting dc pulses into a 0.1 ohm resistor between the circuit ground and the power supply ground. This test was designed to measure upset potential resulting from improper circuit installation or circuit grounding. Although evidence of minor disturbance was apparent on the monitoring oscilloscope, no formal upset was recorded. The maximum injected level for this test was 0.3 V.

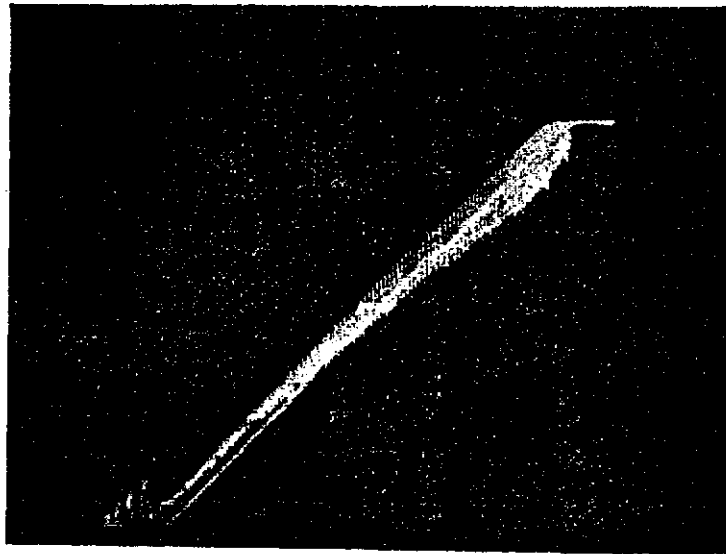
The data in Table 4.13, at upset, was recorded with both positive and negative (zero-to-peak) signals at the 25 and 50 pulse/sec repetition rate. The upset occurred at negative amplitudes which were only about one-half the positive amplitudes.

Pictures of the monitoring oscilloscope display (Figure 4.31), recording the accelerate-decelerate cycle (similar to Figure 4.24), show upset conditions observed during the test. The trace in Figure 4.31(a) was recorded injecting dc pulse amplitudes of +3.4 V with 3 ms pulse width and a 25 Hz repetition rate at pin 2 (the I_o sensor input). The data recorded in Figure 4.31(b) is the accelerate-decelerate cycle using dc pulses of amplitude 3.4 V with 0.3 ms pulse width and a 50 Hz repetition rate. An upset was measured for both of the test runs shown here. The data in Figure 4.31(a) shows evidence of the 25 Hz pulse feeding through the sensor (frequency-to-voltage) convertor.

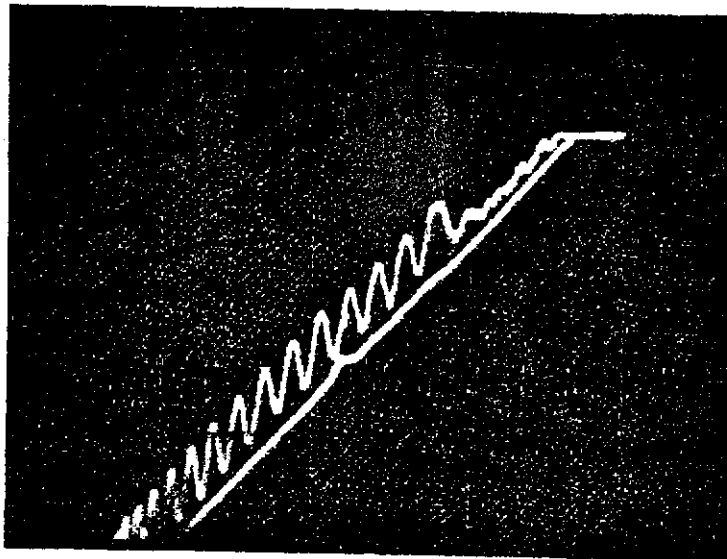
A record of the injected signal which caused upset in Figure 4.31(a) is shown in Figure 4.32(a), superimposed on the sensor input signal at that port. The amplitude and sweep settings were 1 V/div and 5 ms, respectively. The sensor frequency was approximately 1.3 kHz. The sensor signal and dc pulse train which caused an upset displayed in Figure 4.31(b) is shown in Figure 4.32(b).

Table 4.13 DC Pulse Tests (sensor line)

Voltage Polarity	PRR	Width (ms)	Upset Voltage (0-to-Peak)
POS	25	3.00	3.4 V
POS	50	0.30	3.4 V
POS	500	0.03	2.4 V (no upset)
NEG	25	3.00	1.75 V
NEG	50	0.30	1.75 V
NEG	500	0.03	2.30 V (no upset)

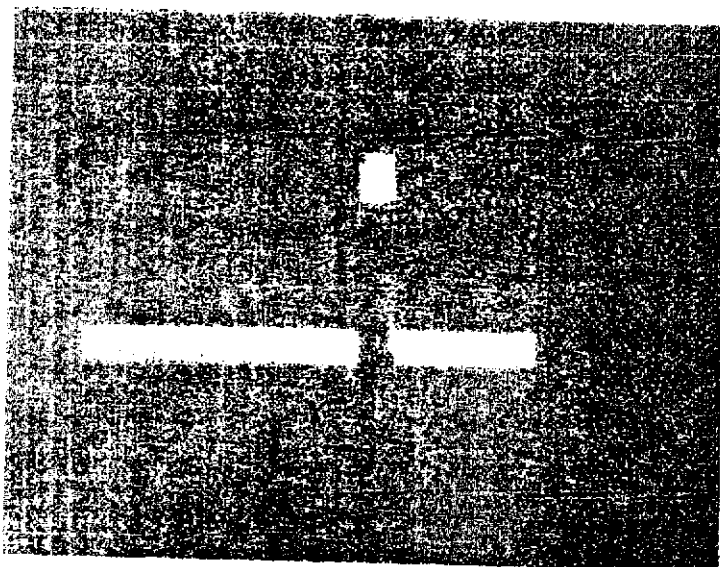


(a)



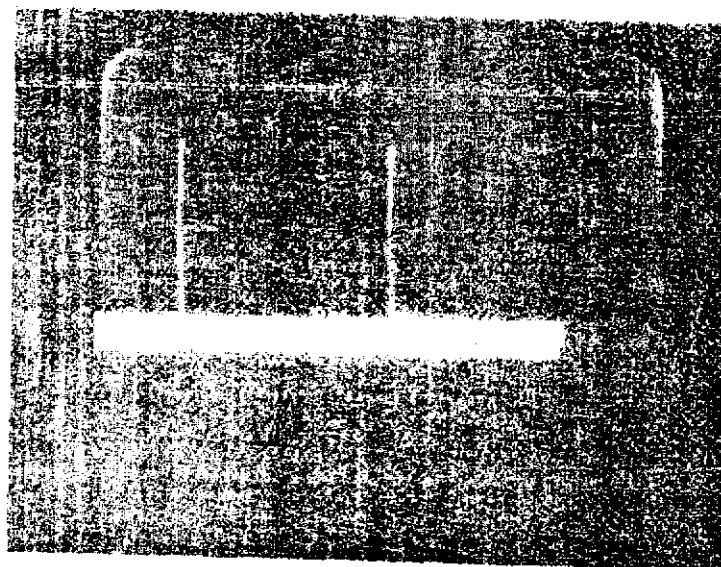
(b)

Figure 4.31 Anti-Skid Accelerate-Decelerate Cycles with System Upset Conditions



Reproduced from
best available copy.

(a)



(b)

Figure 4.32 Anti-Skid Sensor Signal with DC Pulses Superimposed.

5. SUMMARY AND CONCLUSIONS

A measurements task has produced information concerning the characteristics of waveforms which result from the normal activation of the electrical switches and controls of a typical automobile. Data and pictures are presented on waveforms associated with the light switch, air conditioner clutch, the starter, the ignition system, flashers, fan and windshield wiper motors, the alternator, and the horn. In addition to the signals and waveforms generated at the sources, selected coupled signals resulting from the source activity are identified and recorded.

With each switching (energizing or de-energizing) of equipment from the power bus, there is nominally a 12 V dc level change. Transients are sometimes associated with these switching actions which range from 1 V to greater than 100 V in amplitude. The larger transients are generally associated with the de-energizing of inductive loads. Sinusoidal or repetitive waveforms are associated with the motors and vibrators. Their fundamental frequencies are generally below 1 kHz, and their amplitude varied from 0.1 V to more than 3 V. The coupled signals generally appear as exponentially decaying "spikes" and/or as decaying sinusoid. The amplitude and duration of these waveforms are highly dependent on circuit loading and resonance. Typical recorded values range from less than 50 mV to greater than 1 V.

More than fifty measured waveforms are presented in Section 2.2, with comments on the data and details of the measurements. Summary tables of these data are given in Tables 2.2 and 2.3. A review of data obtained in an earlier study on power supply variations and severe transients is given in Section 2.3. Power supply levels as great as 130 V and transients of over 200 V have been observed. Summaries of power supply regulation characteristics and transient characteristics are given in Tables 2.4 and 2.5. The results of dc resistance measurements made at several points in the automobile referred to the power system ground are shown in Table 4.7.

The results of computer program runs to evaluate a simulated field-to-wire coupling of signals from a mobile transmitter to the air-

cushion restraint device cabling are given in Section 3. This analysis demonstrates the character of coupling dependencies on the transmitter operating frequency, the impedance of the signal reception point, the size of aperture, the dimensions of the aperture, body shielding, cable shielding, and cable length. The body shielding depends primarily on the relative positions of the transmitting source and the aperture. The amount of body metal in the direct path between these locations will yield some signal attenuation due to shielding. The cable shielding varies to a small degree as a function of frequency. This is calculated from a routine in the model from a given cable description.

As much as 30 dB variation in received signal level was observed for the frequencies processed across a band from 100 to 200 MHz. This variation resulted from a fixed aperture size. Also, there was an approximately 10 dB increase in received signal when the length of aperture was increased from 4 inches to 40 inches.

The complex interdependence of the several parameters described would indicate that the most useful application of the model would be to analyze specific installations in search of problem areas as opposed to preparation of general data tables to cover a large range of conditions. Sensitivity analyses of this type can be used to indicate aperture and shield integrity requirements for maintenance specifications and to define procedures and thresholds for evaluations required of manufacturers.

An important phase of this study has been the design, instrumentation and analysis of susceptibility testing as applied to two automotive electronic subsystems. The methodology, test plans, and results obtained from the two test series involving an electronic speed control system and an electronic antiskid brake control module are presented in Section 4.

The tests were conducted using a direct-drive facility to inject interference signals at several potentially susceptible circuit or system ports. These ports were selected on the basis of being vulnerable to conducted or induced signals. The character of the injected

signals was based on the results of the data obtained in Section 2. The system "upset" criteria used for evaluation were related to the intended functional performance of the systems.

The test results for the speed control system with rf pulses injected as interference are given in Figures 4.8, 4.9, and 4.10. The results for the same system with dc pulse injected are shown in Tables 4.6 and 4.7. For these tests, an upset resulted if the vehicle speed changed by more than 4 mph from the set speed. The upset conditions observed with rf pulse interference (in the 1 to 75 MHz range) was highly dependent on frequency and all three ports tested (sensor, control line, and power line) showed generally good immunity to rf interference. The lowest measured upset level was about 4 V(p-p). The sensor line was generally more sensitive to dc pulse interference with average upset level of about 1.5 V (zero-to-peak). The control line was much less sensitive, and the power line was not used as an injection port for dc pulses.

The results obtained from the antiskid control tests indicated that this device was more susceptible to rf pulses than the speed control system. A pair of sensor line inputs were used as ports in addition to the power supply input. The injected signals used were rf pulse and cw signals in the 0 to 75 MHz range and dc pulses. The upset criteria were based on a comparison of system performance under interference and interference-free conditions. An upset consisted of abnormal functioning of the braking modulation due to interference. The test results for the rf and cw signals are shown in Figures 4.22, 4.23, 4.28, 4.29, and 4.30. A tabulation of data obtained from dc pulse testing is given in Table 4.12. System upset occurred with injected rf and cw levels of less than 0.5 V(p-p) at the sensor inputs. The results were similar for both types of signals, indicating that the circuit is more sensitive to the cw signal than to the pulse characteristics. Also, the results showed that these ports are much more susceptible to interference at frequencies above 20 to 30 MHz than at lower frequencies. The power supply line input was also quite susceptible to rf interference (the only signal used in the tests at this port). Upsets were recorded at

several frequencies for injected levels below 0.5 V(p-p). The power supply regulator portion of this circuit has built-in transient protection. This protection design appears, however, not to be effective against rf interference. The dc pulse interference to the sensor inputs caused upset at 1.7 V (zero-to-peak) levels. This is similar to the results obtained from the speed control system tests.

These conductive (direct-drive) signal susceptibility tests have proven to be an efficient and useful method of evaluating the effective interference potential of actual motor vehicle electronic subsystems. These test concepts could be expanded to include more ports or system modules and even to evaluate circuit component susceptibility at the design stage.

The results of these tests have shown the dependence of signal characteristics on circuit susceptibility, namely frequency, duty cycle, polarity, etc. Examples are: 1) the low-frequency susceptibility and high frequency immunity of the speed control sensor compared to an opposite situation for the anti-skid module sensor; 2) the sensitivity of the speed control sensor input to dc pulse amplitudes of approximately one-half the sensor peak-to-peak amplitude, and; 3) the similarity of results observed between rf pulse signals and cw signals at the anti-skid sensor inputs, indicating that this circuit is primarily sensitive to rf signals.

Although no detailed analysis has been performed to correlate the results of these tests with the reported malfunctions of anti-skid control modules when exposed to mobile radio emissions, the observed susceptibility levels in the 30 to 75 MHz range do not dispute that such interference and malfunctions could occur. Unshielded or improperly shielded lines and cables between the sensors and the electronic control modules would be very effective in feeding the rf signals to the sensor ports.

6. ACKNOWLEDGEMENTS

The authors express appreciation to the Air Force Weapons Laboratory for the support and cooperation received in using their direct drive test facilities for the susceptibility tests. A special acknowledgement is conveyed to Col. James L. Griggs, Jr., for making available the facilities for our tests; to Mr. Richard Hays for his efforts in planning and arranging our schedules; and to Lt. Allan Snyder, Lt. Richard Elder, Lt. Ralph Carroll, and Mr. Harvey Packard for direct support in conducting the tests.

Also, an appreciation is extended to Mr. Chuck Miller for the drafting of measurement figures and waveform data, and to Marilyn Longan and Kathy Mayeda for typing and preparation of manuscripts.

7. REFERENCES

- Bagdanor, J.L., M.D. Siegel, and J.L. Weinstock (1971), Intra-Vehicle Electromagnetic Analysis Technical Report AFAL-TR-71-155, Parts I, II, and III, July, Air Force Avionics Laboratory, Wright-Patterson AFB, OH.
- Espeland, R.H., L.A. Jacobson, L.R. Teters, and E.L. Morrison, Jr. (1975), Investigation of Electromagnetic Interference Effects on Motor Vehicle Electronic Control and Safety Devices (DOT-HS-801 737), U.S. Dept. of Transportation, NHTSA, Washington, DC 20590.
- Follmer, W.C. (1974), Electronic Speed Control, Society of Automotive Engineers, 740022, New York, NY.
- Ford Motor Company (1974), 1974 Car Shop Manual, Volume 3 - Electrical, Ford Marketing Corporation, Dearborn, MI.
- Greaves, L.D., J.J. Schwarz, H.J. Wagnon, and G.W. Wilson (1975), Subsystem Test Methodology for the AFWL Direct Drive Laboratory, D224-13057-1, AFWL, Kirtland AFB, NM.

Kelsey-Hayes (1974), Marketing Brochure 4-110, June

Lapidus, G. (1973), Transistor Family Tree, IEEE Spectrum, 10, No. 1, pp. 34-35, January.

McCarter, O.T. (1974), What Electronic Devices Face in the Automobile Environment, EDN, January 5, pp. 28-34.

Society of Automotive Engineers, Electronic Systems Subcommittee (SAE, 1974), Preliminary Recommended Environmental Practices for Electronic Equipment Design (proposed), International Colloquium on Automotive Electronic Technology, October, pp. 28-30.

Society of Automotive Engineers (SAE, 1975), Conference Proceedings, International Colloquium on Automotive Electronic Technology, October, pp. 28-30.

Society of Automotive Engineers, Subcommittee on EMI Standards and Tests Methods (1974), Electromagnetic Susceptibility Test Procedures for Vehicle Components (Except Aircraft), International Colloquium on Automotive Electronics Technology, October, pp. 28-30.